Marinella N. Ghezzo

THYMIC STROMAL FACTORS PROMOTING T-CELL LEUKEMIA



UAlg
UNIVERSIDADE DO ALGARVE
DEPARTAMENTO DE CIÊNCIAS BIOMÉDICAS E MEDICINA

2017

Marinella N. Ghezzo

THYMIC STROMAL FACTORS PROMOTING T-CELL LEUKEMIA

PhD Thesis in Biomedical Sciences

Work supervised by:

Nuno Rodrigues dos Santos, PhD



UNIVERSIDADE DO ALGARVE
DEPARTAMENTO DE CIÊNCIAS BIOMÉDICAS E MEDICINA

2017

Thymic stromal factors promoting T-cell leukemia

Declaração de autoria de trabalho

Declaro ser a autora deste trabalho, que é original e inédito. Autores e trabalhos consultados estão devidamente citados no texto e constam da listagem de referências incluída.

_____

Copyright – Marinella N. Ghezzo. *Departamento de Ciências Biomédicas e Medicina, Universidade do Algarve.*

A Universidade do Algarve reserva para si o direito, em conformidade com o disposto no Código do Direito de Autor e dos Direitos Conexos, de arquivar, reproduzir e publicar a obra, independentemente do meio utilizado, bem como de a divulgar através de repositórios científicos e de admitir a sua cópia e distribuição para fins meramente educacionais ou de investigação e não comerciais, conquanto seja dado o devido crédito ao autor e editor respetivos.

Dedicated to my parents

Acknowledgements & funding

To Dr. Nuno Rodrigues dos Santos, who supervised my work during these last few years, all the abstracts and thesis reviewing, and everything else in between, thank you. To my lab colleagues, you have all been part of this journey and I appreciate you for it. Yet I need to thank one in particular, as she was the one to put it best and this says it all: my lab soul mate, Mónica!

I am also very grateful for all the support that Centre for Biomedical Research (CBMR) and its members have given us, in particular Dr. José Belo, Dr. Gabriela Silva and their lab' members. For all the companionship, all the advices on "last-minute" new protocol hesitations, a special thank you to Carolina, Marta, Margaret, Rubi and Zé. To "my" Vanessa, you have been there from the very start and when the time came, "adopting" me into the crew – Bitoque, Sofia, Sónia, Daniela and Susana – with all the silliness and precious musical moments.

Thank you to our collaborators Dr. Matthias Futschik and SysBioLab members, for the experimental design discussions and data analysis on the RNA-seq experiments. Also, Dr. Nuno L. Alves, and Pedro Rodrigues who performed the thymic stromal cell isolation experiments. To the members of my PhD committee, Dr. Wolfgang Link and Dr. Nuno L. Alves, thank you for the valuable discussions.

I would like to thank the University of Algarve and the Department of Biomedical Sciences and Medicine for hosting me in this PhD Program, with a special word of appreciation to the Program's director Dr. Leonor Cancela and secretary Conceição José. The technical assistance provided by André Mozes, Cláudia Florindo, Mauricia Vinhas and Neusa Miguel, the core facilities technicians of the Department/CBMR, was much valued and appreciated.

None of this would have been possible without the financial support given by Portuguese Foundation for Science and Technology (FCT) by means of the PhD studentship (ref. SFRH/BD/80503/2011). Additional funding was also provided by FCT (PTDC/SAU-OBD/103336/2008 and UID/BIM/04773/2013 CBMR), *Núcleo Regional Sul da Liga Portuguesa Contra o Cancro* and *Fundação* Merck Sharpe & Dohme.

Last, but certainly not least, thank you to my family and friends. To my parents and brother, thank you for the support, for the "go for it" when it came time to choose between a "normal" job or doing science. To my friends, thank you for the support, for understanding all my lately-too-frequent absence. To Rato, my best friend, the Yang to my Yin, you Rock!

Resumo

A leucemia linfoblástica aguda de linfócitos T (LLA-T) é uma doença agressiva de percursores de células T, que afeta principalmente crianças e jovem adultos. A LLA-T dissemina-se para vários orgãos, sendo fatal na ausência de diagnóstico precoce e terapia apropriada. Pensa-se que a LLA-T se desenvolva a partir da transformação maligna de percursores de linfócitos T, ou timócitos, como se pode verificar pelos semelhantes perfis imunofenotípicos, genotípicos e transcritómicos de casos de LLA-T e fases específicas de diferenciação intra-tímica de timócitos.

O maturação de timócitos só é atingida através de uma comunicação bidirecional próxima entre estes e células do estroma tímico. Estas interações despoletam alterações no microambiente do timo que são essenciais para a migração, diferenciação e seleção de linfócitos T funcionalmente maduros. Durante o processo de diferenciação dos timócitos, ocorrem alterações genéticas, levando à expressão de oncogenes e ativação de vias de sinalização normalmente envolvidas em cancro. Estas podem igualmente ser ativadas por ligandos associados a células do microambiente. Embora importantes para a génese tumoral, relativamente pouco se sabe acerca dos fatores microambientais do timo que contribuem para a LLA-T. A sua identificação é importante para melhor compreender a patogénese desta doença oncológica, mas apenas recentemente começaram a ser explorados a nível molecular. O nosso grupo identificou um atraso no desenvolvimento de leucemia, num modelo animal transgénico (TEL-JAK2) de LLA-T, provocado pela inativação genética do fator de transcrição RelB e do recetor LTβR em células estromais.

No presente trabalho, procedemos à caraterização das alterações do estroma tímico que ocorrem em várias etapas das doença, verificando que o início da leucemia estava associado à expansão das células tímicas epiteliais (CTE) da medula e redução das equivalentes do córtex. De relevância, verificámos também que a haploinsuficiência do gene *Foxn1*, regulador essencial da diferenciação das CTE, causa atraso no desenvolvimento da leucemia.

Palavras chave

LLA-T, leucemia, TEL-JAK2, timo, microambiente, células epiteliais tímicas.

Abstract

T-cell acute lymphoblastic leukemia (T-ALL) is an aggressive malignancy of T cell precursors that affects mainly children and young adults, disseminates throughout the body invading several organs, and fatal without early diagnosis and appropriate therapy. It is thought that T-ALL arises from the malignant transformation of T-cell precursors or thymocytes, as denoted by similar immunophenotypic, genotypic and transcriptomic profile of T-ALL cases and particular stages of intra-thymic T-cell differentiation.

Thymocyte development is achieved through a close bidirectional communication between stromal cells and the developing thymocytes. These interactions trigger changes in the thymic stromal microenvironment that are essential for thymocyte migration, differentiation and selection of functional mature T cells tolerant to self-antigens. During the intra-thymic development and differentiation process of thymocytes, transformation events lead to the expression of certain oncogenes. Several genetic alterations result in the activation of signaling pathways commonly involved in cancer, any of which can be activated by microenvironmental cell-derived ligands. The cancer microenvironment is crucial for tumorigenesis, yet relatively little is known about the microenvironmental factors contributing to T-ALL. The identification of thymic stromal cell molecular factors that participate in T-ALL is important for a better understanding of T-ALL pathogenesis. The molecular and cellular players involved in stromal support of thymocyte leukemogenesis have only recently began to be explored. Our group has reported that inactivation in stromal cells of the RelB transcription factor and the lymphotoxin-β receptor (LTβR) delayed leukemia development in the TEL-JAK2 transgenic mouse model of thymic T-ALL development.

In this work, we characterized the thymic stromal alteration in various stages of disease and found that thymic leukemogenesis was associated with an expansion of medullary thymic epithelial cells (TEC) and reduction of cortical TECs. More importantly, we found that haploinsufficiency of the *Foxn1* gene, an essential master regulator of TEC differentiation, delayed thymic leukemogenesis.

Keywords

T-ALL, leukemia, TEL-JAK2, thymus, microenvironment, thymic epithelial cells.

List of contents

Acknowledgements & funding ix

Resumo x

Palavras chave x

Abstract xi

Keywords xi

List of contents xiii

List of figures xvi

List of tables xviii

List of abbreviations, acronyms and symbols xix

CHAPTER 1. INTRODUCTION 1

1.1. The hematopoietic system and T lymphocyte development 3

1.1.1. The hematopoietic system 3

1.1.2. Thymocyte development 4

1.1.3. T lymphocytes: main subtypes and functions 7

1.2. The thymus: the T cell cradle 9

1.2.1. Early organogenesis and thymic epithelium generation 9

1.2.2. Thymic microenvironment cellular components 10

1.2.2.1. Thymic epithelial cells 11

1.2.2.2. FoxN1, a master regulator for thymic epithelial differentiation 13

1.2.3. Molecular signals in the thymic microenvironment 16

1.2.3.1. Cell-adhesion molecules and chemokines in T-cell precursor homing and maturation 17

1.2.3.2. NF-κB activation is essential for thymic stromal cell differentiation 18

1.2.3.3. Members of the TNF ligand and receptor superfamilies in mTEC development 19

1.2.3.4. Notch activation is essential for T-cell differentiation 20

1.3. T-cell acute lymphoblastic leukemia 21

1.3.1. Definition and classification 21

1.3.2. Cytogenetics and molecular genetic abnormalities 22

1.3.3. The thymic origin of T-ALL 26

1.3.4. T-ALL experimental models 28

1.3.4.1. TEL-JAK2 transgenic mouse 29

1.4. Aims 30

CHAPTER 2. MATERIALS & METHODS 33

2.1. Mouse strains, breeding and procedures 35

2.1.1. Euthanasia, necropsy and sample preparation 35

2.1.2. Leukemic cell transplantation 36

2.1.3. Blood collection 36

2.1.4. Mouse genotyping 36

2.1.4.1. Polymerase chain reaction 37

2.1.4.2. Restriction enzymatic digestion 37

2.2. Cell culture 39

2.2.1. Leukemic cell co-cultures 39

2.2.2. *Foxn1* stable expression in the 1C6 mTEC cell line 39

2.3. Genomic DNA extraction and *Notch1* mutation detection 40

2.4. Whole transcriptome RNA sequencing (RNA-seq) 40

2.5. Flow cytometry 41

2.5.1. Isolation and analysis of thymic stromal cells 41

2.5.2. Thymocyte/T-cell analysis 42

2.6. Immunofluorescence 42

2.7. mRNA expression analysis 43

2.7.1. Semi-quantitative PCR 43

2.7.2. Real-time quantitative PCR 46

2.8. Statistical analysis 46

CHAPTER 3. RESULTS 49

3.1. Thymic stromal cell alterations during TEL-JAK2-induced murine leukemogenesis 51

3.1.1. TEL-JAK2 leukemic cells depend on microenvironmental cells for survival 51

3.1.2. *Notch1*-activating mutations in the TEL-JAK2 mouse model 53

3.1.3. TEL-JAK2 mouse thymic lymphomas present profound architectural changes as compared to control thymi 55

3.1.4. Early stage thymic lymphomas are marked by the loss of cortical markers and expansion of medullary thymic epithelium 67

3.1.5. The reduction in TEC marker expression starts early in TJ2-induced thymic leukemogenesis 73

3.2. Role of *Foxn1*-dependent thymic stroma in TEL-JAK2-induced leukemogenesis 79

3.2.1. *Foxn1* haploinsufficiency delays the onset of TEL-JAK2-induced leukemia 79

3.2.2. TJ2-Tg-induced early stage thymic leukemogenesis is delayed by *Foxn1* haploinsufficiency 84

3.2.3. The *Foxn1*-dependent thymic microenvironment facilitates leukemic cell expansion 89

3.3. Identification of dose-dependent thymic epithelial cell-specific FoxN1 target genes 91

3.3.1. *Foxn1* haploinsufficiency is associated with reduced target gene expression 91

CHAPTER 4. DISCUSSION & FUTURE PERSPECTIVES 93

4.1. Thymic epithelial architectural alterations associated with thymic leukemogenesis 95

4.2. The FoxN1-dependent thymic microenvironment facilitates thymic leukemogenesis 97

4.3. How does TEC-expressed FoxN1 facilitate thymic leukemogenesis? 98

4.4. Role for other stromal cells in thymic leukemogenesis 100

4.5. Outlook 101

REFERENCES 103

ANNEX. SUPPLEMENTARY DATA 119

List of figures

Chapter 1.

Figure 1.1. Hematopoietic system. 4

Figure 1.2. T cell development. 5

Figure 1.3. Thymic stromal cells and thymocyte migration. 16

Chapter 3.

Figure 3.1. TEL-JAK2 leukemic cell *in vitro* survival is prolonged by co-culture with MS5 stromal cells. 52

Figure 3.2. Co-culture with MS5 cells confers resistance of TJ2-Tg leukemic cells to dexamethasone treatment. 52

Figure 3.3. *Notch1* exon 34 heterozygous mutations at codon 2361. 54

Figure 3.4. TEL-JAK2-induced thymic lymphomas display large keratin-negative areas. 57

Figure 3.5. Detection of thymic stromal markers in wild-type mice. 59

Figure 3.6. Characterization of the thymic stromal cellular alterations in advanced stage thymic lymphomas from TJ2-Tg mice. 61

Figure 3.7. Characterization of the thymic stromal cellular alterations in advanced stage thymic lymphomas from TJ2-Tg mice. 63

Figure 3.8. TEL-JAK2-thymic lymphomas present areas of medullary TEC markers co-localization. 64

Figure 3.9. Fibroblasts are present in keratin-negative areas. 65

Figure 3.10. ICAM-1 often co-localize with $Krt5^+$ TECs. 65

Figure 3.11. Cortical thymic epithelial markers are underrepresented in relation to a medullary TEC marker in whole TJ2-Tg lymphomas. 67

Figure 3.12. Medullary thymic epithelial cell expansion occurs at the early stages of thymic lymphomagenesis. 70

Figure 3.13. Thymic lymphoma blood vessels are surrounded by laminin-containing extracellular matrix. 71

Figure 3.14. Thymic epithelial cell characterization by flow cytometry analysis. 72

Figure 3.15. Young pre-leukemic TJ2-Tg mice have normal thymic weight and cellularity. 73

Figure 3.16. Level of progression of the TJ2-induced leukemia can be quantified by presence of $CD8^+CD25^+$ malignant thymocytes. 74

Figure 3.17. Level of disease progression vs. stromal gene expression in TJ2-Tg mice. 75

Figure 3.18. Presence of leukemic cells in the blood reveals the onset of TJ2-induced leukemia. 77

Figure 3.19. Thymic cellular fractions show enriched expression of specific marker genes. 77

Figure 3.20. Expression of cortical markers becomes reduced from an early stage in TJ2-induced leukemia. 79

Figure 3.21. *Foxn1* haploinsufficiency delays TEL-JAK2-induced leukemia onset. 80

Figure 3.22. *Foxn1* haploinsufficiency does not affect tumor load. 81

Figure 3.23. *Foxn1* haploinsufficient TJ2-Tg thymic lymphomas also display large KNAs. 81

Figure 3.24. Mouse sex does not affect leukemia-free survival. 82

Figure 3.25. Mouse sex does not affect tumor load. 82

Figure 3.26. *Foxn1* haploinsufficiency has no major influence on gene expression in whole TJ2-Tg thymic lymphomas. 83

Figure 3.27. Thymic lymphomas used for gene expression analysis from *Foxn1* haploinsufficient mice were older. 84

Figure 3.28. *Foxn1* haploinsufficiency does not affect weight or cellularity of young asymptomatic TJ2-Tg mice. 85

Figure 3.29. TJ2-induced leukemia initiation takes place in the thymus. 86

Figure 3.30. *Foxn1* haploinsufficiency leads to mild reduction in thymic weight without causing major perturbations in thymic development. 88

Figure 3.31. *Foxn1* haploinsufficiency impairs leukemic cell expansion in recipient mouse thymi. 90

Figure 3.32. *Foxn1* haploinsufficiency leads to reduced target gene expression. 92

Figure 3.33. Overexpression of *Foxn1* correlates with increased *Ccl25* and *Krt5* expression. 92

Chapter 4.

Figure 4.1. Influence of thymic stromal cell signaling in T-ALL. 101

Figure 4.2. Working hypothesis on the role of FoxN1 in TJ2-Tg leukemogenesis. 102

Annex.

Supp. Figure 1. Exclusion of $CD45^+$ cells and doublets prior to flow cytometry analysis of TEC subpopulations. 121

List of tables

Chapter 1.

Table 1.1. Phenotypes of thymic stromal cells. 11

Table 1.2. Main phenotypical differences between cortical and medullary TECs. 12

Table 1.3. Genetically modified *Foxn1* mouse models. 14

Table 1.4. Chemokine expression in the adult thymus. 18

Table 1.5. Characterization of T-ALL. 22

Table 1.6. Main protein families affected by genetic abnormalities in T-ALL. 24

Table 1.7. Most common genetic lesions in T-ALL. 25

Table 1.8. Main genes involved in genetic alterations in the TCR signaling pathway and tyrosine kinases. 26

Chapter 2.

Table 2.1. Primers used for mouse genotyping. 38

Table 2.2. Expected band lengths of wild-type and *nude* alleles in *Foxn1* mice, after restriction enzyme digestion. 38

Table 2.3. Antibodies used in flow cytometry analysis. 44

Table 2.4. Surface markers and secondary reagents used for immunofluorescence. 45

Table 2.5. Oligonucleotide primers used for gene expression analysis. 46

Chapter 3.

Table 3.1. High frequency of exon 34 *Notch1* mutations in TJ2-Tg-induced leukemia samples. 54

Table 3.2. Leukemic cells and TEC populations at the early stages of TJ2-Tg thymic lymphomas. 69

Table 3.3. TJ2-Tg mice monitored for the presence of $CD8^{+}CD25^{+}$ leukemic cells. 76

Annex.

Supp. Table 1. High frequency of exon 34 *Notch1* mutations in TJ2-Tg-induced leukemia samples with distinct genetic backgrounds. 122

Supp. Table 2. Endpoint TJ2-Tg thymic lymphoma samples analyzed by immunofluorescence. 123

Supp. Table 3. DEGs upregulated in WT sample. 124

Supp. Table 4. DEGs upregulated in TJ2-Tg sample. 129

Supp. Table 5. Overlapping genes between the high-throughput RNA-sequencing and the study performed by Ki and colleagues (2014). 140

List of abbreviations, acronyms and symbols

#	
ºC	degrees Celcius
x*g*	times gravity
1C6	1C6 murine mTEC cell line
hi	high
lo	low

A

A	adenosine
AGM	aorta-gonad mesonephros (region)
AIRE	autoimmune regulator
ALL	acute lymphoblastic leukemia
APC	allophycocyanin

B

B-ALL	B-cell acute lymphoblastic leukemia
BM	bone marrow
BMP	bone morphogenic protein
bp	base pair (lenghth)

C

C	cytosine
CAM	cell-adhesion molecule
CD	cluster of differentiation
CD4SP	$CD4^+$ single-positive
CD8SP	$CD8^+$ single-positive
CDKN	cyclin-dependent kinase inhibitor
cDNA	complementary DNA
CLP	common lymphoid progenitor
CMJ	corticomedullary junction
CMP	common myeloid-erythroid progenitor

CNS	central nervous system
CO_2	carbon dioxide
CPM	count-per-million
CTE	*células tímicas epiteliais*
cTEC	cortical thymic epithelial cell
Cy	cyanine

D

DAPI	4',6-diamidino-2-phenylindole
DC	dendritic cell
DEGs	differentially expressed genes
DLL	Delta-like ligand
DN	CD4-CD8- double-negative
DNA	deoxyribonucleic acid
DNM2	DNA methylase 2
DP	$CD4^+CD8^+$ double-positive

E

E	embryonic day (of development)
ECM	extracellular matrix
EDTA	ethylenediaminetetraacetic acid
EGIL	European Group for the Immunological Characterization of Leukemias
ELP	early lymphoid precursor
ETP	early T-cell precursor
ETV6	ETS variant 6

F

F	female
FACS	fluorescence-activated cell sorting
FBS	fetal bovine serum
FC	fold-change
FDR	false discovery rate
FGF	fibroblast growth factor
FITC	fluorescein isothiocyanate

FLT3	fms related tyrosine kinase 3
FOX	forkhead box
FSC-A	forward scatter – area
FSC-H	forward scatter – height

G

G	guanine
GMP	granulocyte-macrophage progenitor

H

HCl	hydrochloric acid
HLA	human leukocyte antigen
HSC	hematopoietic stem cell

I

ICAM	Ig cellular-adhesion molecule
ICN	intracellular-Notch
ID	(mouse) identification
IFN	interferon
Ig	immunoglobulin
IGF-1	insulin-like growth factor 1
IGF-1R	insulin-like growth factor 1 receptor
IL	interleukin
IL-7R	interleukin-7 receptor
IκB	inhibitor of NF-κB

J

JAK	Janus kinase

K

KNA	keratin negative area
Krt	keratin

L

LEF1	lymphoid enhancer factor 1
LLA-T	*leucemia linfoblástica aguda de linfócitos T*
LTβR	lymphotoxin-β receptor
LTi	lymphoid tissue inducer

M

M	male
$MgCl_2$	magnesium chloride
MHC	major histocompatibility complex
MHCII	major histocompatibility complex class II
MEP	megakaryocyte-erythroid progenitor
min	minute
MLLT	mixed lineage leukemia
MPP	multipotent progenitor
mRNA	messenger RNA
MS5	MS5 murine bone marrow stromal cell line
mTEC	medullary thymic epithelial cell
$mTEC^{hi}$	mature mTEC
$mTEC^{lo}$	immature mTEC

N

nº	number
n/a	non-available
NaCl	sodium chloride
NaN3	sodium azide
NCC	neural crest cell
NF-κB	nuclear factor-κB
NH_4Cl	ammonium chloride
NK	natural killer (cell)

P

PBS	phosphate-buffered saline
PCR	polymerase chain reaction

PDGF	platelet-derived growth factor
PE	R-phycoerythrin
PECAM-1	Platelet endothelial cell adhesion molecule-1
PerCP	peridinin-chlorophyll proteins
pH	potential of hydrogen
PI3K	phosphatidylinositol 3-kinase
PICALM	phosphatidylinositol-binding clathrin assembly protein
PSGL-1	P-selectin glycoprotein ligand-1
Ptcra	pre-TCR α chain

R

RAG	Recombination activating gene
RB1	retinoblastoma 1
RBC	red blood cell
RHD	REL homology domain
RNA	ribonucleic acid
RNA-seq	whole transcriptome RNA sequencing
RT	reverse trancriptase (reaction)
RT-PCR	semi-quantitative PCR
RT-qPCR	real-time quantitative PCR
RUNX1	runt related transcription factor 1

S

S1P	sphingosine-1-phosphate
Sca-1	stem cell associated antigen-1
SHH	sonic hedgehog
SP	single-positive ($CD4^+$ or $CD8^+$)
STAT	signal transducer and activator of transcription
Supp.	Supplementary

T

T	thymidine
T-ALL	T-cell acute lymphoblastic leukemia
T-LBL	T-cell lymphoblastic lymphoma

TAL	T-cell acute lymphocytic leukemia
T_C	T cytotoxic (cell)
T_{CM}	central memory T (cell)
TCR	T-cell receptor
TE	Tris-EDTA (buffer)
TEC	thymic epithelial cell
T_{EM}	effector memory T (cell)
T_{FH}	Follicular helper T (cell)
T_H	T helper (cell)
TJ2	TEL-JAK2
TJ2-Tg	TEL-JAK2 transgenic (mouse)
TK	tyrosine kinase
TLX	T cell leukemia homeobox
TM	tamoxifen
TMAP	Torrent Mapping Alignment Program
TNF	tumor-necrosis factor
TNFSF	TNF ligand superfamily
TNFRSF	TNF receptor superfamily
T_{REG}	regulatory T (cell)
Tris	Tris (hydroxymethyl) aminomethane

U

UEA-1	*Ulex europaeus* agglutinin I

V

vs.	versus

W

WNT	wingless-int
WT	wild-type
WT1	Wilms tumor 1

Chapter 1.

Introduction

1.1. The hematopoietic system and T lymphocyte development

1.1.1. The hematopoietic system

Hematopoiesis is the process that leads to the formation of mature blood cells. Through a highly regulated differentiation process, hematopoietic stem cells (HSCs) originate all blood cell types (Figure 1.1) (Hu and Shilatifard, 2016; Owen et al., 2013).

The ontogeny of the hematopoietic system, in humans and other vertebrates (including the mouse), is characterized by two waves: a first, *primitive* wave and a second, *definitive* wave. The *primitive* wave takes place in the extraembryonic yolk sac, producing transitory hematopoietic cell populations – mainly short-lived primitive erythrocytes, macrophages and primitive megakaryocytes (Jagannathan-Bogdan and Zon, 2013; Julien et al., 2016). The primary function of this first wave is to promote tissue oxygenation during the initial rapid growth of the developing embryo (Orkin and Zon, 2008). *Definitive* hematopoiesis originates later in development and occurs at different sequential sites. The first site of settlement of the definitive HSCs is the aorta-gonad mesonephros (AGM) region, followed by the fetal liver and, before birth, the bone marrow (BM), where it is maintained throughout life (Hu and Shilatifard, 2016; Jagannathan-Bogdan and Zon, 2013; Julien et al., 2016).

HSCs, as *bona fide* stem cells, are defined by their ability to self-renew and to differentiate into multiple cell lineages (multipotency). Each stem cell division originates daughter cells that either maintain the characteristics of the mother cell or differentiate into multipotent progenitor cells that lose the self-renewal capacity and become gradually more committed to a particular blood cell lineage (Owen et al., 2013). The two main lineage commitment choices result in the generation of common myeloid-erythroid progenitors (CMP) or common lymphoid progenitors (CLP). CMPs will give rise to the megakaryocyte/erythroid lineage (all red blood cells and platelets) and other myeloid lineage cells (granulocytes, monocytes and macrophages). CLPs will originate the lymphoid lineage, consisting of T lymphocytes (T cells), B lymphocytes (B cells) and natural killer (NK) cells (Doulatov et al., 2012; Owen et al., 2013). Of note, both lymphoid and myeloid lineages can generate different subsets of dendritic cells (DC) (Moore and Anderson, 2013; Owen et al., 2013).

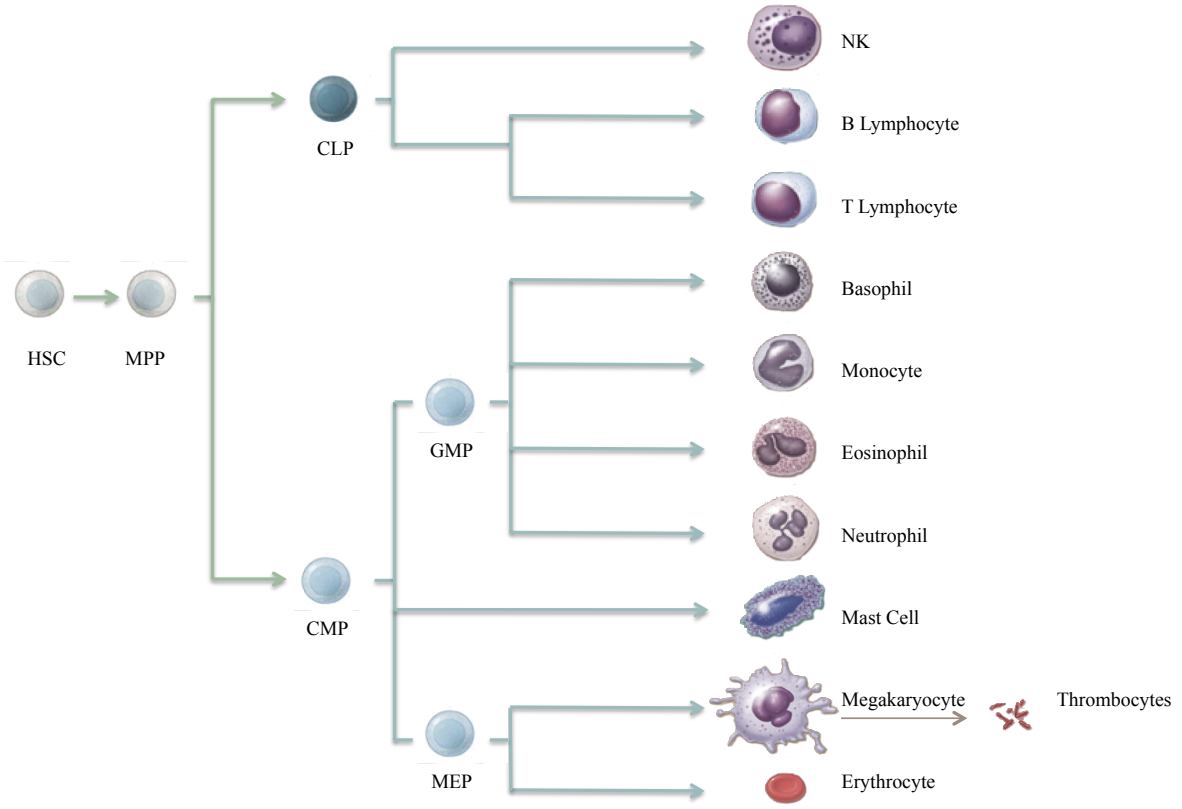

Figure 1.1. Hematopoietic system. Hematopoietic stem cells (HSC) ultimately give rise to all cells of the hematopoietic system. HSCs first start to loose self-renewal abilities, differentiating from long-term to short-term repopulating HSCs, and then into multipotent progenitor (MPP). Progressively, multipotency potencial is lost by differentiation into common lymphoid or myeloid progenitors (CLP or CMP, respectively), which will further differentiate into the different cell types of each lineage (GMP, granulocyte-macrophage progenitor; MEP, megakaryocyte-erythroid progenitor; NK, natural killer). (Adapted from Hu and Shilatifard, 2016; Orkin and Zon, 2008.)

1.1.2. Thymocyte development

T cell development occurs in the thymus, as discovered by Jacques Miller in 1961 (Miller, 1961). Pre-thymic progenitors, descendants of HSCs and originated from the fetal liver or the BM, include early lymphoid precursors (ELP, $Lin^{-}Sca\text{-}1^{+}CD117^{+}FLT3^{+}CD27^{+}IL\text{-}7R\alpha^{-/+}$), CLP ($Lin^{-}Sca\text{-}1^{lo}CD117^{lo}IL\text{-}7R\alpha^{+}$) and LSK precursors ($Lin^{-}Thy\text{-}1.1^{-}Sca\text{-}1^{+}CD117^{+}CD62L^{+}$) (Wu, 2006; Yui and Rothenberg, 2014). The T cell progenitors that seed the thymus maintain the absence of lineage marker (Lin^{-}) phenotype, meaning that they have not yet fully committed to the lymphoid or any other lineage. Recent evidence indicates that the earliest thymic-seeding progenitors retain lymphoid and myeloid potential (Luis et al., 2016). Thymic-seeding progenitors express factors associated with early progenitor cells, such as

stem cell antigen-1 (Sca-1, also known as Ly6a), CD117 (KIT, also known as c-Kit) and the growth-factor-receptor tyrosine kinase FLT3 (Figure 1.2) (Rothenberg et al., 2008; Wu, 2006; Yui and Rothenberg, 2014).

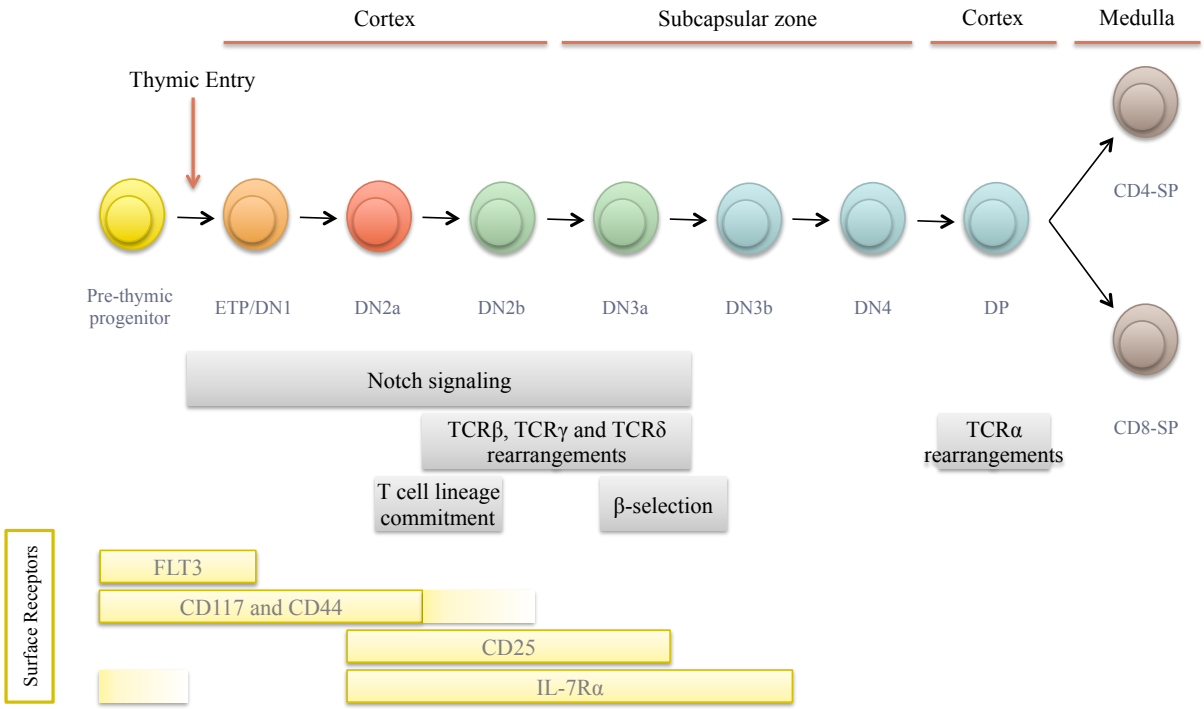

Figure 1.2. T cell development. T cell progenitors migrate from the BM through the blood stream to the thymus, where they undergo a series of differentiation steps associated with the expression of different surface molecules in different areas of the thymus. (Adapted from Koch and Radtke, 2011; Yui and Rothenberg, 2014.)

The T-cell progenitor thymic homing is not a continuous process. It proceeds in waves, as the specific thymic microenvironmental niches are liberated from the developing thymocytes. Pre-thymic progenitors circulating in the blood enter the thymus by a multistep process, essentially regulated by P-selectin and P-selectin glycoprotein ligand-1 (PSGL-1), and by CCL21 and CCL25 chemokines (see section 1.2.3.1). These activate their respective receptors, CCR7 and CCR9, in progenitors homing to the thymus (Scimone et al., 2006; Wu, 2006; Zlotoff et al., 2010).

Once in the thymus, progenitors are not yet fully T cell-committed and are often designated as early thymic progenitors (ETP). In the earliest stage of thymocyte development, thymocytes are CD4 and CD8 double-negative (DN). Murine DN thymocytes are subdivided into four stages (DN1 to DN4). DN1 thymocytes (corresponding to ETPs) populate the corticomedullary junction (CMJ) and are characterized by high levels of expression of CD117, CD44 and low levels of CD25. These cells retain potential to differentiate into

lineages other than T-cell, including NK, DCs and myeloid lineages. As DN1 cells migrate to the cortex, they undergo differentiation into DN2 stage, where they maintain expression of CD117 and CD44, also acquiring CD25 expression (Koch and Radtke, 2011).

Although the DN2 stage retains potential to originate DCs and NK cells, it marks the stage when T-cell identity genes are upregulated and RAG recombinase-mediated rearrangements of the T-cell receptor (TCR) *γ*, *δ* and *β loci* take place (Koch and Radtke, 2011; Rothenberg et al., 2008). The DN2 stage is further subdivided into two subsets: DN2a and DN2b, according to decreasing CD117 expression (Koch and Radtke, 2011). The transition from DN2b to DN3 ($CD24^{+}CD25^{+}CD44^{lo}CD117^{lo}$) stage is marked by the upregulation of the pre-TCR α chain (*Ptcra*) and *Rag1* genes. Early DN3 thymocytes (called DN3a) that successfully rearrange the TCR γ- and δ-chains are qualified for γδ T cell fate specification, while TCRβ expression elicits the β-selection checkpoint. This consists on the selective survival and proliferative expansion of αβ thymocyte precursors that form a pre-TCR complex consisting of the correctly rearranged β-chain, the pTα-chain and CD3 family chains. At this point and beyond, T-cell identity is set (Koch and Radtke, 2011; Rothenberg et al., 2008). As post-β-selection DN3 thymocytes (designated as DN3b) at the subcapsular thymic zone make their way back towards the inner cortex, they mature to DN4 thymocytes ($CD24^{+}CD25^{-}CD44^{-}CD117^{-}$). These cells go though a transitional CD8 immature single-positive stage before also upregulating CD4 to become double-positive (DP) thymocytes (Koch and Radtke, 2011; Yui and Rothenberg, 2014).

Once thymocytes reach the DP stage of development, *Rag* genes are reexpressed and the recombination of the TCRα (*Tcra*) gene locus takes place. The correct assembly of the αβ TCR complex at the cell membrane and its competence to bind to major histocompatibility complex (MHC) ligands is critical for the positive selection checkpoint (Koch and Radtke, 2011). DP thymocytes that fail to recognize or display low level of binding affinity to self-MHC/peptide complexes die by apoptosis. This process is know as death by neglect and is impelled by the lack of survival signaling to the thymocytes through their TCR molecules (Owen et al., 2013). DP thymocytes that display intermediate binding affinity to self-MHC/peptide complexes are positively selected and go on to commit to either $CD4^{+}CD8^{-}$ single-positive (CD4SP) or $CD4^{-}CD8^{+}$ single-positive (CD8SP) thymocytes, according to the ability to interact with either MHC class II or class I molecules (see section 1.1.3) (Koch and Radtke, 2011; Owen et al., 2013).

SP thymocytes migrate into the thymic medulla, in a CCR7-dependent manner and are then submitted to the negative selection checkpoint. Thus, SP cells displaying TCRs with high affinity for self-antigens bound to MHC (expressed by epithelial cells or DCs) are either eliminated through apoptosis (Koch and Radtke, 2011; Owen et al., 2013) or differentiate into the regulatory T-cell lineage (Klein et al., 2014; Malchow et al., 2013). Thymocytes that withstand negative selection undergo further maturation. Upregulation of sphingosine-1-phosphate (S1P) expression by SP thymocytes allows their egress from the thymus, as naïve mature T-cells (Cyster and Schwab, 2012; Matloubian et al., 2004).

1.1.3. T lymphocytes: main subtypes and functions

T lymphocytes are a key component of adaptive immunity, which is characterized by the interaction of variable cell-surface TCRs with MHC/antigen complexes. MHC molecules are classified into two classes: class I molecules – expressed by nearly all nucleated cells of the body – and class II – predominantly expressed by antigen-presenting cells (Owen et al., 2013). As fully matured T cells exit the thymus, they are designated as naïve. Their activation occurs when presented to antigenic peptides bound to MHC molecules. Upon activation, T cells become effector T cells, which can be grouped into two main subtypes: T helper (T_H) cells and T cytotoxic (T_C) cells. Essentially, T_H cells are $CD4^+$, restricted to recognize antigen bound to MHC class II molecules and orchestrate adaptive immune responses through cytokine secretion, while T_C cells are $CD8^+$, restricted to recognize antigen bound to MHC class I molecules and display cytotoxic action (Owen et al., 2013).

Effector $CD4^+$ helper T cells can be further subdivided into different subsets, according to their cytokine profiles and specific functions. Two types were first identified: T_H1 and T_H2. T_H1 cells are characterized by the production of interferon-gamma (IFN-γ), interleukin (IL)-2 and tumor-necrosis factor alpha (TNFα), and have a key role in cell-mediated immune responses. T_H2 are characterized for the secretion of several interleukin molecules (IL-4, IL-5, IL-13, IL-9 and IL-10) and have a key role in humoral-mediated immunity (Bromley et al., 2008; Raphael et al., 2015). More recently, other subsets of $CD4^+$ T cells have been reported. Follicular helper T (T_{FH}) cells are closely related to T_H2 cells, and are characterized by the secretion of IL-6 and IL-21 (Golubovskaya and Wu, 2016; Owen et al., 2013). T_H17 cells

express the transcription factor RORγt, secrete IL-17 and are involved in auto-immune processes of inflammation and tissue damage (Bromley et al., 2008; Raphael et al., 2015). Also identified, but with exact mechanisms of actions still to be further studied, are the T_H22 cells (characterized by the secretion of IL-22) and the T_H9 cells (characterized by IL-9 secretion) (Raphael et al., 2015).

Regulatory T (T_{REG}, $CD25^+FOXP3^+$) cells have an important role in T cell homeostasis. The main site of development of T_{REG} cells is the thymus – like for other T cells – however, they can also differentiate in the periphery. Of note, although T_{REGs} are commonly classified as $CD4^+$, in the human thymus a subset of $CD8^+$ single positive cells has been identified displaying T_{REG} characteristics (Caramalho et al., 2015).

In the cell-mediated immune response, effector $CD8^+$ cytotoxic T cells are key in the process of eliminating intracellular pathogens (e.g. viruses) and tumor cells (Owen et al., 2013; Tscharke et al., 2015). Similarly to the T_H subtypes, $CD8^+$ cytotoxic T cells can be classified into two subtypes: T_C1 and T_C2. Likewise, this classification is based on the secreted cytokine profile and cytokines that regulate their development (Owen et al., 2013).

Most effector T cells undergo apoptosis after pathogen clearance. The remaining cells persisting in the body become antigen-specific memory T cells, able to develop secondary immune responses to the same pathogen/antigen. Memory T cells can be further classified as central memory (T_{CM}) or effector memory (T_{EM}) T cells according to different criteria, including location, expression of surface markers and function (Owen et al., 2013).

Also of reference are the NKT cells, a type of cytolytic lymphocyte that shares the characteristics of NK and T_C cells. NKT cells also develop in the thymus and express a TCR complex (which in humans is invariant) although it is not able to recognize MHC-bound peptides. These cells can act both as helper and cytotoxic cells, do not originate memory cells and their exact role in the immune system is yet to be fully defined (Owen et al., 2013).

Lineage commitment of T cells to the TCRγδ lineage in detriment of the TCRαβ lineage fate is still under discussion (Zarin et al., 2015). In the mouse thymus, the branching of the two lineages occurs at the DN3 stage of development (see 1.1.2). During fetal development, TCRγδ T cells are the first to emerge but after birth their production declines (Owen et al., 2013). Despite this decline, TCRγδ T cells remain relevant for tissue homeostasis and of immunity, specifically as components of the innate immunity branch (Zarin et al., 2015).

1.2. The thymus: the T cell cradle

1.2.1. Early organogenesis and thymic epithelium generation

Located in the thoracic cavity, just above the heart, the thymus is the main site of differentiation for developing T cells. It is composed of two lobes, each one surrounded by a connective tissue capsule and, in some mammalian species (e.g. humans and rats), organized in compartments or lobules (Marchevsky and Wick, 2014; Pearse, 2006). In mice, a second single-lobed thymus has been revealed near the cervical vertebrae with similar thymic structure and thymocyte phenotype when compared to the thoracic thymus (Terszowski et al., 2006).

Early embryonic development of the thymus is closely tied to that of the parathyroid glands, as they both derive from the endodermal gut tube, more specifically the third pharyngeal pouch (Gordon and Manley, 2011). Several transcription factors are thought to have a role in the early stages of murine pouch formation, such as the Hox-Eya-Pax-Six network and the sonic hedgehog (Shh), bone morphogenic protein (Bmp), wingless-int (Wnt), fibroblast growth factor (Fgf) signaling pathways, as well as signals from surrounding neural crest cells (NCCS) (Gordon and Manley, 2011).

As early as embryonic day (E-)11, the FoxN1 transcription factor becomes expressed in the murine thymic rudiment. Thymic organogenesis involves an initial *Foxn1*-independent phase, with the generation of the thymic primordium, and a subsequent *Foxn1*-dependent phase, when TEC progenitor differentiation and homing of lymphocyte progenitors takes place (Blackburn and Manley, 2004). Although it is early expressed in the thymic rudiment, FoxN1 is not required for the initial organogenesis, but critical for thymic-specific differentiation (Blackburn and Manley, 2004; Gordon and Manley, 2011). In mice, immigration of lymphoid precursor cells begins by E11.5, occurring at specific developmental stages and in successive discrete waves (Gordon and Manley, 2011).

The thymic primordium contains a population of *Foxn1*-expressing bipotent thymic epithelial progenitor cells that ultimately originate the epithelial cells composing the cortical and medullary compartment (Bleul et al., 2006; Hamazaki, 2015; Rossi et al., 2006). At E12, this progenitor cell population expresses the epithelial markers EpCAM, keratin-5 and -8 (Krt5

and Krt8, respectively) and the MTS24 surface marker, reported to define a subpopulation of early thymic epithelial progenitors (Rossi et al., 2006; Rossi et al., 2007a). Additionally, specific progenitors for medullary and cortical thymic epithelial cells (mTEC and cTEC, respectively) have also been identified (Hamazaki, 2015). The kinship between these bipotent and lineage-specific thymic epithelial progenitors is yet to be fully understood. Two models have been proposed to explain thymic epithelial cell (TEC) development (Alves et al., 2014). The *synchronous* model postulates that uncommitted bipotent progenitors simultaneously diverge into lineage-specific cortical and medullary TEC progenitors. The *serial progression* model refers to a transitional TEC progenitor, with characteristics associated with cTECs, which *asymmetrically* can generate both TEC lineages, being the cortical the default one. Alternatively, the (still to be identified) transitional TEC progenitor *symmetrically* displays both cTEC and mTEC characteristics, before committing to cTEC or mTEC fate (Alves et al., 2014).

1.2.2. Thymic microenvironment cellular components

The thymic microenvironment is essential for and where thymocyte differentiation takes place. It is constituted by a complex network of different cell types (Table 1.1), often designated as stromal cells, which include epithelial cells, reticular fibroblasts, macrophages, dendritic and endothelial cells (Boyd et al., 1993).

Together with mTECs, DCs have a major role in negative selection (Ladi et al., 2008; Lopes et al., 2015). In general, DCs are considered professional antigen-presenting cells with the ability to activate naïve T cells and trigger immune responses (Moore and Anderson, 2013). Based on the expression of cell surface markers, different subsets of DCs have been identified. They can also have distinct developmental origin, transcriptional regulation, pattern of migration and localization (Moore and Anderson, 2013). Three DC subsets constitute the thymic DCs: the $CD8^+$ and $CD8^-$ conventional DCs (characterized as $CD11c^{hi}CD11b^-CD8\alpha^{hi}Sirp\alpha^-$ and $CD11c^{hi}CD11b^+CD8\alpha^{lo}Sirp\alpha^+$, respectively) and plasmacytoid DCs (characterized as $CD11c^{int}B220^+PDCA\text{-}1^+$) (Lopes et al., 2015; Moore and Anderson, 2013). Within the thymus, they are mainly present in the medulla although also detected in the cortex (Kurobe et al., 2006; Ladi et al., 2008).

Table 1.1. Phenotypes of thymic stromal cells. (Adapted from Gray et al., 2002; Gray et al., 2007.)

Thymic stromal cell subset	Phenotype
Dendritic cells	$CD45^{+}$, $CD11c^{hi}$, $MHCII^{hi}$
Myeloid-derived cells	$CD45^{+}$, $CD11b^{+}$, $CD11c^{-/lo}$, $MHCII^{-/+}$
Epithelial cells	$CD45^{-}$, $EpCAM^{+}$, $MHCII^{+}$
Fibroblasts	$CD45^{-}$, $MTS15^{+}$, $Ly51^{+}$, $CD31^{-/lo}$, $EpCAM^{-}$, $MHCII^{-}$
Endothelial cells	$CD45^{-}$, $CD31^{+}$, $EpCAM^{-}$, $MHCII^{-/lo}$, $MTS15^{-/+}$

Mesenchymal-derived fibroblasts are responsible for the establishment of the thymic extracellular matrix (ECM), a key component of the thymic microenvironment through the sequestration and presentation of soluble growth factors (Jenkinson et al., 2003; Suniara et al., 2000). Furthermore, fibroblasts were shown to be essential for thymic epithelial cell differentiation and maintenance (Itoi et al., 2007; Jenkinson et al., 2003; Sun et al., 2015).

1.2.2.1. Thymic epithelial cells

Thymic epithelial cells constitute the main component of the thymic stroma with a prominent role in both thymic organogenesis and thymocyte differentiation. TECs can be subdivided into two main groups, based on their location in the thymus, distinct functions, phenotype (Table 1.2) and morphology (Alves et al., 2009a).

The most commonly used molecular markers to distinguish between TEC populations are the cytokeratins. Cortical TEC are characterized by positive expression of Krt8 and Krt18, while medullary TEC express Krt5 and Krt14 (Sun et al., 2014). Immunostaining of murine thymic sections has shown that Krt8 expression is also detected in the medulla, although at a lower level than in cortical regions (Alexandropoulos and Danzl, 2012).

Through expression of specific molecular cues, cTECs are closely involved in commitment, expansion, development and homing of T cell progenitors and in positive selection of DP thymocytes. Cortical TECs are regularly defined or identified by expression of the protein markers Krt8, Ly51 (also named BP-1), CD205 (also named Ly75, or DEC205) and MHC class II (Alves et al., 2009a; Anderson and Takahama, 2012). The expression of thymus-

specific proteasome protein β5t subunit (encoded by *Psmb11*) has been exclusively attributed to cTECs in the mouse thymus (Murata et al., 2007). Additionally, β5t underlies the role of cTECs in the presentation of MHC class I-bound peptides and consequential influence in the development of $CD8^+$ T cells (Nitta et al., 2010).

Table 1.2. Main phenotypical differences between cortical and medullary TECs. Cardinal molecular markers detected (+) in cTECs and mTECs. (Adapted from Shakib et al., 2009; Sun et al., 2014.)

	cTECs	mTECs
CD45	-	-
EpCAM	+	+
MHCII	+	+
CD40	+	+
Ly51	+	-
CD80	-	+
UEA-1	-	+
Keratins	Krt8, Krt18	Krt5, Krt14

Medullary TECs are usually associated with the markers Krt5, the *Ulex europaeus* agglutinin I (UEA-1) lectin, CD80 and the autoimmune regulator Aire protein (Anderson and Takahama, 2012). Murine mTECs can be classified according to their maturation level. Immature mTECs ($mTEC^{lo}$) display low levels of expression of MHC class II and CD80, while functionally mature mTECs ($mTEC^{hi}$) display higher levels of those proteins. The mature mTEC stage of development is also accompanied by the ability to express Aire (Alves et al., 2009a). A post-Aire stage has been identified, where part of the $Aire^+$ $mTEC^{hi}$ population downregulate Aire and reduce MHC class II and CD80 expression levels, but maintain the high levels of involucrin, a suggested marker for the last stages of mTEC development (Lopes et al., 2015; Metzger et al., 2013). Aire is a transcriptional regulator with a crucial role in the expression of tissue-restricted self-antigens, together with the less studied Fezf2 transcription factor (Lopes et al., 2015; Takaba et al., 2015). Through the genome-wide expression of multiple tissue-restricted self-antigens (Aire-dependent or Aire-independent), mTECs are involved in the process of negative selection (Alves et al., 2009a; Takahama, 2006). Globally, the medullary compartment is crucial for the establishment of central tolerance through negative selection and generation of T_{REG} cells. These mechanisms are

maintained by mTECs working together with DCs, where DCs play a more critical part in T_{REG} development (Leventhal et al., 2016; Lopes et al., 2015; Perry et al., 2014).

1.2.2.2. FoxN1, a master regulator for thymic epithelial differentiation

The FoxN1 transcription factor belongs to the large forkhead box (FOX) family, which is composed by functionally diverse transcription factors sharing a homologous winged-helix DNA-binding domain and associated with an equally diverse range of cellular processes (Coffer and Burgering, 2004). Since the *Foxn1* gene is expressed in epithelial cells of both thymus and skin, its loss causes the *nude* phenotype in mice, rats and human, consisting of hairlessness and congenital athymia. The spontaneously originated *nude* mutation is autosomal, recessive and caused by a single nucleotide deletion in the *Foxn1* gene coding sequence, resulting in a frameshift leading to an aberrant protein lacking the DNA-binding domain (Coffer and Burgering, 2004). Other than the *Foxn1*$^{nu/nu}$ mice, different genetically modified mouse models (with loss- or gain-of-function) have been used to study the functions of this transcription factor in the thymus (Table 1.3).

As previously mentioned (section 1.2.1), *Foxn1* is essential for the development of a mature thymus. The athymic phenotype present in homozygous *nude* mice results from the absence of all main types of TECs (Coffer and Burgering, 2004). Furthermore, downregulation of *Foxn1* in mice causes a progressive loss of functional TECs (Chen et al., 2009). In the postnatal thymus, all TECs are *Foxn1* dosage-sensitive, however mTECs seem to be particularly more affected by changes in *Foxn1* expression (Chen et al., 2009; Cheng et al., 2010). It was also found that loss of *Foxn1* expression is one of the key factors that contribute to age-related thymic involution, since this involution is accompanied by downregulation of *Foxn1* expression in cTECs (O'Neill et al., 2016) and enforced FoxN1 TEC expression led to thymic regeneration (Bredenkamp et al., 2014).

Besides the critical role in epithelial cells (and consequentially in thymocytes), *Foxn1* has also been reported to be required indirectly for proper thymic mesenchymal development and consequent vascularization of the thymus (Mori et al., 2010; Nowell et al., 2011). In sum, FoxN1 activity not only is crucial for epithelial differentiation but also for the development and function of other thymic cell types.

Table 1.3. Genetically modified *Foxn1* mouse models.

	Feature	Phenotype	TECs	Thymocytes	Observations	Reference
Loss-of-function						
***Foxn1*$^{\Delta/\Delta}$**	Most of the N-terminal domain of the protein is deleted	Thymus-specific phenotype, with milder defects than the null (*Foxn1*$^{nu/nu}$); absence of cortical and medullary regions	Differentiation is halted	ETPs enter the thymus but fails to develop, severe hypocellularity and apparent loss of CD25^{+} immature thymocytes	Hypomorphic mutant	(Su et al., 2003)
***Foxn1*^{LacZ}**	Insertion of an IRES-lacZ cassette into the 3' untranslated region, generating a bicistronic message	Thymic compartment degeneration, CMJ disorganization	Loss of specific TEC subsets (MHCII^{hi} and UEA-1^{hi})	Reduced T-cell population	After ~1 week after birth, there is a reduction in *Foxn1* expression, effects are dose-dependent	(Chen et al., 2009)
***Foxn1*^{fx}(fx)**	Generated by a gene-targeting strategy, using Cre-*loxP* and Flp-*FRT* recombinase systems	Acute thymic atrophy (with the K5-CreER^{T} transgene)	Significant reduction of mTEC population	Presence of all mature thymocyte populations, with lower percentage of DP population (compared to WT)	By crossbreeding with mice carrying tamoxifen (TM)-inducible ubiquitous Cre-recombinase, *Foxn1* deletion is obtained	(Cheng et al., 2010)
***Foxn1*$^{R/R}$**	Revertible hypomorphic *Foxn1* allele by crossing *Foxn1*$^{R/+}$ mice with ZP2^{Cre} deletor strain	Severe hypoplastic thymi (instead of the expected complete thymic aplasia), with clear cortical and medullary regions	Normal mTEC and cTEC morphology, but with impaired TEC functionality	Impaired commitment of ETPs to the T cell lineage, increased DP and reduced CD4SP and CD8SP thymocyte populations (compared to WT)	Expresses low levels of *Foxn1* mRNA and protein	(Nowell et al., 2011)

(cont.)

Table 1.3. Genetically modified *Foxn1* mouse models. (Continuation.)

	Feature	Phenotype	TECs	Thymocytes	Observations	Reference
Gain-of-function						
***Foxn1*Tg**	*Foxn1* overexpression driven by the human keratin14 promoter	Attenuated thymic involution and intact thymic architecture in aged *Foxn1*Tg mice	High numbers of $EpCAM^{+}$ cells in aged *Foxn1*Tg mice	High levels of ETPs in aged *Foxn1*Tg mice	Increased endogenous *Foxn1* overexpression	(Zook et al., 2011)
R26*Foxn1*ER	Conditional, TM-inducible overexpression of *Foxn1*	Increase of thymic size	Increase in numbers of $EpCAM^{+}$ TECs, $MHCII^{hi}$ TECs, UEA-1^{hi} and $AIRE^{+}$ mTECs	Increase in total thymocyte numbers (by more than 2.5-fold)	Upon *Foxn1* promoter-driven Cre expression, a $FOXN1ER^{T2}$ fusion protein is produced	(Bredenkamp et al., 2014)
Reporters of expression						
***Foxn1*$^{G/+}$**	Generation of a revertible functionally null allele by insertion of a cassette containing *eGFP* cDNA.	Age-related thymic involution (both in weight and cellularity) was equivalent to wild-type mice	n/a	n/a	Activation of the *Foxn1* promoter is reported by GFP expression in *Foxn1*$^{G/+}$ mice	(O'Neill et al., 2016)
***Foxn1*$^{wt*/wt*}$**	*Foxn1*$^{nu/nu}$ mice transgenic for a bacterial artificial chromosome (BAC) encoding FoxN1 tagged with a Flag-octapeptide	Similar to WT mice, with ordered stromal architecture and normal FoxN1 expression	Cellularity mildly reduced in mice 4 weeks or older	Similar to WT mice, except for CD4SP and CD8SP which were mildly reduced	FoxN1-Flag protein is expressed under normal control of *Foxn1* regulatory elements and allows immunoprecipitation	(Zuklys et al., 2016)

n/a: non-available.

1.2.3. Molecular signals in the thymic microenvironment

The morphological structure of the thymus originates different microenvironmental niches composed of different thymic stromal cell populations. The complex three-dimensional structure of the thymus and how the different stromal cell populations are organized grant the adequate thymic microenvironment for the correct sequential steps of thymocyte development (Gordon and Manley, 2011; Takahama, 2006). Reciprocal signaling between developing thymocytes and thymic stromal cells provide the necessary cues for thymocytes to orderly migrate through the different microenvironmental niches associated with specific maturation steps (Figure 1.3). This bidirectional exchange of signals between thymocytes and stromal cells is known as *thymic crosstalk* and is crucial not only for thymocyte development but also thymic stromal cell differentiation and maintenance. Thymic crosstalk signals consist of a large variety of molecules, among which are cell-adhesion molecules, chemokines and TNF superfamily receptors and ligands (Gordon and Manley, 2011; Petrie and Zuniga-Pflucker, 2007; Takahama, 2006).

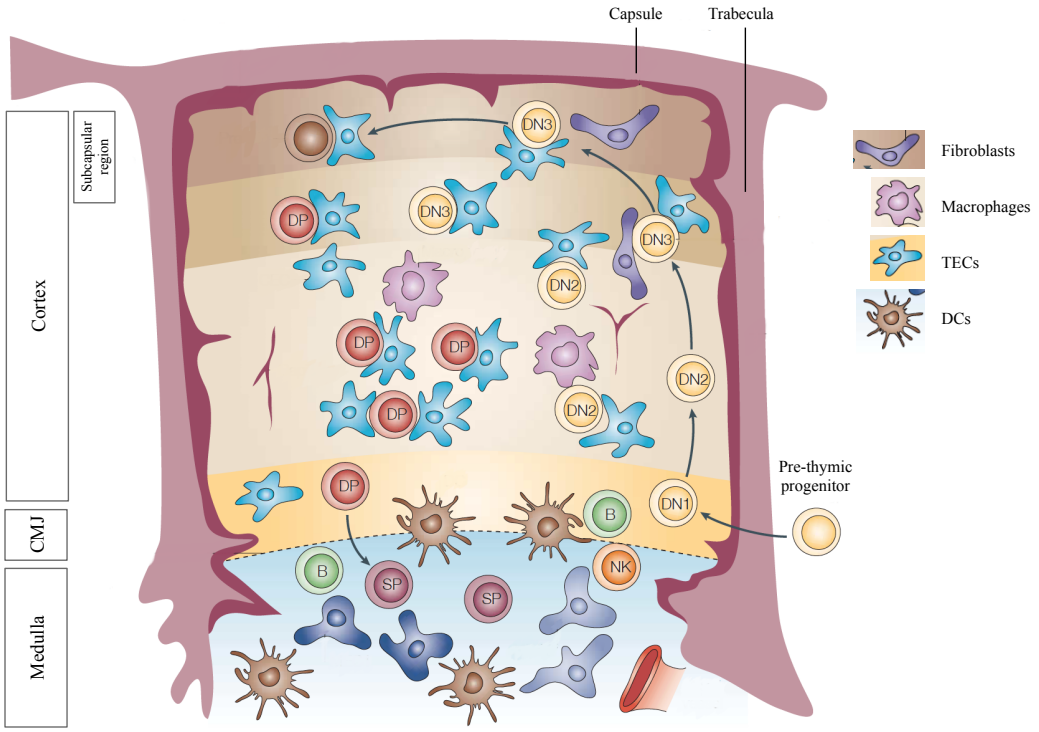

Figure 1.3. Thymic stromal cells and thymocyte migration. Upon entry in the corticomedullary junction (CMJ) region of the thymus, T-cell precursors follow a specific pattern of migration. Interaction with different stromal cells and microenvironmental niches favor the correct sequential differentiation steps towards the production of mature T cells. (Adapted from Blackburn and Manley, 2004.)

1.2.3.1. Cell-adhesion molecules and chemokines in T-cell precursor homing and maturation

Cell-adhesion molecules (CAMs) are essential for cell-cell interactions. These proteins include four major receptor/ligand families: selectin, mucin-like, the integrin family and the immunoglobulin (Ig) superfamily. The Ig cellular-adhesion molecules (ICAMs) superfamily includes proteins such as ICAM-1 (CD54), VCAM-1 (CD106) and PECAM-1 (CD31). ICAMs are known to be expressed by endothelial cells and to bind several integrin molecules (Owen et al., 2013). Specific CAMs have been implicated in the seeding of thymocyte progenitors to the postnatal thymus. This process results from a signaling cascade that involves the interaction between P-selectin (expressed on blood vessels) and its main ligand (PSGL-1; expressed on homing lymphoid progenitors) and the adhesion molecules VCAM-1 and ICAM-1 (expressed on blood vessels) to the integrins α4β1 and αLβ2, respectively (expressed on homing lymphoid progenitors) (Scimone et al., 2006).

Chemokines are also involved in the early steps of fetal thymus colonization by T cell precursors, through the action of the CCL21/CCR7, CCL25/CCR9 and CXCL12/CXCR4 chemokine ligand/receptor pairs (Calderon and Boehm, 2011; Nitta and Suzuki, 2016; Takahama, 2006). While several of these chemokines continue to be part of the crosstalk signals necessary at different steps of the thymocyte development, their role in the seeding of the postnatal thymus is less dominant than in embryogenesis (Bunting et al., 2011).

Chemokines are chemotactic cytokines, small peptides, involved in different processes such as migration, activation and proliferation of different cell types. Chemokine signaling is able to induce the transcription of target genes that are involved in these processes through signaling pathway activation, including the PI3K (phosphatidylinositol 3-kinase) and nuclear factor (NF)-κB pathways (Balkwill, 2004; Richmond, 2002). The best studied chemokine receptors contributing to different steps of thymocyte development are CCR7, CCR9 and CXCR4 (Bunting et al., 2011). Chemokine gradients allow the migration of cells towards sites of higher chemokine concentration. The dynamic change of expression of chemokine receptors in the developing thymocytes orchestrates their correct stepwise migration through the thymus, following the chemokine gradient generated by stromal cells (Table 1.4) (Balkwill, 2004; Bunting et al., 2011).

The cTEC-expressed CCL25 and CXCL12 chemokines and VCAM-1 are involved in the outward migration of DN thymocytes (expressing respectively the CCR9 and CXCR4

chemokine receptors and the receptor integrins α4β1 and α4β7) from the CMJ region to the subcapsular zone (Nitta and Suzuki, 2016). The chemokine signaling pair CXCL12/CXCR4 is also involved in β-selection thymocyte survival (Trampont et al., 2010). The CCL19 and CCL21 chemokines, produced by mTECs and medullary fibroblasts, engage the migration of CCR7-expressing SP thymocytes to the medulla and subsequent submission to the negative selection checkpoint (Forster et al., 2008; Nitta and Suzuki, 2016).

Table 1.4. Chemokine expression in the adult thymus. (Adapted from Bunting et al., 2011.)

Chemokine	Cellular source
CCL19	CMJ, medulla, low in cortex/high in mTEC^{lo}, mTEC^{hi}, fibroblasts, endothelium, low in cTECs, high mTEC CD80^{hi}, moderate in mTEC CD80^{lo}, low in cTEC
CCL21	CMJ, medulla, low in cortex/high in fibroblasts, endothelium, moderate in mTEC^{lo}, cTEC, high in mTEC CD80^{lo}, low in mTEC CD80^{hi}
CCL25	Cortex, low in medulla/DCs, high in cTEC, fibroblasts, endothelium, moderate in mTEC^{hi}, low in mTEC^{lo}, high in mTEC CD80^{hi}, moderate in mTEC CD80^{lo}, low in cTEC
CXCL12	CMJ, cortex, subcapsular zone, medulla/high in cTEC, mTEC^{lo} and fibroblasts, moderate in endothelium

1.2.3.2. NF-κB activation is essential for thymic stromal cell differentiation

In the thymus, signals activating the NF-κB pathways are critical for thymic medulla and thymocyte development (Nitta and Suzuki, 2016; Takahama, 2006; Webb et al., 2016). The mammalian NF-κB family is composed of five related transcription factors: p50 (NF-κB1), p52 (NF-κB2), p65 (RELA), REL (also known as cREL) and RELB. All five members share the REL homology domain (RHD). RELA and RELB contain transactivation domains, while NF-κB1 and NF-κB2 are longer isoforms that are processed into the active-DNA-binding forms (p105 and p100 into p50 and p52, respectively). In their inactive state, NF-κB subunit homo- or heterodimers are bound to inhibitor of NF-κB (IκB) proteins, retaining them in the

cytoplasm. Phosphorylation of IκBs by an IκB kinase (IKK), leads to their ubiquitylation and proteasomal degradation, releasing NF-κB to translocate to the nucleus and activate gene target expression (Ghosh and Hayden, 2008; Perkins, 2012).

NF-κB signaling can follow two pathways: canonical or alternative. The canonical pathway is usually triggered by exposure to proinflammatory cytokines, by TCR or B-cell receptor stimulation or in response to microbial and viral infections. This pathway activates NF-κB dimers composed of cREL, RELA and p50. The alternative, non-canonical, pathway is mainly activated through members of the TNFR superfamily, which activate the IKKα subunit of IKK, as well as the protein kinase NIK. Through degradation of the inhibitory p100 isoform, this pathway activates mainly p52, which preferentially dimerizes with RELB (Ghosh and Hayden, 2008; Karin et al., 2002). Both pathways are thought to be involved in the development of mTECs expressing Aire and tissue-restricted self-antigens (Akiyama et al., 2008).

1.2.3.3. Members of the TNF ligand and receptor superfamilies in mTEC development

The TNF ligand and receptor superfamilies (TNFSF and TNFRSF, respectively) are involved in several biological mechanisms, such as regulation of innate and adaptive immunity, induction of apoptosis and regulation of bone homeostasis (Eissner et al., 2004).

Within the thymus, the TNFRSF members RANK, CD40 and LTβR are expressed in mTECs and activate the NF-κB pathways, upon ligation of the corresponding ligands (Nitta and Suzuki, 2016; Sun et al., 2014; Webb et al., 2016).

The RANK/RANKL signaling controls the emergence of $Aire^+$ mTECs in the embryonic thymus. RANKL is expressed by cells of the innate system, $CD4^+CD3^-$ lymphoid tissue inducer (LTi) cells and invariant $V\gamma5^+$ dendritic epidermal T cell progenitors (Desanti et al., 2012; Rossi et al., 2007b), and by positively selected thymocytes and TCR-stimulated DP thymocytes (Hikosaka et al., 2008). At the embryonic stage, RANK/RANKL signaling has a major role in the initial steps of thymic medulla development and consequent importance in the regulation of central tolerance. In the postnatal thymus, signaling involving RANK and CD40 maintain both singular and overlapping functions in the development of mature $Aire^+$

mTECs (Akiyama et al., 2012; Lopes et al., 2015). Irla and colleagues (2008) described the formation of a functional medulla as a two different processes. First, the medulla formation relies on positively selected thymocytes, regardless of their commitment to the $CD4^+$ or $CD8^+$ lineage. Second, the expansion of mature mTECs is highly dependent on $CD4^+$ thymocytes, which upregulate both RANKL and CD40L (Irla et al., 2008).

Signaling involving LTβR and its two known ligands, LTα1β2 heterotrimers and LIGHT homotrimers (Fernandes et al., 2016), in the mTEC differentiation is yet to be fully understood. Thus far, it is known to participate in supporting the three-dimensional structure of the thymus, to regulate expression of several Aire-independent tissue-restricted self-antigens in mTECs and of chemokines important in the process of thymocyte migration to medullary regions (Boehm et al., 2003; Lopes et al., 2015; Seach et al., 2008). LTβR has more recently been shown to contribute to RANK signaling in the differentiation of mTECs (Mouri et al., 2011).

1.2.3.4. Notch activation is essential for T-cell differentiation

The Notch signaling pathway is an evolutionary conserved mechanism involved in the regulation of cell fate determination and differentiation processes during embryonic development and organogenesis. In mammals, the transmembrane Notch receptor family has four members (Notch1–Notch4) that can be activated by five ligands (Jagged1 and -2 and Delta1, -3 and -4) (Radtke et al., 2004; Weerkamp et al., 2006). Notch signaling is initiated through the interaction of the extracellular domain of the Notch receptor with a membrane-bound ligand, leading to proteolytic cleavage of the receptor and consequent release of the intracellular part of Notch (ICN). This fragment then translocates to the nucleus and binds to the transcription factor CSL (also designated RBP-Jκ). Heterodimerization of ICN-CSL acts as a transcriptional activator, inducing the transcription of Notch-specific target genes (Radtke et al., 2004; Weerkamp et al., 2006).

Notch signaling is involved in T-cell fate determination with Notch ligands – mainly Delta4 (Dll4) – being expressed by thymic stromal cells (mainly cTECs) and the receptors expressed at the surface of hematopoietic progenitor cells and DN thymocytes. As demonstrated by genetic inactivation in mice, *Notch1* is required for the T-cell commitment of thymic

progenitors and further steps of thymocyte differentiation (from DN1 through to DP) including survival of post-β-selected thymocytes (Koch and Radtke, 2011; Weerkamp et al., 2006).

1.3. T-cell acute lymphoblastic leukemia

1.3.1. Definition and classification

Acute lymphoblastic leukemia (ALL) is the most common type of childhood cancer (Cooper and Brown, 2015; Hunger and Mullighan, 2015). Childhood ALL cases are more frequent in male than female infants, with a peak of incidence between the ages of 2 and 5 years (Pui, 2006).

The T-cell subtype of acute lymphoblastic leukemia, T-ALL, is a neoplastic disorder of immature T-cell precursors and represents approximately 15% of all childhood ALL cases (You et al., 2015). It is an aggressive malignancy that results in diffuse infiltration of the BM by immature T cell lymphoblasts, high white cell counts, mediastinal masses with pleural effusions, and frequent infiltrations of the central nervous system (CNS) (Van Vlierberghe and Ferrando, 2012). T-ALL is closely related, regarding genetic alterations and transcriptomic profiling, to T-cell lymphoblastic lymphomas (T-LBL) (Basso et al., 2011; Burkhardt, 2010). In some studies, T-ALL and T-LBL are considered as being different manifestations of the same disease (Karrman and Johansson, 2017). By definition, T-ALL involves the BM in the disease, containing at least 20-25% of blast cells while T-LBL refers to cases where the neoplastic disorder is confined to a mass lesion with minimal or no involvement of blood or BM (Chiaretti et al., 2014; Mullighan, 2010).

Significant advances in treatment have been made and several options are now available, leading to approximate survival rates of 70% for 5-year event-free and 80% of overall survival for pediatric T-ALL (Karrman and Johansson, 2017). Yet, close to 20% of patients

will relapse, remaining with a lower cure rate (Cooper and Brown, 2015; Karrman and Johansson, 2017).

T-ALL is a heterogeneous disease regarding immunophenotype, cytogenetics, molecular genetic abnormalities and or/ clinical features (Graux et al., 2006). The European Group for the Immunological Characterization of Leukemias (EGIL) has proposed a four-group classification of T-ALL subtypes, according to the expression of cytoplasmic CD3 and other T-cell lineage markers (Table 1.5) (Bene et al., 1995). An additional subgroup, early T-cell precursor (ETP)-ALL has more recently been identified. In parallel with normal ETPs, ETP-ALL is characterized by absence of CD1a and CD8, weak expression of CD5 and expression of one or more myeloid or stem cell-associated markers (CD117, CD34, human leukocyte antigen [HLA]-DR, CD13, CD33, CD11b, or CD65) (Coustan-Smith et al., 2009).

Table 1.5. Characterization of T-ALL. Based on the initial EGIL's immunophenotypic characterization, a more embracive characterization according to expression of CD markers. (Adapted from Bene et al., 1995; Coustan-Smith et al., 2009; Karrman and Johansson, 2017; Pui, 2006.)

Subtype	Name	Key markers (cytoplasmic $CD3^+$ with)
T-I	Pro-T-ALL	$CD7^+$ ($CD1a^-$ $CD2^-$ $CD5^-$ $CD4^-$ $CD8^-$ $CD10^-$ $CD34^{+/-}$)
T-II	Pre-T-ALL	$CD7^+$ $CD2^+$ and/or $CD5^+$ and/or $CD8^+$ ($CD1a^-$)
T-III	Cortical T-ALL	$CD7^+$ $CD1a^+$ ($CD2^+$ $CD5^-$ $CD34^-$)
T-IV	Mature T-ALL	$CD7^+$ surface $CD3^+$ surface TCRαβ or γδ ($CD1a^-$ $CD2^+$ $CD34^-$)
ETP	ETP-ALL	$CD7^+$ $CD5^{weak/-}$ HSC/myeloid markers ($CD1a^-$ $CD8^-$)

1.3.2. Cytogenetics and molecular genetic abnormalities

Conventional karyotyping techniques have been able to identify structural chromosomal aberrations in about 50% of T-ALL cases (Graux et al., 2006). Translocations involving the TCR *loci* are present in approximately 30-35% of T-ALL cases (Graux et al., 2006; Le Noir et al., 2012). During the RAG-mediated TCR *loci* V(D)J recombination events in thymocyte development, other genes become vulnerable to the action of those recombinases. Strong promoter and enhancer elements of the TCR genes may then become juxtaposed to transcription factor proto-oncogenes. This results in an aberrant expression of these genes in developing thymocytes, driving the initiation of T-ALL (Graux et al., 2006). Generation of

fusion genes results mainly from translocations, where two genes located at the chromosomal breakpoints become fused 'in frame' and encode a new chimeric protein carrying oncogenic properties (Graux et al., 2006). Cryptic deletions are also frequent and can accumulate with other alterations. These often lead to loss of tumor suppressor genes or to the activation of proto-oncogenes due to the deletion of negative regulatory elements (Karrman and Johansson, 2017).

Several oncogenic mutational steps are required to achieve the leukemic transformation of an immature thymocyte, culminating in a developmental arrest in any of nearly all stages of thymocyte development (Van Vlierberghe et al., 2008). Most cases of ALL (both T and B subtypes) are not a consequence of an existing predisposing genetic condition (a notable exception is Down syndrome in B-cell precursor ALL in patients under 5 years of age), rather resulting instead from somatically acquired genetic changes that disturb the normal development (Pui, 2006). Those alterations affect genes involved in different biological processes such as cell cycle, apoptosis, gene regulation, signaling and regulation of lymphoid differentiation (Pui et al., 2011).

Van Vlierberghe and colleagues (2008) tentatively classified genetic alterations in T-ALL into two categories, accordingly to their influence in the patients' aberrant gene expression signature. 'Type A' mutations are dominant in that role, defining T-ALL molecular subtypes (e.g., *TAL1*, *LMO1*, *LMO2*, *TLX1*, *TLX3*, and *MYB* mutations and *PICALM-MLLT10* and *SET-NUP214* fusions), while 'type B' mutations comprise other mutational events (mutations affecting e.g. *CDKN2A*, *NOTCH1*, *FBXW7*, *PTEN*, and *NF1* genes and *NUP214-ABL1* fusion) that occur across T-ALL subtypes and accumulate simultaneously with 'type A' mutations (Van Vlierberghe et al., 2008). 'Type A' mutations include genetic abnormalities that facilitate the arrest of thymocyte development at specific stages (Table 1.6) (Graux et al., 2006; Van Vlierberghe et al., 2008). 'Type B' mutations affect genes involved in different cellular processes, such as cell cycle regulation, self-renewal, TCR signaling, T-cell differentiation or tyrosine kinase (TK) activation (Van Vlierberghe et al., 2008). Two of the most common genetic alterations that occur in T-ALL cases (Table 1.7) are the 'type B' activation of the *NOTCH1* signaling pathway (present in over 60% of the cases) and inactivation of the cell cycle inhibitor *CDKN2A* and *CDKN2B* (present in 65 to 70% of T-ALL cases) (Tosello and Ferrando, 2013; Van Vlierberghe et al., 2008; Weng et al., 2004).

Table 1.6. Main protein families affected by genetic abnormalities in T-ALL. (Adapted from Pui, 2006; Van Vlierberghe and Ferrando, 2012.)

Protein family	Gene	Translocation
Basic helix-loop-helix	*MYC*	t(8;14)(q24;q11)
(bHLH)	*TAL1*	t(1;7)(p32;q35)
	TAL1	t(1;14)(p32;q11)
	TAL1	1p32 deletion
	TAL2	t(7;9)(q34;q32)
	LYL1	t(7;19)(q34;p13)
	BHLHB1	t(14;21)(q11;q22)
Homeodomain	*HOX11*	t(10;14)(q24;q11)
(Hox)	*HOX11*	t(7;10)(q35;q24)
	HOX11L2	t(5;14)(q35;q32)
	TLX1	t(11;14)(p15;q11)
	TLX3	t(11;14)(p15;q11)
	HOXA	Inv(7)(p15q34)
	HOXA	t(7;7)(p15;q34)
Cysteine-rich	*LMO1*	t(11;14)(p15;q11)
(LIM)	*LMO1*	t(7;11)(q34;p15)
	LMO2	t(7;11)(q35;p13)
	LMO2	t(11;14)(p13;q11)
	LMO2	11p13 deletion
	LMO3	t(7;12)(q34;p12)

Table 1.7. Most common genetic lesions in T-ALL. (Adapted from Belver and Ferrando, 2016.)

Gene	Genetic lesion(s)	Frequency (%)
Transcription factor oncogenes		
TAL1	1p32 deletion	25
TLX1	t(10;14)(q24;q11)	5–10 (pediatric T-ALL)
TLX1	t(7;10)(q35;q24) del(10)(q24q26)	30 (adult T-ALL)
TLX3	t(5;14)(q35;q32)	20–25 (pediatric T-ALL) and 5 (adult T-ALL)
PICALM–MLLT10	t(10;11)(p13;q14)	5-10
NOTCH1 pathway		
NOTCH1	activating mutation	>60
NOTCH1	inactivating mutation	8-30
Cell cycle		
CDKN2A and *CDKN2B*	9p21 deletion Methylation	>70
RB1	13q14.2 deletion	12 (pediatric T-ALL)
CDKN2B	12p13.2 deletion	12
Transcription factor tumor suppressors		
WT1	Inactivating mutation or deletion	10
LEF1	Inactivating mutation or deletion	10-15
ETV6	Inactivating mutation or deletion	13
BCL11B	Inactivating mutation or deletion	10
RUNX1	Inactivating mutation or deletion	10-20
Signal transduction		
PTEN	Inactivating mutation 10q23 deletion	10-15
JAK1	Activating mutation	4-18
FLT3	Activating mutation	5-10
IL7R	Activating mutation	10
DNM2	Inactivating mutation	15

Genes involved in TCR signaling are also affected by mutations in T-ALL (Table 1.8) (Van Vlierberghe et al., 2008). In normal T cell development, several TKs are involved in (pre-)TCR signaling, as well as in regulation of T-cell survival, proliferation, differentiation and T-cell immune response. Although occurring at a low frequency, genetic alterations in the TKs are of clinical interest because they can potentially be studied as objects of targeted therapy (Graux et al., 2006; Van Vlierberghe et al., 2008). TCR activation by itself was recently shown to be tumor-suppressive for T-ALL, so raising the possibility of using TCR/CD3 stimulation as a therapeutic strategy (Trinquand et al., 2016).

Table 1.8. Main genes involved in genetic alterations in the TCR signaling pathway and tyrosine kinases. (Adapted from Graux et al., 2006.)

Gene	Function
***ABL1* fusions**	ABL1 is a cytoplasmic TK, involved in TCR signaling
JAK2	TK; signaling transmission from cytokine receptors to downstream signaling
LCK	TK; T-cell-expressed
FLT3	Receptor TK; development of hematopoietic stem cells
RAS	Survival signaling from the cell membrane to the intracellular transduction pathways
PI3K* and *PTEN	PI3K is involved in TCR signaling, negatively controlled by the tumor suppressor PTEN

1.3.3. The thymic origin of T-ALL

As mentioned before, the malignant transformation of thymocytes during crucial steps of their development, along with expression of certain oncogenes, leads to the arrest of normal thymocyte development and results in T-ALL (Aifantis et al., 2008).

Several of the molecular factors involved in thymocyte development and thymic function may become altered in T-ALL (Aifantis et al., 2008). Some have already been here mentioned, such as the activating mutations of *NOTCH1*, a key regulator of T-cell fate, survival and differentiation.

Activation of signaling pathways commonly involved in cancer, particularly the PI3K/AKT, Ras/MAPK and JAK/STAT pathways can be activated by microenvironmental cell-derived ligands (Passaro et al., 2016; Steelman et al., 2008). It is well established that the cancer

microenvironment is crucial for tumorigenesis, yet much remains to be explored about the microenvironmental factors contributing to T-ALL. The molecular signals potentially exchanged by leukemic and stromal cells include a wide range of molecules, including growth factors, cytokines, chemokines and adhesion molecules (Tlsty and Coussens, 2006).

In vitro studies have shown that stromal cells support the survival of established T-ALL cell lines and patient-derived T-ALL cells (Armstrong et al., 2009; Winter et al., 2001; Winter et al., 2002). Various extrinsic factors promoting T-ALL growth *in vitro* and *in vivo* have been identified, including IL-7 (Silva et al., 2011; Touw et al., 1990), IL-18 (Uzan et al., 2014), insulin-like growth factor (IGF)-1 (Medyouf et al., 2011), DLL4 (Indraccolo et al., 2009; Minuzzo et al., 2015), ICAM-1 (Winter et al., 2001) and CXCL12 (Passaro et al., 2015; Pitt et al., 2015). The CCL19 and CCL21 chemokines, which activate the CCR7 receptor, were found to be important for T-ALL dissemination to the central nervous system (Buonamici et al., 2009; Jost et al., 2016). Moreover, CXCR4 activation by the CXCL12 chemokine and IGF-1 receptor (IGF-1R) activation were found to be important for T-ALL-initiating activity in recipient mice (Medyouf et al., 2011; Passaro et al., 2015; Pitt et al., 2015). In a recent study, IGF-1R was also found to be highly expressed by T-ALL cells and thymic tumor-associated DCs were found to secrete high levels of IGF-1, thus promoting leukemic cell survival (Triplett et al., 2016).

Together, the aforementioned reports highlight the importance of stromal cell-derived signals for leukemia maintenance and progression, but did not always provide clues to whether T-ALL development is promoted by signals from its native microenvironment. Human T-ALL has often been associated with thymic enlargement (Kersey et al., 1975; Sen and Borella, 1975) and patient T-ALL cells were shown to expand in NOD/SCID mouse fetal thymus organ culture without the addition of exogenous factors (Ma et al., 2002). Furthermore, it has long been recognized that the thymic microenvironment is essential for T-cell acute leukemia/lymphoma in mouse models (Kaplan, 1950; McEndy, 1944).

Contact with thymic microenvironmental cells in co-cultures was shown to improve survival of rodent primary leukemic T cells derived from the thymus, further indicating that stromal signals are important for leukemia maintenance (Hiai et al., 1981; Ioachim and Furth, 1964). In addition, structural and immunophenotypic studies showed that the thymic stroma undergoes profound alterations throughout the murine thymic leukemogenic process (Davey et al., 1996; Metcalf, 1966; Siegler and Rich, 1963). However, the molecular and cellular

players involved in stromal support of thymocyte leukemogenesis have only recently began to be explored.

1.3.4. T-ALL experimental models

Immortalized human T-ALL cell lines are important experimental models to understand the molecular mechanisms of this disease, especially to understand how specific genetic alterations or activated signaling pathways may promote leukemogenesis. Cell lines have also provided information on specific microenvironment requirements and have been used to investigate how they respond to certain stimuli. Despite the valuable information that can be taken from the *in vitro* studies, animal models are more appropriate to understand the behavior of leukemic cells in their native or tumorigenic environments (Ma et al., 2002).

Murine models have been a powerful source in understanding the potential initiators of leukemogenesis (Jacoby et al., 2014). Different approaches have been used, including carcinogen-induced, viral-induced, radiation-induced, transgenic, mosaic, knockout and xenograft models (Cook and Pardee, 2013). Alternative animal models exist, although still relatively little explored, such as the transgenic zebrafish expressing the human *NOTCH1-ICN* mutant (Chen et al., 2007) or the *MYC* oncogene (Langenau et al., 2003).

Given the heterogeneous range of genetic alterations and targeted genes/pathways, several mouse models have been used to study T-cell leukemia/lymphoma. Many of the transgenic or knockout mouse models developed were based on naturally occurring genetic alterations identified in human T-ALL.

The frequent *NOTCH1* activating mutations in T-ALL render this pathway one of the most investigated *in vitro* and *in vivo*. One murine model commonly used employs transplantation of lethally irradiated mice with BM progenitor cells transduced with mutant activated forms of Notch1. Several weeks after, the resulting chimeric mice develop T-ALL in the BM and blood, without thymic involvement (Allman et al., 2001; Aster et al., 2000; Pear et al., 1996). Other studies, using transgenic murine models, targeted the overexpression of T-ALL oncogenes such as *TAL1*, *TLX1*, *LMO2* and *LYL1* to the T-cell lineage (Condorelli et al., 1996; De Keersmaecker et al., 2010; Larson et al., 1996; Zhong et al., 2007). These mice develop T-ALL that models the pathogenesis of specific human molecular subgroups. For

example, *TLX1* transgenic mice developed T-ALL with similar gene expression profile as T-ALL samples classified in the TLX1/3 molecular subgroup (De Keersmaecker et al., 2010). Transgenic mice overexpressing oncogenes develop T-ALL with involvement of the thymus but leukemogenesis is somewhat delayed and often incompletely penetrant. Nevertheless, all the different models have contributed to the understanding of development and progression of T-cell leukemia (Aifantis et al., 2008).

1.3.4.1. TEL-JAK2 transgenic mouse

The present work was based on the study of a transgenic mouse model – the EμSRα-TEL-JAK2 mice – based on the expression of the TEL-JAK2 fusion protein in the lymphoid lineage. The TEL-JAK2 protein is encoded by the *ETV6-JAK2* fusion gene, which was previously identified in a T-ALL patient (Lacronique et al., 1997) and in chronic myelogenous leukemia and B-ALL patients (Peeters et al., 1997).

TEL, a member of the ETS-like family of transcription factors, is encoded by the *ETV6* gene located on chromosome 12p13 and is frequently involved as a fusion partner with several proto-oncogenes in human leukemia (Lacronique et al., 1997; Pui, 2006). JAK2 is a member of the Janus-tyrosine kinase (JAK) family, involved in the JAK/signal transducer and activator of transcription (STAT) signaling pathway, which is activated by different cytokines. The self-association of the TEL-JAK2 protein mediated by the TEL moiety prompts the tyrosine kinase activity of the JAK2 component. JAK2 constitutive kinase activity underlies the oncogenic features of the fusion protein (Carron et al., 2000; Lacronique et al., 1997).

The TEL-JAK2 transgenic (TJ2-Tg) mice were generated to express the fusion gene isolated from the original T-ALL patient (Lacronique et al., 1997). TJ2-Tg mice develop a fully penetrant fatal immature $CD8^+$ T-cell leukemia characterized by highly invasive leukemic cells with constitutive activation of STAT5. In these mice, T-cell leukemia is accompanied by lymphomas due to organ (thymic, spleen and/or lymph nodes) infiltration with TJ2-Tg leukemic cells. The expression of the TEL-JAK2 fusion protein by lymphoid cells is thought to be the primary genetic event, requiring the activation of secondary events for the induced leukemia to manifest (Carron et al., 2000). Further studies have shown that pre-TCR

signaling, but not RAG-mediated recombination facilitates leukemogenesis (dos Santos et al., 2007). Although *JAK2* fusions are rare in T-ALL, activation of the JAK-STAT pathway due to other mechanisms (e.g. *JAK1*, *JAK3* and *IL7R* mutations) is relatively frequent (Chen et al., 2012; Vainchenker and Constantinescu, 2013).

Altogether, the clinical and molecular features presented by the TJ2-Tg mice are consistent with the human counterpart of T-ALL, providing an amenable model for the study of this disease, or at least those patients that show JAK-STAT pathway activation. In relation to T-ALL mouse models expressing transcription factor proto-oncogenes (e.g. *TAL1*, *LMO1/2*, *TLX1/3*), which represent a specific molecular subgroup of T-ALL, the TJ2-Tg mice model T-ALL with JAK-STAT activation, which occurs across different molecular subgroups. Furthermore, this animal model develops spontaneous thymic leukemia/lymphoma, unlike BM transduced chimeric models expressing *NOTCH1* or other oncogenes, which renders it useful to study thymic leukemigenesis.

1.4. Aims

One important aim of our research team is to obtain a better understanding on the role of the thymic microenvironment in T-cell leukemia development.

Previous findings revealed that the expression of the RelB transcription factor in normal non-hematopoietic cells was required for rapid and aggressive T-cell leukemia development in the TEL-JAK2 transgenic mouse model of T-ALL (dos Santos et al., 2008). In addition, our group has recently shown that inactivation of a thymic stromal cell receptor protein, LTβR, delayed leukemogenesis (Fernandes et al., 2015). Based on this knowledge and on the notion that thymic stromal cell signaling is important for thymocyte development, we conceived a working model where an evolving crosstalk between leukemic and thymic stromal cells develops during TEL-JAK2-induced leukemogenesis. It is possible that during this process, transformed thymocytes express proteins (e.g. lymphotoxin) that interact with and induce thymic stromal cells to produce pro-leukemogenic factors. Having this model in mind, we

proposed to identify thymic stromal molecular and cellular alterations linked to T-cell leukemogenesis. Given the essential role of the TEC-specific FoxN1 transcription factor in the generation of a functional, thymocyte-supportive thymic microenvironment, we were also interested to analyze whether this protein was also important for thymic leukemogenesis.

As such, the goals of this thesis were twofold:

1) Identify thymic stromal cell alterations during TEL-JAK2-induced murine leukemogenesis.

2) Determine the role of *Foxn1*-dependent thymic stroma in TEL-JAK2-induced leukemogenesis.

By achieving these goals, we expected to gain further insights into how a thymocyte malignancy arises in the thymus.

Chapter 2.

Materials & methods

2.1. Mouse strains, breeding and procedures

Mice were maintained at the University of Algarve/CBMR specific pathogen-free Animal House, with 12 h light/dark cycles and food (4RF25; Mucedola, Settimo Milanese, Italy) and water *ad libitum*. Microorganism screening detected presence of opportunistic pathogens (*Helicobacter spp.*, *Pasteurella pneumotropica* and murine norovirus) in the housing room. All experimental procedures were authorized by the host institution and performed in strict accordance with recommendations from the European Commission (Directive 2010/63/UE) and Portuguese authorities (*Decreto-Lei* n°113/2013).

EμSRα-TEL-JAK2 transgenic (TJ2-Tg) mice (Carron et al., 2000), and *Foxn1*$^{+/nu}$ mice (carrying a *nude* mutant allele), obtained from *Instituto Gulbenkian de Ciência* (Oeiras, Portugal) were maintained in the C57BL/6 background. *Foxn1* mice were maintained both as a separate lineage and used to breed with TJ2-Tg mice. Cohorts of TJ2-Tg;*Foxn1*$^{+/+}$ and TJ2-Tg;*Foxn1*$^{+/nu}$ were monitored for the development of TEL-JAK2-induced leukemia (see section 2.1.1).

2.1.1. Euthanasia, necropsy and sample preparation

All mice were killed by CO_2 inhalation. TJ2-Tg mice and leukemic cell recipient mice were frequently monitored for signs of leukemia, and were killed when manifesting visible symptoms of disease and reaching pre-defined endpoints (dyspnea, perceptible loss of activity, enlargement of lymph nodes and/or abdomen). The symptoms are a consequence of expansion of leukemic cells in the thymus and/or their consequent dissemination to other organs such as bone marrow, lung and liver. Thus, at endpoint we also refer to mice as being at an advanced stage of the disease. When required for analysis, wild-type (WT) control mice and mice with other genetic backgrounds were killed, as mentioned in the presented results (see Chapter 3).

Collected organs at necropsy were maintained briefly in cold PBS, previous to organ weighing and sample preparation. Thymic sample fractioning was performed using a mechanical method, by dissociation of the thymic tissue through a cell strainer (BD Falcon) in PBS. Stromal cell-enriched fractions were retained in the strainer, while thymocyte suspensions washed through and were pelleted by centrifugation.

2.1.2. Leukemic cell transplantation

Thymic-derived leukemic cells were prepared from diseased TJ2-Tg mice, and 4 x 10^6 cells in phosphate-buffered saline (PBS) solution were intravenously injected into 6- to 9-week-old *Foxn1*$^{+/+}$ and *Foxn1*$^{+/nu}$ littermate mice.

2.1.3. Blood collection

To detect malignant thymocytes at early stages of TEL-JAK2-induced leukemia, peripheral blood from mice (8 to 16 weeks of age) was collected from the submandibular vein. The location where the facial and submandibular veins meet at the rear end of the mandibular bone was punctured with a blood lancet (Marienfeld Superior) and few drops (about 50 µl) were collected into a microtube containing 50 mM EDTA (approximately 1 volume of EDTA [Sigma-Aldrich] for 10 volumes of blood). To lyse red blood cells, samples were transferred to 15 ml conical tubes and centrifuged at 300 x*g* for 5 min at 4°C. After discarding the supernatant, the pellet was resuspended in 5 ml of red blood cell (RBC) lysis solution (1 volume of 170 mM Tris-HCl [Sigma-Aldrich] with 9 volumes of 160 mM NH_4Cl [Sigma-Aldrich]), and incubated for 5 min at room temperature. Following another centrifugation for 5 min at 4°C, the supernatant was discarded and the cell pellets were resuspended in cold PBS before proceeding for immunostaining (see section 2.5.2).

2.1.4. Mouse genotyping

DNA from mouse's tail tips was extracted by digesting with 100 µg/ml proteinase K (Fermentas) in 500 µl of lysis buffer (200 mM NaCl [BDH Prolabo], 100 mM Tris-HCl, pH 8.3, 5 mM EDTA, 1% Triton X-100 [Sigma-Aldrich]), and incubating at 55ºC overnight. After vortex mixing the suspension, proteinase K was inactivated by a 10-min incubation at 90ºC. The supernatant collected from a 15-min 13000 rpm centrifugation was transferred to a new microtube, and mixed with 500 µl of isopropanol (BDH Prolabo). To collect the precipitated DNA, the suspension was centrifuged for 10 min and the supernatant was discarded. The DNA pellet was washed with 500 µl of 70% ethanol (BDH Prolabo) and the microtube was inverted several times to mix the contents. Then, after a 5 min centrifugation,

the supernatant was discarded and the pellet was allowed to dry at room temperature. Finally, DNA was resuspended in TE buffer, pH 7.4 (10 mM Tris-HCl, pH 7.4 1 mM EDTA, pH 8) and stored at 4 ºC.

2.1.4.1. Polymerase chain reaction

Polymerase chain reaction (PCR) on the extracted DNA was performed in 25 µl volumes of the mixture containing 2 µl of suspended DNA, GoTaq Flexi Buffer 1x, 1.5 mM $MgCl_2$, 0.2 mM PCR nucleotide mix, primers (Table 2.1), 0.5 U GoTaq DNA polymerase (Promega) and sterilized deionized MilliQ water (Millipore). PCR amplification was performed on a C1000 Thermal Cycler (Bio-Rad), under the following conditions: initial denaturation at 95ºC for 5 min; 30 to 35 cycles of denaturation at 95ºC for 45 seconds; annealing at the indicated temperature (Tm) (Table 2.1) for 45 seconds; extension at 72ºC for 1 min; a final extension step at 72ºC for 10 min was also performed. PCR products (digested or not, accordingly; see 2.1.4.2) were analyzed by electrophoresis in a Greensafe Premium (NZYTech)-stained 3% or 2% agarose (Lonza) gel (for *Foxn1* or *TEL-JAK2*, respectively) prepared in TAE buffer (40 mM Tris base [Sigma-Aldrich], 20 mM glacial acetic acid [BDH Prolabo], 1 mM EDTA) and visualized under UV light (Gene Flash, Syngene BioImaging).

2.1.4.2. Restriction enzymatic digestion

In order to be able to identify the WT from the *nude* allele, genotyping of *Foxn1* mice (performed according to Hirasawa et al., 1998) required an additional enzymatic digestion, before electrophoretic visualization of the DNA bands (Table 2.2). Restriction enzyme digestion of the PCR products was performed with BseDI (Thermo Fisher Scientific), according to the manufacturer's protocol, overnight at 55ºC.

Table 2.1. Primers used for mouse genotyping.

Target	Primer	Primer sequence	Allele and expected band length	Final concentration for PCR reaction (µM)	Tm (ºC)	nº of cycles (annealing step)
TEL-JAK2	TJ2-Tg(+)	GGGAAGGGAAGCCCATCAACC	**transgenic** 441 bp	0.2	63	30
	TJ2-Tg(-)	CCGCACTGTAGCACACTCCC		0.2		
Foxn1	Nude 1	GGCCCAGCAGGCAGCCCAAG	**wild-type** 168 bp	0.2	55	35
	Nude 3	AGGGATCTCCTCAAAGGCTTCCAG	***nude*** 167 bp	0.2		

Table 2.2. Expected band lengths of wild-type and *nude* alleles in *Foxn1* mice, after restriction enzyme digestion.

after BSEDI digestion:	**Band lengths**
WT allele	88, 64, 16 bp
***Nude* allele**	103, 64 bp

2.2. Cell culture

2.2.1. Leukemic cell co-cultures

The MS5 murine bone marrow stromal cell line, provided by Dr. Françoise Pflumio (CEA, Fontenay-aux-Roses, France), was maintained in αMEM medium (Gibco), supplemented with 10% FBS, EU approved (PAA), 2 mM L-glutamine (Lonza) and 100 units penicillin/streptomycin (Lonza). TJ2-Tg leukemic cells ($1x10^6$ cells/ml) were monocultured or co-cultured in triplicate with confluent MS5 cells in complete RPMI medium (Lonza). Monocultured and co-cultured leukemic cells in suspension were then collected for flow cytometry analysis. For dexamethasone treatments, TJ2-Tg leukemic cells were either cultured alone or in co-culture with MS5 cells as described above and vehicle or dexamethasone (Sigma-Aldrich) was added at the indicated concentrations. Cells in suspension were collected and the remaining culture was washed twice with PBS and then incubated with enzyme-free cell dissociation buffer (Gibco) at 37ºC. Collected cell suspensions and correspondent dissociated cells were pooled before immunostaining. Leukemic cells were discriminated from MS5 through flow cytometry immunodetection of the CD8 T-cell surface marker (see 2.5.2).

2.2.2. *Foxn1* stable expression in the 1C6 mTEC cell line

The 1C6 mouse mTEC cell line, provided by Dr. George Holländer (University of Basel, Switzerland), was used to stably overexpress the *Foxn1* gene. The thymic epithelial cell origin was confirmed by detecting expression of the *Krt5* marker gene. The 1C6 cell line and the Plat-E retroviral packaging cell line (provided by Dr. Toshio Kitamura [University of Tokyo, Japan]) were cultured in DMEM (Lonza) supplemented with 10% FBS, 2 mM L-glutamine and 100 units penicillin/streptomycin. Plat-E cells were transfected by the calcium phosphate method with the retroviral plasmids pBABEpuro-FoxN1 and negative control pBABEpuro-GFP, provided by Dr. David Prowse (Queen Mary University of London, UK). In brief, 12.5 μg of plasmid DNA was diluted in water with $CaCl_2$ (250 mM) and added drop-by-drop onto equal volume of 2x HEBS. After allowing precipitate formation for 10 min, the mixture was added to the Plat-E cells (cultured for 24 h without antibiotics). Culture medium

(without antibiotics) was changed approximately 20 h after transfection. Two days after transfection, Plat-E supernatants were collected, 0.45 μm filtered and used to infect 1C6 cells. After transfectant selection with 2 mg/ml puromycin (Sigma-Aldrich) for 17 days, FoxN1- or GFP-transduced 1C6 clones were isolated with the aid of cloning cylinders (Corning Inc.).

2.3. Genomic DNA extraction and *Notch1* mutation detection

Genomic DNA was extracted from thymic TJ2-Tg leukemic cells using the GeneJET Genomic DNA purification kit (Thermo Fisher Scientific), following the manufacturer's protocol. The exon 34 of *Notch1* was PCR amplified as previously described (O'Neil et al., 2006). Briefly, the PCR protocol was followed as described in section 2.1.4.1, with the following alterations: performed in 50 μl volumes of the mixture, 1 μl of genomic DNA, 1.0 U GoTaq DNA polymerase and primers (forward 5'-ATAGCATGATGGGGCCACTA-3' and reverse 5'-CTTCACCCTGACCAGGAAAA-3') at a final concentration of 0.4 μM. PCR amplification was performed in 30 cycles, with annealing temperature of 54ºC. PCR products were purified using the PCR Clean-Up kit (Machery-Nagel) protocol and Sanger sequenced (CCMAR, Faro, Portugal). Visualization of the obtained sequences to detect double peaks was done on 4Peaks (Nucleobytes) and Sequence Scanner Software 2 (Applied Biosystems). Sequence alignment was performed using the online MultAlin tool (Corpet, 1988).

2.4. Whole transcriptome RNA sequencing (RNA-seq)

Thymic stromal-enriched fractions from wild-type (WT; 5 males) and TJ2-Tg (2 males and 1 female) mice were obtained as described above (section 2.1.1) and total RNA was extracted using Trizol (Life Technologies) and the Direct-zol RNA Miniprep kit (Zymo Research). Next, mRNA was isolated using the NEBNext Poly(A) mRNA Magnetic Isolation Module (New England Biolabs, Ipswich, MA, USA), following the manufacturer's instructions. mRNA samples from WT and TJ2-Tg samples were pooled and purified using the RNeasy

MinElute Cleanup kit (Qiagen) and further processed using the Ion Total RNA-Seq kit v2 (Thermo Fisher Scientific). Sequencing was performed on Ion Torrent PGM (Thermo Fisher Scientific) using Ion 316 Chip kits v2 (Thermo Fisher Scientific) for the WT pooled sample and for the TJ2-Tg pooled sample. Quality check of the sequence data through both FastQC (available online at www.bioinformatics.babraham.ac.uk/projects/fastqc/) and Prinseq (Schmieder and Edwards, 2011) indicated high sequence quality except for a residual adapter sequence in a subpopulation of reads. The latter was removed from the data by Cutadapt software (Martin, 2011). Additionally, reads were trimmed if the corresponding Phred score fell below 25. Subsequently, reads were aligned to the mouse genome (UCSC, mm10) by the Torrent Mapping Alignment Program (TMAP). In total, 3,204,955 and 3,125,039 reads were mapped to the genome for the WT and TJ2-Tg sample, respectively. Expression levels of genes were derived by HTseq-count and differential gene expression was assessed with Bioconductor package edgeR (McCarthy et al., 2012; Robinson et al., 2010). Bioinformatic data analysis was performed by our collaborators from the SysBioLab, led by Dr. Matthias Futschik (CCMAR, Faro, Portugal).

2.5. Flow cytometry

2.5.1. Isolation and analysis of thymic stromal cells

Thymic tumor samples were shipped on ice to Dr. Nuno L. Alves and collaborators (IBMC, Porto, Portugal) to perform the isolation and flow cytometric analysis of thymic stromal cells. Briefly, thymic stromal cells were isolated by enzymatic digestion as previously described (Alves et al., 2009b). TECs were further enriched by depleting hematopoietic cells using a MACS-based $CD45^+$ cell depletion kit (Miltenyi Biotec). Before immunostaining, cells were treated with Fc block (anti-CD16/CD32 antibodies TruStain FcX; Biolegend). Cell suspensions were stained as described (Alves et al., 2009b) with R-phycoerythrin (PE)-conjugated anti-CD80 (16-10A1) and anti-Ly51 (6C3); peridinin-chlorophyll proteins (PerCP)-cyanine (Cy)-5.5-conjugated anti-CD45.2 (104); allophycocyanin (APC)/eFluor660-conjugated anti-CD80 (16-10A1); APC/eFluor780-conjugated anti-I-A/I-E (M5/114-15-2) and eFluor450-conjugated anti-EpCAM (G8.8). The binding of biotinylated *Ulex europaeus*

agglutinin-1 (UEA-1) or anti-Ly51 (6C3) was revealed by PE-Cy7-conjugated streptavidin. Intracellular staining with APC/eFluor660-conjugated anti-Aire (5H12) antibody was performed according to the supplier's protocol. Two sets of analysis were performed for thymic stromal cell populations. The antibodies/target molecules for each set are discriminated in Table 2.3. The combination of antibodies used for TEC populations are Flow cytometry was performed on a FACSCanto II and LSRFortessa, with data analyzed on FlowJo software (Tree Star).

2.5.2. Thymocyte/T-cell analysis

Single-cell suspensions from collected organs were prepared by dissociation against a 70 μm cell strainer (BD Biosciences) in PBS. 1 x 10^6 cells were resuspended in cold staining buffer (PBS with 10% fetal bovine serum [FBS; PAA Laboratories] and 10 mM NaN_3). Single-cell suspensions were centrifuged at 300 x*g* for 5 minutes at 4ºC. The cells were stained with fluorochrome-labeled antibodies, in 50 μl of staining buffer, and incubated for 1 hour on ice, in the dark. Fluorescein isothiocyanate (FITC)-, PE- or PE-Cy5-conjugated antibodies specific for CD25 (PC61), CD4 (GK1.5) and CD8 (53-6.7) (BioLegend) were used (Table 2.3). Then, cells were washed twice with 1 ml of cold staining buffer and resuspended in 1 ml of 10 mM NaN3 in PBS solution, and analyzed in a FACS Calibur flow cytometer (BD Biosciences). Isotype negative controls and cells stained with each antibody individually were also prepared to adjust the FACS Calibur settings. Propidium iodide (Sigma-Aldrich) staining was used to gate viable cells for analysis. Analyses were performed on CellQuest (BD Biosciences).

2.6. Immunofluorescence

Whole thymi were included and frozen in OCT compound (VWR). Thymic cryosections of 6-10 μm on Superfrost Plus glass slides (Thermo Scientific) were dried at 37ºC for 30 min before cold acetone fixation for 10 min at room temperature. Sections were re-hydrated in PBS, washed with PBSW solution (PBS with 0.1% Tween20 [VWR]) and incubated with blocking solution (10% BSA [Sigma-Aldrich], 20% FBS in PBSW) for 1 h. Primary

antibodies (Table 2.4) were incubated overnight at 4ºC, washed with PBSW, followed by 1 h incubation with secondary antibodies (Table 2.4) at room temperature. Slides were washed with PBS and mounted with Mowiol reagent and 0.15% DAPI (Biotium), using glass cover slips. Images were acquired with a Zeiss Axio Imager Z2 fluorescence microscope. Image analysis was performed using open-source ImageJ (Schindelin et al., 2015; Schneider et al., 2012) and Fiji (Schindelin et al., 2012) software. Assembly of sequential images was performed using Pairwise Stitching plugin (Preibisch et al., 2009) in Fiji.

2.7. mRNA expression analysis

Total RNA from whole, stromal- or thymocyte-enriched thymic samples, or from mTEC 1C6 cells was prepared using Trizol reagent (Life Technologies) followed by phenol:chloroform extraction, according to the manufacturer's instructions. Quality and concentration of the RNA samples was determined by Experion (Bio-Rad) and NanoDrop 2000c (Thermo Scientific) analysis. In order to remove any possible remaining genomic DNA in the samples, 1 µg of RNA samples were treated with 1U/µl DNase I (Thermo Fisher Scientific), following the manufacturer's protocol. Reverse transcription was performed using the First Strand cDNA Synthesis Kit (Thermo Fisher Scientific) and oligo$(dT)_{18}$ primers, according to the manufacturer's instructions.

2.7.1. Semi-quantitative PCR

Semi-quantitative PCR (RT-PCR) was performed as described in the polymerase chain reaction section (see 2.1.4.1), with the following alterations: 1.0 µl of serial dilutions (1/20, 1/60, and 1/180) of template cDNA was used for each sample. PCR reaction protocol was as follows: an initial denaturation step of 94ºC for 5 min, 26 to 35 cycles at 94ºC for 1 min, 60ºC for 1 min and 72ºC for 1 min, with a final extension step of 72ºC for 7 min. Primers (each at a final concentration of 0.1 mM) used for each reaction are described in Table 2.5. PCR products were analyzed by electrophoresis in Greensafe premium-stained a 2% agarose gel prepared in TAE buffer and visualized under UV light.

Table 2.3. Antibodies used in flow cytometry analysis. Different sets were used to analyze thymocyte/T cells (thymocyte analysis) and thymic stromal cell (TEC analysis I and II) populations.

Target molecule	Conjugated fluorochrome	Analysis set	Conjugated fluorochrome	Analysis set	Source
CD25 (PC61)	FITC	thymocyte analysis			BioLegend
CD4 (GK1.5)	PE	thymocyte analysis	-	-	BioLegend
CD8 (53-6.7)	PE-Cy5	thymocyte analysis			BioLegend
CD45.2 (104)	PerCP-Cy5.5	TEC analysis I	PerCP-Cy5.5	TEC analysis II	eBioscience
EpCAM (G8.8)	eFluor450	TEC analysis I	eFluor450	TEC analysis II	eBioscience
I-A/I-E (M5/114-15-2)	APC/eFluor780	TEC analysis I	APC/eFluor780	TEC analysis II	eBioscience
CD80 (16-10A1)	APC/eFluor660	TEC analysis I			eBioscience
Ly51 (6C3)	PE	TEC analysis I	-	-	eBioscience
biotinilayed UEA-1	PE-Cy7-conjugated streptavidin *	TEC analysis I			Vector Laboratories
Aire (5H12)			APC/eFluor660	TEC analysis II	eBioscience
CD80 (16-10A1)	-	-	PE	TEC analysis II	eBioscience
biotinilayed Ly51 (6C3)			PE-Cy7-conjugated streptavidin *	TEC analysis II	eBioscience

* source of the conjugated fluorochrome: eBioscience

Table 2.4. Surface markers and secondary reagents used for immunofluorescence.

	Source	Clone/ species	Dilution
Primary reagents			
Keratin 5 (Krt5)	Covance	AF 138 Rabbit polyclonal	1/1000
Keratin 8 (Krt8)	Dr. Rolf Kemler (Max Planck Institute, Freiburg, Germany)	Clone Troma1, Rat monoclonal IgG2a	1/100
ER-TR7	Dr. J.L. Dooley (University of Leuven, Belgium)	Clone ER-TR7, Rat monoclonal IgG2a	1/100
F4/80 (Emr1/Ly71)	Dr. J.L. Dooley	Clone F4/80, Rat monoclonal IgG2a	1/50
DEC205 (Ly75/CD205)	Dr. J.L. Dooley	Clone NLDC-145, Rat monoclonal IgG2a	1/100
ICAM-1	Dr. Dietmar Vestweber (Max Planck Institute, Münster, Germany)	Clone 25ZC7, Rat monoclonal IgG	1/100
CCL21 (Exodus-2)	PeproTech	Rabbit polyclonal	1/100
Laminin	Abcam	Rabbit polyclonal	1/125
CD31 (PECAM-1)	BD Biosciences	Clone MEC13.3, Rat IgG2a	1/100
Biotinylated UEA-1 *(Ulex Europaeus* Agglutinin I)	Sigma-Aldrich	–	1/200
Secondary reagents			
Streptavidin, Alexa Fluor® 546 conjugate	ThermoFisher Scientific	–	1/500
Anti-Rabbit IgG DyLight 488	Jackson ImmunoResearch	Goat	1/1000
Anti-Rat IgG DyLight 488	Jackson ImmunoResearch	Goat	1/1000
Anti-Rabbit IgG DyLight 594	Jackson ImmunoResearch	Goat	1/1000
Anti-Rat IgG DyLight 594	Jackson ImmunoResearch	Goat	1/1000

2.7.2. Real-time quantitative PCR

For real-time quantitative PCR (RT-qPCR), 2 µL of 1/20 diluted cDNA, SsoFast EvaGreen Supermix (Bio-Rad) and 300 nM of primers (Table 2.5) in a 20 µL reaction were analyzed on a C1000 Thermal Cycler coupled to a CFX 96 Real-time PCR detection system (Bio-Rad). RT-qPCR results were analyzed by Bio-Rad CFX Manager software and the mean fold change in expression of the gene of interest was calculated in relation to expression of a reference gene (*Hprt* and *Gapdh* were both used, rendering similar results) by the comparative C_T method ($2^{-\Delta\Delta C(T)}$ method).

Table 2.5. Oligonucleotide primers used for gene expression analysis.

Gene name	Forward primer	Reverse primer
Ccl19	CTGCCTCAGATTATCTGCCAT	CTTCCGCATCATTAGCACCC
Ccl21a	CCCTGGACCCAAGGCAGT	AGGCTTAGAGTGCTTCCGGG
Ccl25	AATGTGAAGAGGGCGATGAG	GGGTTCTCCACCTTGGACTT
Cd3e	TCTCGGAAGTCGAGGACAGT	ATCAGCAAGCCCAGAGTGAT
Epcam	GGAGATCACGTGCTCCGAGCG	CTTGAAGCGCAGTCTGCAAGCTCT
Foxn1	ACTCTTCCCAAAGCCCATCT	GCACTTGTTGAGGGACAGGT
Gapdh	GGTGAAGGTCGGTGTGAACG	ACCATGTAGTTGAGGTCAATGAAGG
Hprt	GCTGGTGAAAAGGACCTCT	CACAGGACTAGAACACCTGC
Krt5	GAGATCGCCACCTACAGGAA	TCCTCCGTAGCCAGAAGAGA
Krt8	CTCCGGCAGATCCATGAAGA	GCTCGGCTGCGATTGG
Ltbr	CCAGATGTGAGATCCAGGGC	GACCAGCGACAGCAGGATG
Psmb11	CTCTGTGGCTGGGACCACTC	TCCGCTCTCCCGAACGTGG

2.8. Statistical analysis

Graphs and statistical analyses were performed with GraphPad Prism (GraphPad Software, Inc.). Statistical tests were performed as indicated in each figure legend. Samples were assumed to have a Gaussian distribution and therefore parametric unpaired *t* tests were

applied. Welch's correction was applied when variances values were not equal. Comparison of survival curves of TJ2-Tg;*Foxn1* cohorts was done by plotting Kaplan-Meier curves and using the log-rank (Mantel-Cox) statistical test. Hazard ratio of survival curves was obtained by the Mantel-Haenszel approach, referencing the TJ2-Tg;*Foxn1*$^{+/nu}$ mice as the control group. *P* values were considered statistically significant when lower than 0.05, as indicated (*, $P < 0.05$; **, $P < 0.01$; ***, $P < 0.001$; ****, $P < 0.0001$).

Chapter 3.

Results

3.1. Thymic stromal cell alterations during TEL-JAK2-induced murine leukemogenesis

3.1.1. TEL-JAK2 leukemic cells depend on microenvironmental cells for survival

Leukemia/lymphoma development in TEL-JAK2 transgenic (TJ2-Tg) mice was previously shown to be assisted by stromal expression of RelB and LTβR, two components of the non-canonical NF-κB pathway (dos Santos et al., 2008; Fernandes et al., 2015). Other studies, using different models, have also highlighted the importance of microenvironmental cells and derived factors in the development and maintenance of T-ALL (Passaro et al., 2016).

To establish whether TJ2-Tg leukemic cells are dependent on microenvironmental factors, *ex vivo* collected cells were maintained in standard culture medium, with bovine serum but no addition of growth factors, or in co-culture with the MS5 murine bone marrow stromal cell line. When cultured alone (isolated) leukemic cells from TJ2-Tg mice did not proliferate or survive longer than 2-3 weeks (data not shown). When co-cultured *in vitro* with the MS5 cell line, TJ2-Tg leukemic cells remained partly in suspension but often adhered to those cells (Figure 3.1A). Upon three days of culture, TJ2-Tg leukemic cells maintained significantly higher cell viability than when cultured alone (Figure 3.1B). Co-culture with stromal cells improved survival of leukemic cells, as compared to when cultures in isolation, for at least six days (Figure 3.1C). Expression of the DLL1 Notch ligand in MS5/DL1 cells did not further improve leukemic cell survival (not shown). Furthermore, in a single experiment (using one biological sample), we detected that survival of TJ2-Tg leukemic cells in the presence of the chemotherapeutic agent dexamethasone was improved upon co-culture with MS5 cells (Figure 3.2). Although requiring more extensive investigation, this result indicates that stromal cells can confer chemoresistance to at least a subset of TJ2-Tg leukemic samples. The increased survival of TJ2-Tg leukemic cells can result from the combination of two factors: direct contact between leukemic and stromal cells or secretion of soluble factors released to the culture medium by the stromal cells. When co-cultured with human T-ALL cells, MS5 cells have been shown to secrete IL-18, a tumor-promoting factor in this setting (Uzan et al., 2014). Further experiments are warranted to determine whether stromal cell-bound, soluble factors, or both are involved in TJ2-Tg leukemic cell survival.

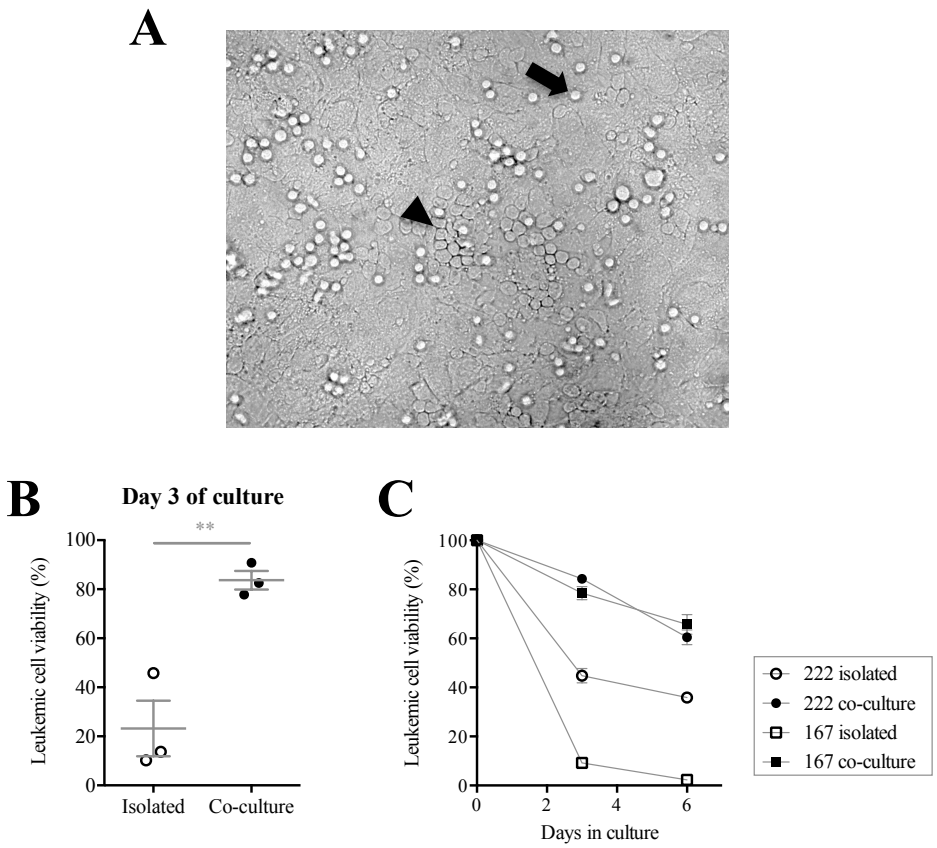

Figure 3.1. TEL-JAK2 leukemic cell *in vitro* survival is prolonged by co-culture with MS5 stromal cells. (A) Phase contrast microscopy depicting TJ2-Tg leukemic cells in co-culture with, adhering (arrowhead) or not adhering (arrow) to, the MS5 bone marrow stromal cell line, after 3 days of co-culture. (B-C) TJ2-Tg primary leukemic cell viability (as measured by propidium iodide exclusion and flow cytometry), in culture medium alone (isolated) or in co-culture with MS5 cells. (B) Representative results of three biological replicates, after 3 days of *in vitro* culture. Data expressed as mean ± SEM, *P* values determined by two-tailed, unpaired *t*-test (**, $P < 0.01$). (C) Results from two (mice IDs nº 167 and nº 222) out of three biological replicates, expressed as the mean ± SEM of technical triplicates.

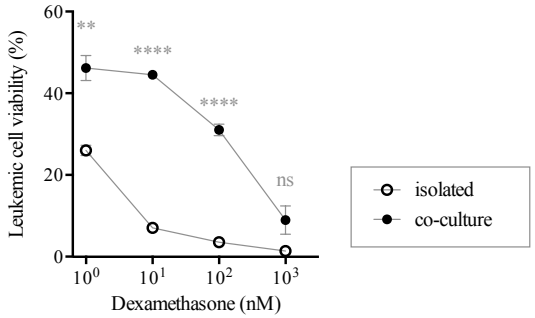

Figure 3.2. Co-culture with MS5 cells confers resistance of TJ2-Tg leukemic cells to dexamethasone treatment. Leukemic cells were cultured *in vitro* alone (isolated) or with MS5 cells (co-culture) for 3 days, in the presence of the indicated concentrations of dexamethasone. Leukemic cell viability was determined by propidium iodide exclusion by gated $CD8^+$ cells. Data expressed as the mean ± SEM of experimental triplicates, from one single biological sample. Statistical analysis of leukemic cell viability for isolated and in co-culture leukemic cells, for each dexamethasone concentration. *P* values determined by unpaired *t*-test (****, $P < 0.0001$; **, $P < 0.01$; ns, non-significant).

3.1.2. *Notch1*-activating mutations in the TEL-JAK2 mouse model

Similarly to other mouse models of T-ALL (Dumortier et al., 2006; Lin et al., 2006; Martins et al., 2014; O'Neil et al., 2006; Tremblay et al., 2010) and to human patients (Weng et al., 2004), primary leukemic cells in TJ2-Tg mice frequently acquire (> 60%) activating mutations in *Notch1* exon 34 (Table 3.1). For this analysis, we extracted genomic DNA from leukemic cells and performed sequencing directly after PCR amplification of exon 34 and product purification. By doing so, we observed either only non-mutated sequence or mixed sequences comprising both wild-type and mutated sequence, which indicated the occurrence of heterozygous mutations (Figure 3.3). The samples presented here are part of a larger study performed by our group, which included primary leukemic cells of TJ2-Tg mice with distinct genetic background mutations, namely at the *Rag2* and *Ltbr* genes (Supp. Table 1). The *Notch1* exon 34 activating mutations consisted of deletions and/or insertions leading to frameshifts, premature stop codons, and predicted loss of the C-terminal PEST domain and affecting mostly codons 2361, 2398 and 2399 (Table 3.1 and Supp. Table 1). Of note, some of the amplified sequences presented possible underrepresented mutated sequences in addition to the wild-type sequence (data not shown). Two samples with underrepresented mutations were ambiguous as to whether they were caused by the presence of a small leukemic cell population with a heterozygous mutation or by an artifactual contamination, so those were therefore excluded from the analysis. Although we did not investigate exons 26 and 27, which encode the heterodimerization domain and are mutated in some but not all T-ALL mouse models (De Keersmaecker et al., 2010; Karlsson et al., 2008; Lin et al., 2006; Martins et al., 2014; O'Neil et al., 2006), our potentially underestimated data shows nevertheless that *Notch1* mutations occur with high frequency in TJ2-Tg-induced leukemia.

Table 3.1. High frequency of exon 34 *Notch1* mutations in TJ2-Tg-induced leukemia samples.

Samples	*Notch1* ex34.2	Mutated codon	Mutation
TJ2-Tg and TJ2-Tg;*Foxn1*$^{+/+}$			
113	**mut**	2361	Del G, Ins CC
320	**mut**	2361	Ins ACAG
263	**mut**	2431	Ins A
311	**mut**	2377	Ins C
599	wt	-	-
613	wt	-	-
633	wt	-	-
TJ2-Tg;*Foxn1*$^{+/nu}$			
292	**mut**	2398	Ins TTCC
579	**mut**	2361	Del G, Ins CC
580	wt	-	-

mut, mutated sequence; wt, wild-type sequence.

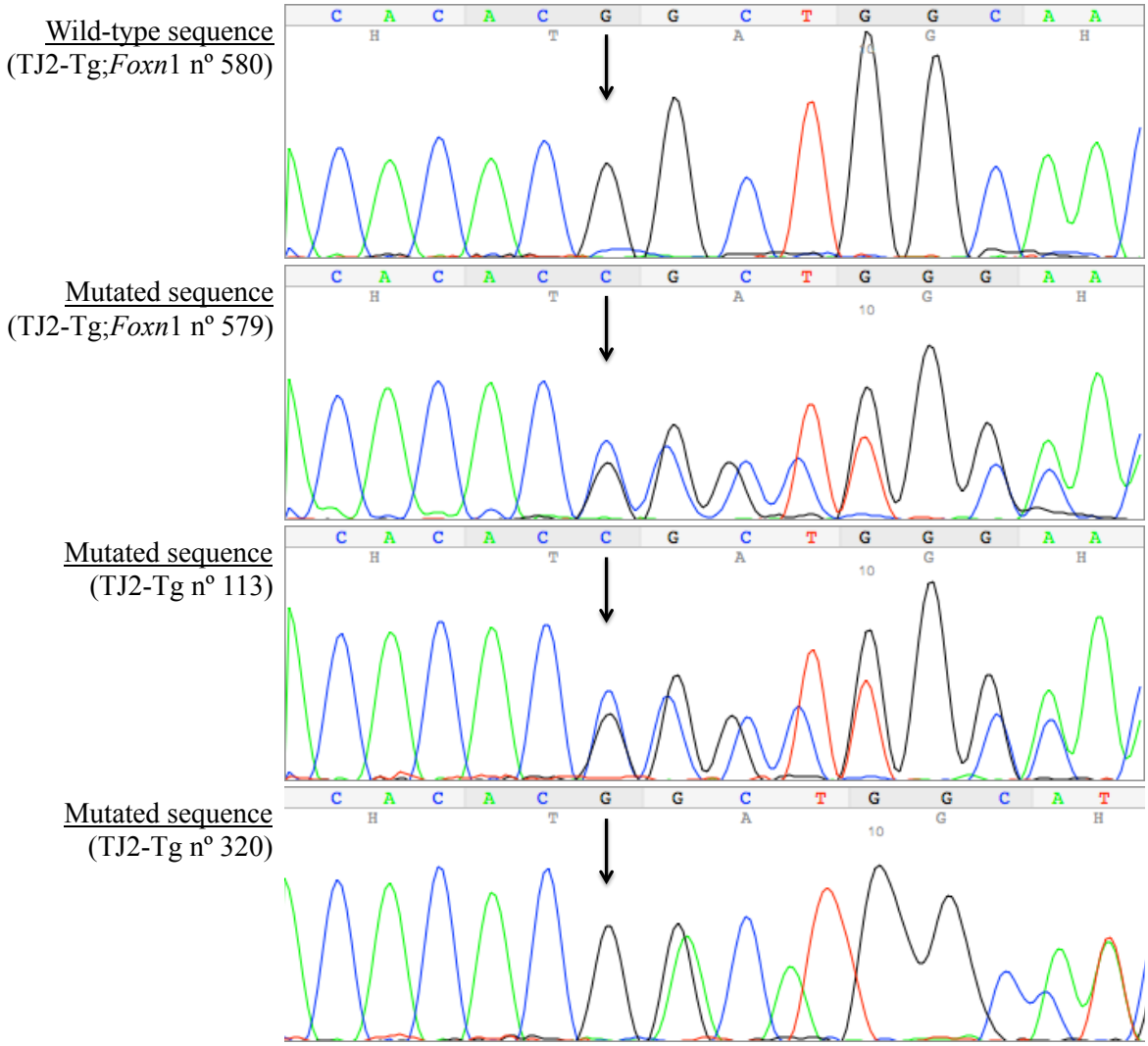

Figure 3.3. *Notch1* exon 34 heterozygous mutations at codon 2361. Mutated sequences can be identified by the presence of double-peaks, representing the two bases. The examples showed here represent a wild-type and mutated sequences at codon 2361 (CGG, black arrow), as presented in Table 3.1.

3.1.3. TEL-JAK2 mouse thymic lymphomas present profound architectural changes as compared to control thymi

Thymic lymphomas from mice manifesting visible symptoms of TJ2-Tg-induced leukemia often become 10-20 times heavier than age-matched control thymi. In these advanced cases, the classical thymic compartmentalization in cortex and medulla becomes effaced (Carron et al., 2000), as typically found in other thymic lymphoma mouse models (Dunn et al., 1961; Goodman and Block, 1963).

To understand how the thymic microenvironment is involved in TJ2-Tg-induced leukemogenesis, we first set out to assess the spatial distribution of several thymic stromal cell types in mice with advanced stage TJ2-Tg-induced leukemia. Immunofluorescence analysis of thymic cryosections with antibodies against the Krt5 and Krt8 epithelial proteins revealed large regions with no staining, here designated as keratin-negative areas (KNA) (Figure 3.4A). The Krt5 and Krt8 proteins are widely used as medullary and cortical TEC markers, respectively. As previously described for wild-type (WT) thymic samples (Alexandropoulos and Danzl, 2012), we observed that medullary regions also presented Krt8-positive staining, although not as intense as in cortical regions (Figure 3.5). While in the WT thymus, medullary and cortical regions were clearly discernible by Krt5 and Krt8 double-immunostaining (Figure 3.4B and Figure 3.5), keratin-positive areas in most TJ2-Tg thymic lymphomas showed co-staining with both Krt5 and Krt8 without the typical cortical Krt8 single staining (Figure 3.4B,C and Figure 3.6). Only one (out of eight analyzed endpoint thymic lymphomas; Supp. Table 2) presented KNA and maintained a keratin-positive area with Krt5/Krt8 labeling similar to wild-type cortico-medullary regions (Figure 3.7). At the individual cell level, Krt5 and Krt8 often stained distinct cells although a subset expressed both proteins (Figure 3.4B,C).

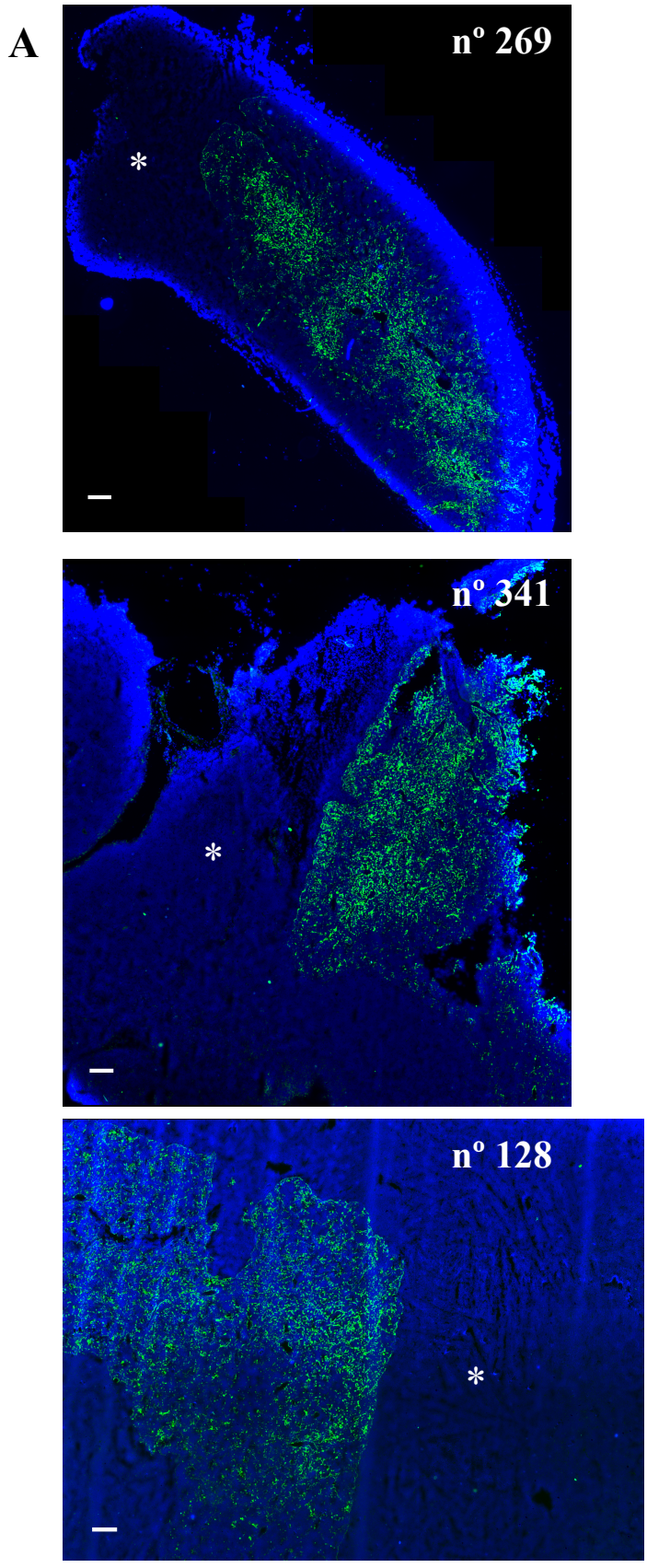
A
nº 269
nº 341
nº 128
B
nº 341
WT
C
nº 133

Figure 3.4. TEL-JAK2-induced thymic lymphomas display large keratin-negative areas. Thymic cryosections from TJ2-Tg mice with progressed disease were immunostained for Krt5 (green). (A) Stitched images for a wider view of the keratin-positive and –negative areas (representative of eight analyzed samples). (B-C) Keratin-positive areas in TJ2-TJ thymic lymphomas express both Krt5 and Krt8 (red) without their normal cortico-medullary distribution as in wild-type (WT) thymi. Cryosections were also stained with DAPI (blue), represented in (A) and (C). Asterisks indicate keratin-negative areas; mouse ID nº at the top right corner of each panel; according to positioning on each panel, scale bars: lower left = 200 μm, lower right = 100 μm. **(Previous page.)**

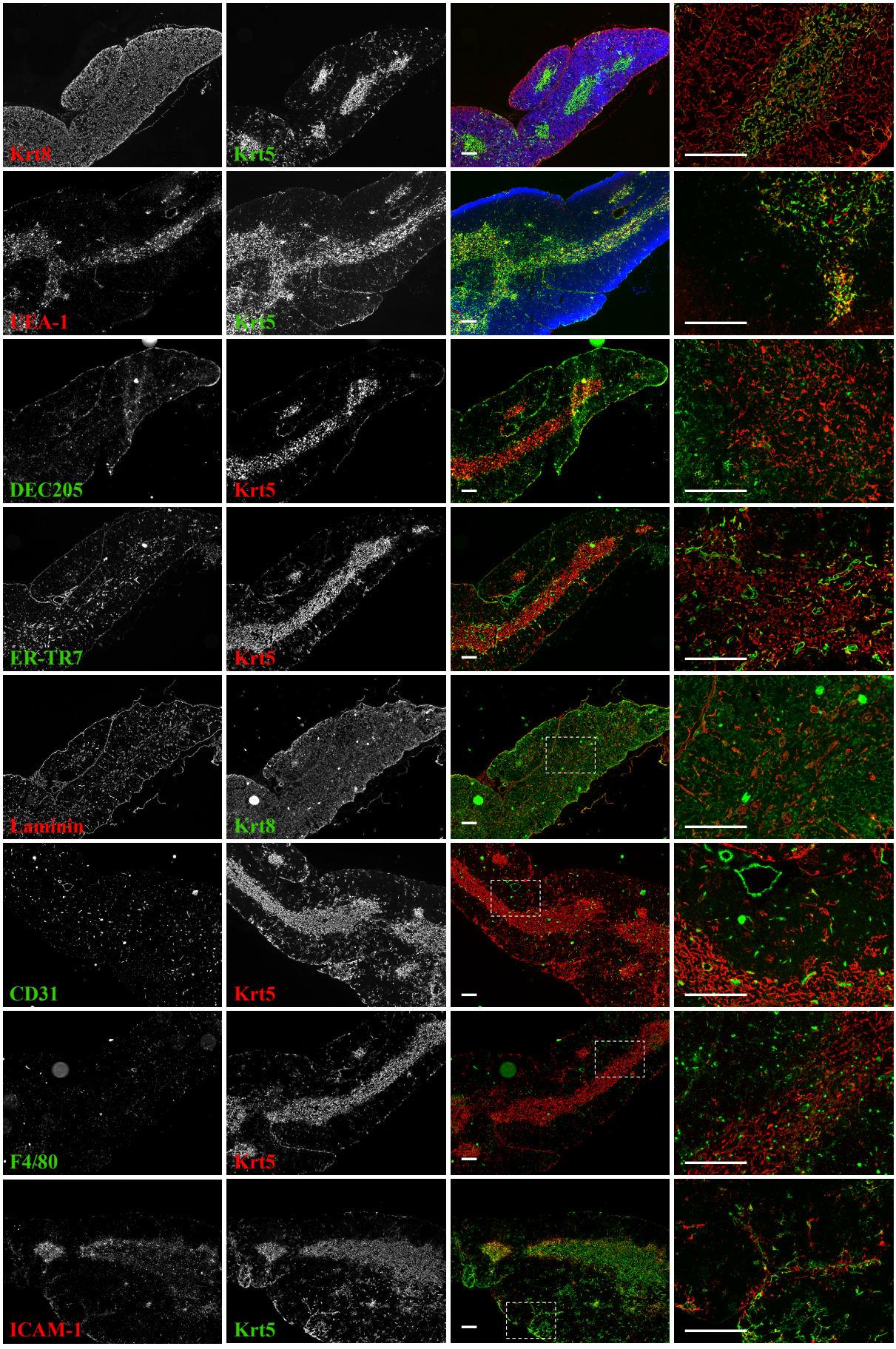
Krt8
Krt5
UEA-1
Krt5
DEC205
Krt5
ER-TR7
Krt5
Laminin
Krt8
CD31
Krt5
F4/80
Krt5
ICAM-1
Krt5

Figure 3.5. Detection of thymic stromal markers in wild-type mice. Double immunofluorescence staining of a wild-type thymus, with antibodies against the indicated markers. The third column images represent pseudocolored merging of images shown in the first and second columns, while the fourth column depicts a higher magnification area (when applicable, dashed-line rectangles represent the magnified area). In the first and second row, the lower magnification pseudocolored panels also depict the DAPI staining (blue). Scale bars = 200 μm. **(Previous page.)**

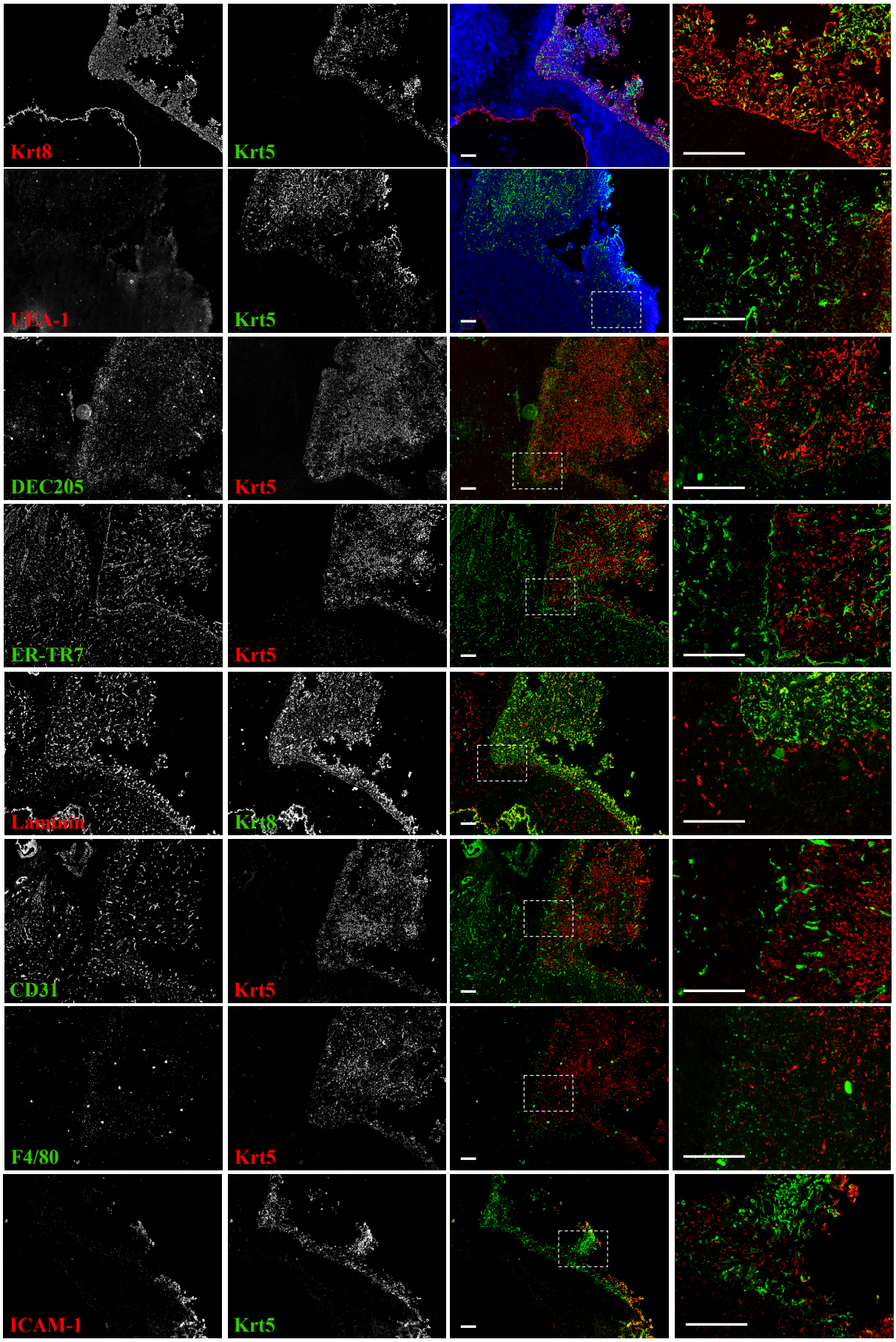
Krt8
Krt5
UEA-1
Krt5
DEC205
Krt5
ER-TR7
Krt5
Laminin
Krt8
CD31
Krt5
F4/80
Krt5
ICAM-1
Krt5

Figure 3.6. Characterization of the thymic stromal cellular alterations in advanced stage thymic lymphomas from TJ2-Tg mice. Double immunofluorescence staining of a representative TJ2-Tg thymic lymphoma (mouse ID nº 341) of two (out of at least three) analyzed with antibodies against the indicated markers. The third column images represent pseudocolored merging of images shown in the first and second columns, while the fourth column depicts a higher magnification of the keratin-positive and negative boundaries. For the first and second row, DAPI staining (blue) was shown for the lower magnification pseudocolored panels. When applicable, dashed-line rectangles represent the magnified area; scale bars = 200 μm. **(Previous page.)**

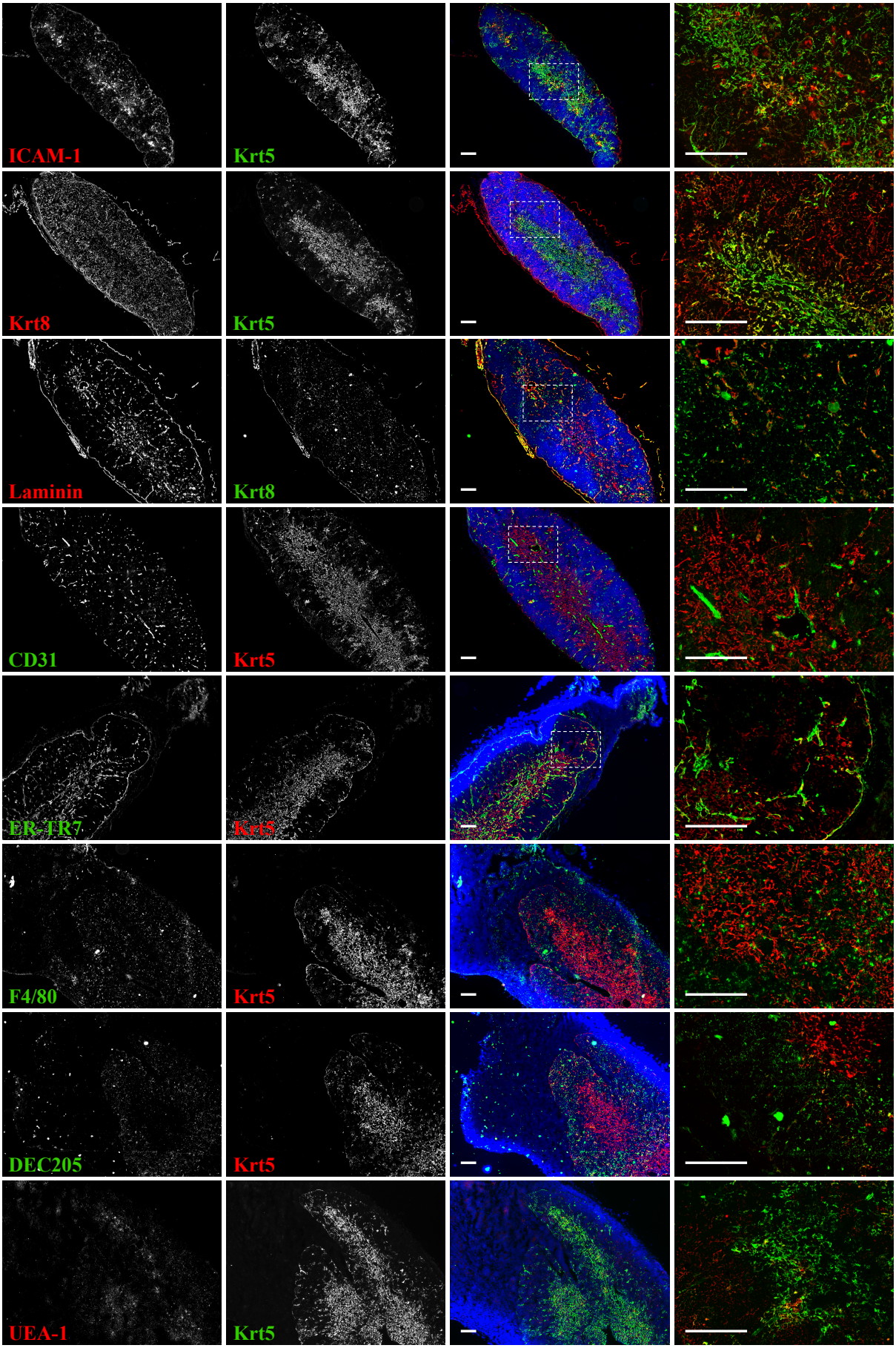
ICAM-1
Krt5
Krt8
Krt5
Laminin
Krt8
CD31
Krt5
ER-TR7
Krt5
F4/80
Krt5
DEC205
Krt5
UEA-1
Krt5

Figure 3.7. Characterization of the thymic stromal cellular alterations in advanced stage thymic lymphomas from TJ2-Tg mice. Double immunofluorescence staining of a TJ2-Tg thymic lymphoma (mouse ID nº 269), with antibodies against the indicated markers. The third column images represent pseudocolored merging of images shown in the first and second columns, with DAPI staining (blue), while the fourth column depicts a higher magnification area (when applicable, represented by dashed-line rectangles). Scale bars = 200 μm. NOTE: take relevance to the fact that this figure does not follow the same order of immunofluorescence staining as the previous two figures. **(Previous page.)**

WT medullary TECs express UEA-1, often with subcellular co-localization with Krt5 (Figure 3.5, higher magnification panel). In TJ2-Tg thymic lymphomas, UEA-1 was also detected within keratin-positive areas, but in some tumors with lower expression levels (Figure 3.6 and Figure 3.7) than others (Figure 3.8). Cortical TECs can also be detected through expression of the DEC205 marker (also known as CD205 and encoded by the *Ly75* gene), although the latter is also expressed in thymic DCs (Kraal et al., 1986). TJ2-Tg thymic lymphomas revealed a dense DEC205 staining in keratin-positive regions, notably higher in zones with less intense Krt5 staining, suggesting that DEC205 labels residual cortical areas marked by ectopic Krt5 expression. Interestingly, DEC205 also marked many cells in KNA from thymic lymphomas, which suggests the presence of DCs.

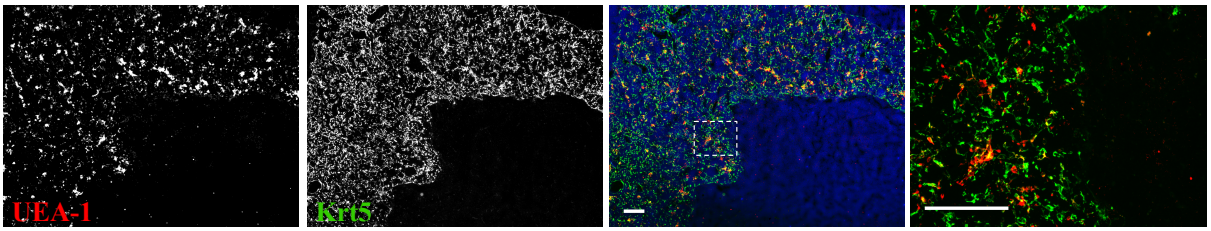

Figure 3.8. TEL-JAK2-thymic lymphomas present areas of medullary TEC markers co-localization. Thymic cryosections from TJ2-Tg mice (ID nº 128) at advanced-stage disease were immunostained against UEA-1 and Krt5 mTEC markers. The third panel represents pseudocolored merge of images shown in the first and second panels, with DAPI staining (blue), while the fourth panel depicts a higher magnification area (represented by a dashed-line rectangle). Scale bars = 200 μm.

Fibroblasts detected by the ER-TR7 antibody in WT thymic tissue are not restricted to particular regions, but are more abundant in the thymic capsule, trabeculae, and lining of blood vessels (Van Vliet et al., 1986). In TJ2-Tg thymic lymphomas, the pattern of expression of ER-TR7 was similar in both keratin-positive and keratin-negative areas, although a layer of ER-TR7-positive staining often marked the border between these two areas (Figure 3.6, Figure 3.7 and Figure 3.9). Of note, like ER-TR7, laminin staining was also observed at the border between keratin-positive and keratin-negative areas (Figure 3.6). Similar to ER-TR7^{+} fibroblasts, extracellular matrix and endothelial cells (detected by anti-laminin and anti-CD31/PECAM-1 antibodies, respectively) were present throughout the lymphoma tissue, irrespective of keratin labeling (Figure 3.6).

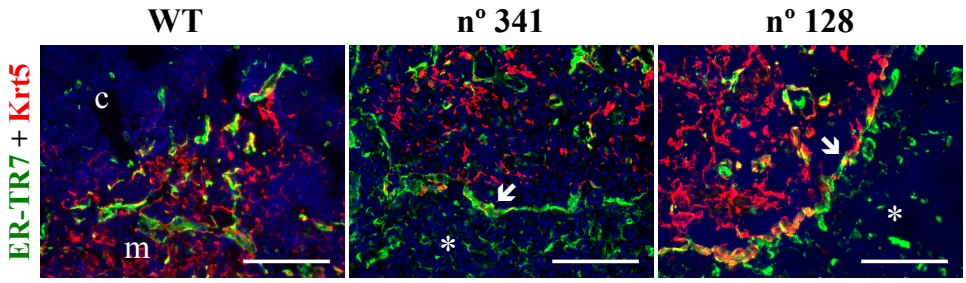

Figure 3.9. Fibroblasts are present in keratin-negative areas. ER-TR7^{+} fibroblasts are present throughout the tissue in wild-type (WT) thymus and TJ2-Tg thymic lymphomas (mouse IDs nº 341 and nº 128). In thymic lymphomas, a layer of ER-TR7^{+} cells (arrow) separates the keratin-positive and –negative areas. Asterisks indicate keratin-negative areas; DAPI staining in blue – faded to highlight other labeling; m, medulla; C, cortex; scale bars = 100 µm.

Scattered macrophages in normal thymic tissue were detected by the anti-F4/80 antibody (Figure 3.5). F4/80^{+} cells were also distributed throughout TJ2-Tg thymic lymphomas, but more prevalently in keratin-positive areas (Figure 3.6 and Figure 3.7). Finally, we also analyzed the distribution pattern of the integrin-interacting ICAM-1 adhesion molecule. As previously reported (Lepique et al., 2003; Ueda et al., 2012), ICAM-1 was detected both in cortex and medulla of WT thymic samples, but with much more prominent expression in the medulla (Figure 3.5). Ueda et al. (2012) reported that the cells expressing ICAM-1 were medullary DCs and mTECs. In TJ2-Tg thymic lymphomas, ICAM-1 expression was higher in areas of stronger Krt5 labeling (Figure 3.6 and Figure 3.7), often co-localizing at the subcellular level (Figure 3.10), thus indicating that also in the thymic lymphoma context mTECs express ICAM-1.

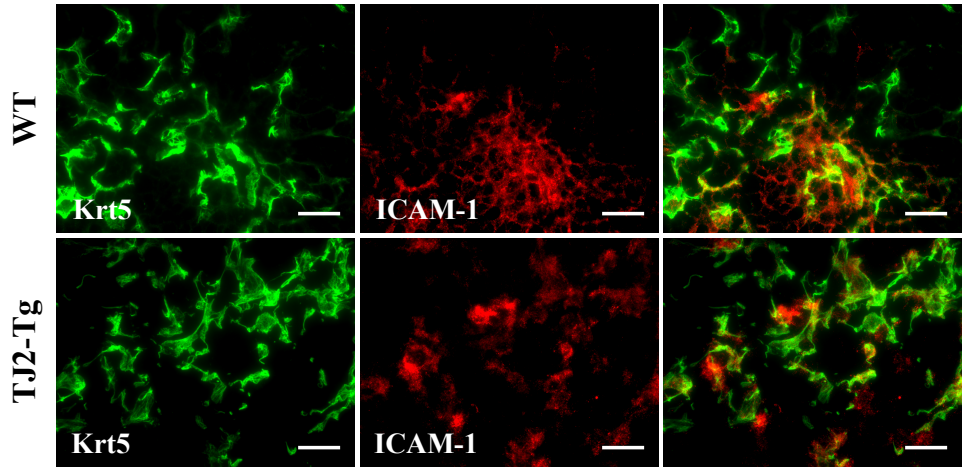

Figure 3.10. ICAM-1 often co-localize with Krt5^{+} TECs. Higher magnification of double immunostaining and of Krt5 and ICAM-1 revealed subcellular co-localization in the medullary region of wild-type (WT) thymic cryosections and Krt5-positive areas of TJ2-Tg thymic lymphomas (mouse ID nº 133). Scale bars = 20 µm.

The immunohistological results indicate that TEC subpopulations undergo profound alterations in spatial distribution and organization upon lymphoma development. Two of the main thymic lymphoma features observed here were the presence of large KNAs and an underrepresentation of Krt8 expression in relation to Krt5. To confirm the presence of these features through another method, we determined by RT-qPCR the relative expression levels of TEC marker genes in whole thymic lymphoma samples as compared to WT. Proportional changes in specific cell populations within the whole thymus should correlate with expression changes in marker genes for those cells. The *Krt8* and *Psmb11* cTEC marker genes and the *Krt5* mTEC marker gene were significantly less expressed in whole TJ2-Tg thymic lymphomas than in wild-type thymi (Figure 3.11). This indirectly confirms that the proportion of epithelial cells in lymphomas was reduced, as compared to normal whole thymi. Two features suggest that cortical epithelial domains are lost during lymphoma development: first, immunohistology showed that expression of Krt5 encompassed all epithelial areas in thymic lymphomas. Second, unlike in WT thymi, no areas positive for Krt8 and negative for Krt5 were observed. Supporting the notion that mTEC-like cells ($Krt5^+$) were overrepresented as compared to cTEC-like cells ($Krt8^+$), the ratio of *Krt5*/*Krt8* mRNA relative expression was higher in TJ2-thymic lymphomas than in normal thymi (Figure 3.11).

Expression of the epithelial adhesion molecule marker *Epcam* (Figure 3.11) was, however, not similarly decreased in TJ2-Tg samples. Although this discrepancy remains unclear without RT-qPCR analysis of purified thymic cells, it appears that *Epcam* expression can be upregulated in thymic lymphomas, either in TECs or in other cell types. Of note, higher levels of *Epcam* were found in malignant and normal cancer-associated epithelial cells in other types of cancers (Mukherjee et al., 2009; Patriarca et al., 2012), so it is possible that *Epcam* may favor leukemogenesis. Expression of other thymic stromal genes, namely those encoding the chemokine ligand *Ccl21a* and lymphotoxin-β receptor *Ltbr* was not significantly altered during lymphomagenesis (Figure 3.11). Thymic expression of *Ccl21a* and *Ltbr* is normally not restricted to TECs (Misslitz et al., 2004; Shi et al., 2016; Takahama, 2006). The lack of correlation between TEC underrepresentation and high *Ccl21a* and *Ltbr* expression in whole thymic lymphomas, suggests that other thymic stromal cell types, perhaps fibroblasts or endothelial cells, express these genes. Alternatively, it is possible that TECs express higher levels of *Ccl21a* and *Ltbr* genes. Again, gene expression analysis in purified populations should be undertaken to answer this question.

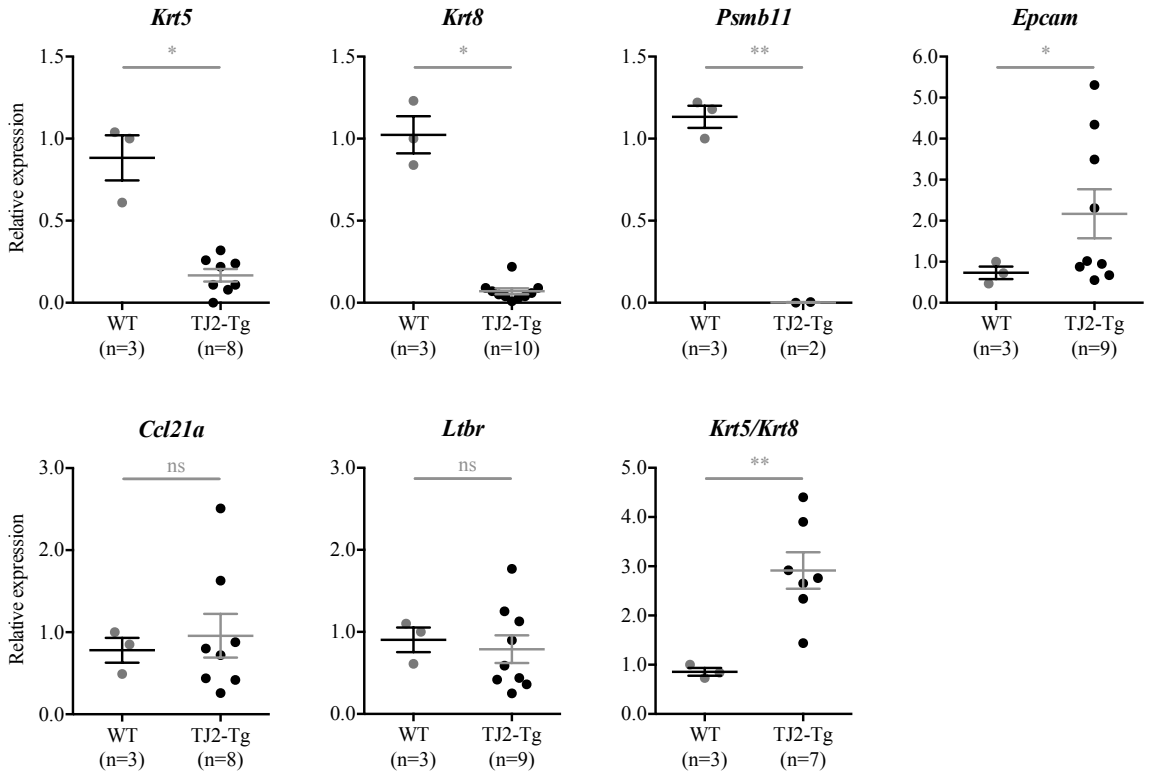

Figure 3.11. Cortical thymic epithelial markers are underrepresented in relation to a medullary TEC marker in whole TJ2-Tg lymphomas. RT-qPCR quantification of *Krt5*, *Krt8*, *Psmb11*, *Epcam*, *Ccl21a* and *Ltbr* thymic stromal gene expression in whole 20-week-old wild-type (WT) thymi and TJ2-Tg thymic lymphomas relative to expression of the *Hprt* reference gene. *Krt5/Krt8* refers to *Krt5* expression relative to *Krt8* expression in WT and TJ2-Tg samples. All data are expressed with mean ± SEM error bars, with the number of samples given between parentheses. *P* values determined by two-tailed, unpaired *t*-test with Welch's correction (**, $P < 0.01$; *, $P < 0.05$; ns, non-significant).

3.1.4. Early stage thymic lymphomas are marked by the loss of cortical markers and expansion of medullary thymic epithelium

The aforementioned data were obtained from the immunohistological analysis of advanced-stage diseased TJ2-Tg mice, which displayed significant thymic enlargement (average thymic weight of 573 mg, with average age of 18 weeks). To gain insights into cellular alterations in earlier stages of disease, we also performed immunohistology on smaller (average thymic weight of 288 mg) TJ2-Tg thymic lymphomas, from younger animals (average age of 13 weeks) (Table 3.2). These analyses revealed two striking features. First, Krt5 and Krt8 detection showed expansion of Krt5 but not Krt8 labeling and concomitant loss of the normal

cortico-medullary compartmentalization. Second, the extension of KNAs in this set of TJ2-thymic lymphomas correlated with lymphoma weight (Figure 3.12).

Like in larger lymphomas, KNAs in small thymic lymphomas contained abundant ER-TR7$^+$ fibroblasts (Figure 3.12). Since a more evident expansion of Krt5-positive in relation to Krt8-positive areas was recurrently detected in TJ2-Tg thymic lymphomas, we have also immunostained thymic lymphomas for medullary markers Ccl21 and UEA-1 (Ueno et al., 2004). UEA-1 expression in thymic lymphoma samples was similar to that of Krt5, while Ccl21 was detected throughout the lymphoma, including in KNAs (Figure 3.12). Of note, in keratin-positive areas Ccl21 showed little subcellular co-localization with UEA-1, rather labeling adjacent cells, septae and vasculature (Figure 3.12). These results indicate that Krt5$^+$/UEA-1$^+$ TECs expanded in detriment of Krt8$^+$ TECs. Additionaly, other non-TEC stromal cells, both adjacent to mTECs in keratin-positive areas and localized in KNAs, express Ccl21. Double immunofluorescence showed that all CD31$^+$ lymphoma blood vessels co-localized with laminin (Figure 3.13).

Since the initial immunohistological analyses indicated an enrichment in mTEC markers, our collaborators, led by Dr. Nuno L. Alves, purified stromal cells and analyzed the TEC compartment of eight thymic lymphomas, four of low (127-240 mg) and four of intermediate (295-668 mg) thymic weight, all presenting abnormal proportions of malignant CD8$^+$CD25$^+$ thymocytes (Table 3.2). In order to perform both experiments on each thymic lymphoma, one thymic lobe was used for immunofluorescence and the other was sent for TEC analysis by flow cytometry.

Table 3.2. Leukemic cells and TEC populations at the early stages of TJ2-Tg thymic lymphomas. Cellularity of $CD8^+CD25^+$ and $CD45^-EpCAM^+$ populations was calculated based on the percentages obtained by flow cytometry and the initial cellularity of T-cell suspension and CD45-depleted stromal fractions, respectively. Values for $Ly51^+$ and $CD80^{hi}Aire^{hi}$ populations are relative to $CD45^-EpCAM^+$ population.

				$CD8^+CD25^+$		$CD45^-EpCAM^+$		$Ly51^+$		$CD80^{hi}Aire^{hi}$		Classification (thymic weight)
ID	**Sex**	**Age (weeks)**	**Thymus (mg)**	**(x 10^5 cells)**	**(%)**	**(x 10^4 cells)**	**(%)**	**(x 10^4 cells)**	**(%)**	**(x 10^4 cells)**	**(%)**	
146	F	13	127	48.1	41.5	23.5	11.1	1.0	4.2	14.9	63.4	Low
164	F	10	135	16.1	19.2	25.5	18.2	1.5	5.9	13.8	54.0	Low
401	F	12	161	108.8	46.1	24.5	27.8	0.5	2.2	20.0	81.9	Low
142	F	14	240	99.6	48.8	37.6	24.1	1.2	3.3	22.3	59.3	Low
55	F	14	295	88.2	16.7	166.8	55.6	11.8	7.1	59.7	35.8	Intermediate
187	F	6	310	153.1	43.0	342.1	28.8	75.3	22.0	39.3	11.5	Intermediate
400	M	16	367	212.9	50.7	179.0	45.2	13.2	7.4	58.9	32.9	Intermediate
144	M	18	668	170.2	34.6	448.2	46.4	33.6	7.5	189.2	42.2	Intermediate
				8.1	0.6	138.5	88.8	21.2	15.3	98.8	71.3	Wild-type
				4.6	0.6	87.3	70.4	11.3	13.0	54.5	62.4	Wild-type

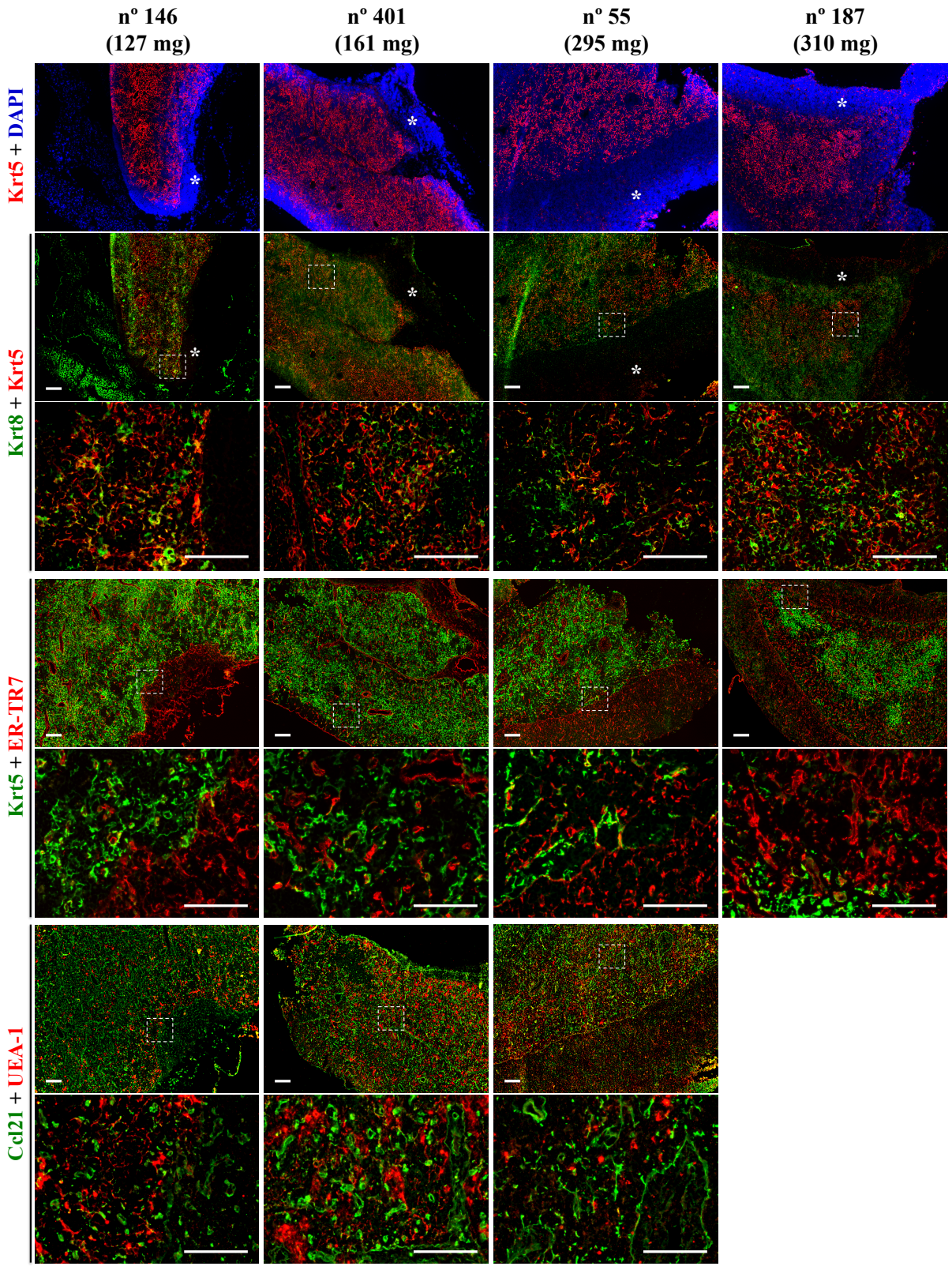

Figure 3.12. Medullary thymic epithelial cell expansion occurs at the early stages of thymic lymphomagenesis. Thymic cryosections from a different set of relatively younger/smaller size TJ2-Tg thymic lymphomas were immunostained for Krt5, Krt8, and UEA-1 thymic epithelial markers, the ER-TR7 fibroblast marker, and the Ccl21 chemokine. Asterisks indicate keratin-negative areas; mouse ID nº at the top, with thymic weight between parenthesis; dashed-line rectangles represent the area magnified in the panel immediately below; according to positioning on each panel, scale bars: lower left = 200 μm, lower right = 100 μm.

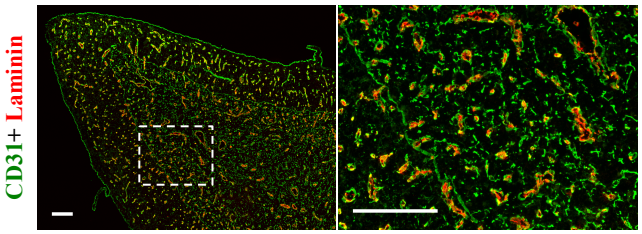

Figure 3.13. Thymic lymphoma blood vessels are surrounded by laminin-containing extracellular matrix. Double immunofluorescence labeling of a representative (of four) TJ2-Tg thymic lymphomas with antibodies against the CD31 endothelial cell marker and laminin. Scale bars = 200 μm.

Sample preparation prior to flow cytometry analysis of the stromal population fraction involved depletion of $CD45^+$ cells. Cellularity of the CD45-depleted fractions was used to determine the cellularity of $CD45^-EpCAM^+$ cells. Cellularity for each TEC subpopulation, based on $CD45^-EpCAM^+$ cellularity and on the percentage of Ly^+ and $CD80^+Aire^+$ cells obtained from the flow cytometry data analysis (Table 3.2). Thymic epithelial cells were selected first by viable $CD45^-$ and doublet exclusion (Supp. Figure 1). Two approaches were undertaken to identify TEC subpopulations. First, by selecting the population of $MHCII^+EpCAM^+$ cells, cTECs were detected through $Ly51^+$ expression and mTECs through $CD80^{hi}Aire^{hi}$ expression (Figure 3.14A and Table 3.2). The second approach was based on selection of $CD80^+MHCII^+EpCAM^+$ cells and identification of $CD80^{hi}UEA\text{-}1^{hi}$ mTECs (Figure 3.14A).

Fitting the notion that cTECs become underrepresented with leukemogenesis, the percentage of TECs expressing the Ly51 marker (encoded by the *Enpep* gene) was, in seven out of eight samples, lower in TJ2-Tg thymic lymphomas (most notably in the smaller lymphomas) (Figure 3.14B). Expression of the CD80 and Aire mTEC markers in small lymphomas remained similar to that in control thymi, but was significantly lower in intermediate sized lymphomas (Figure 3.14B). Meanwhile, high CD80- and UEA-1-expressing TECs, in six out of eight samples, presented lower percentages of this mTEC population in comparison to the WT samples (Figure 3.14B).

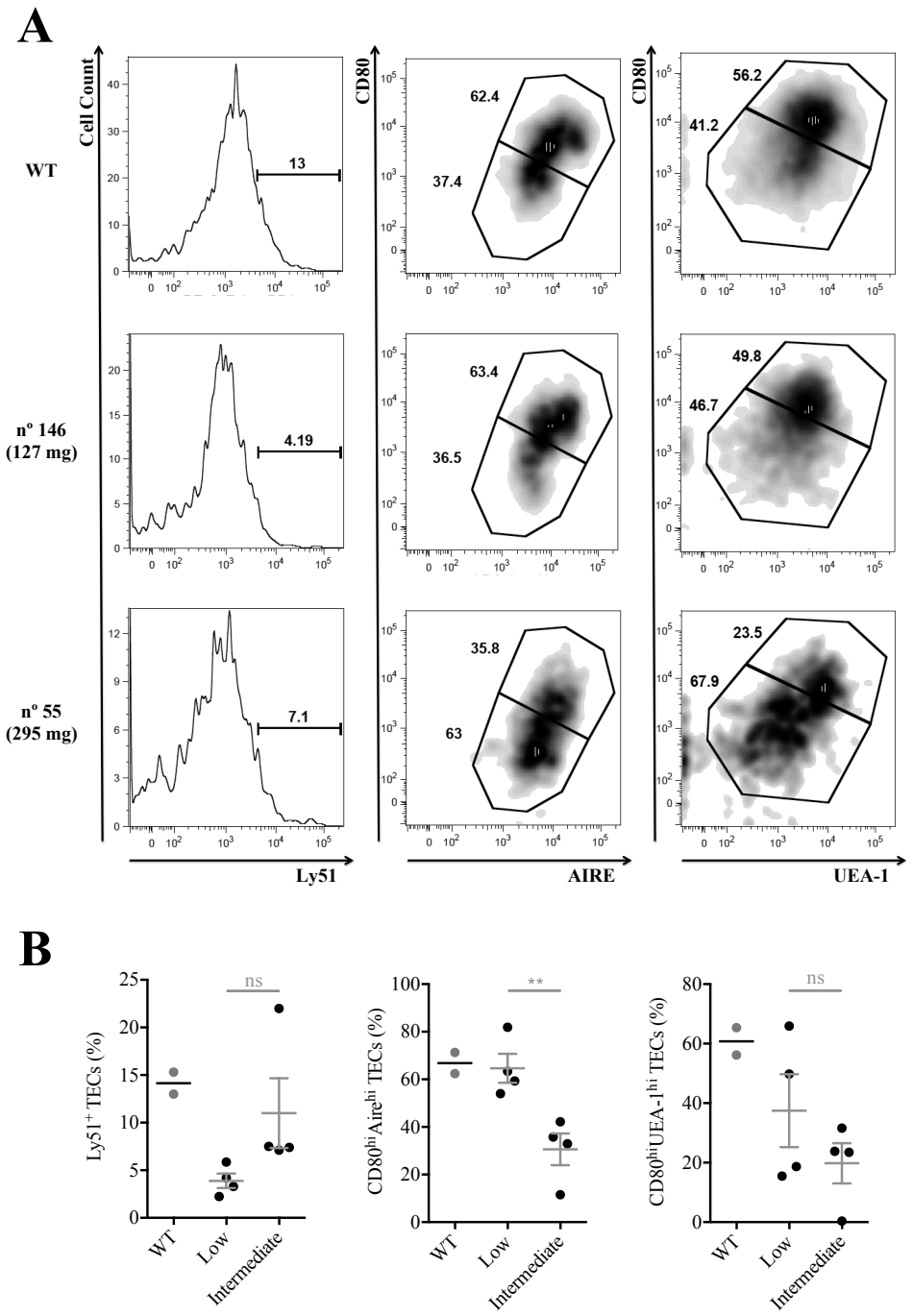

Figure 3.14. Thymic epithelial cell characterization by flow cytometry analysis. (A) Flow cytometry analysis of representative two wild-type (WT) and eight TJ2-Tg (mouse IDs nº 146, of low thymic weight, and nº 55, of intermediate thymic weight) thymic stromal cell suspensions showing total Ly51$^+$ TECs and expression of TEC-specific markers CD80, Aire and UEA-1 (gated as CD45$^-$EpCAM$^+$). (B) Flow cytometry analysis of the same samples was performed to estimate the percentage of total Ly51$^+$ TECs, CD80^{hi}Aire^{hi} and CD80^{hi}UEA-1^{hi} mTECs. TJ2-Tg thymic lymphomas were grouped by thymic weight range: low (127-240 mg, n=4) or intermediate (259-668 mg, n=4). Data are expressed with mean (WT samples) and mean ± SEM error bars (TJ2-Tg samples). *P* values determined by two-tailed, unpaired *t*-test (**, $P < 0.01$; ns, non-significant).

3.1.5. The reduction in TEC marker expression starts early in TJ2-induced thymic leukemogenesis

Our results so far were based on the analysis of mice with clear signs of disease, which presented more or less enlarged thymi. We aimed to know whether stromal alterations were detectable before disease manifestation. Thus, we collected thymi from TJ2-Tg mice without signs of disease (also termed as pre-leukemic), and cells were analyzed by flow cytometry for CD4, CD8 and CD25 expression. The TEL-JAK2 mouse model allows the identification of leukemic thymocytes by flow cytometry because these aberrantly co-express CD8 and CD25. At 8 weeks of age, most TJ2-Tg mice presented normal or near normal thymic weight and cellularity (Figure 3.15). However, in several mice increased proportions of $CD4^{-}CD8^{+}$ cells were observed (Figure 3.16, upper panels). Most of these cells aberrantly express CD25, indicating the presence of $CD8^{+}CD25^{+}$ leukemic cells among normal thymocytes (Figure 3.16, lower panels). The proportion of these aberrant cells was variable from mouse to mouse, which is expected when considering the observed variable age of disease onset (dos Santos et al., 2007) and the stochastic nature of secondary genetic alteration acquisition.

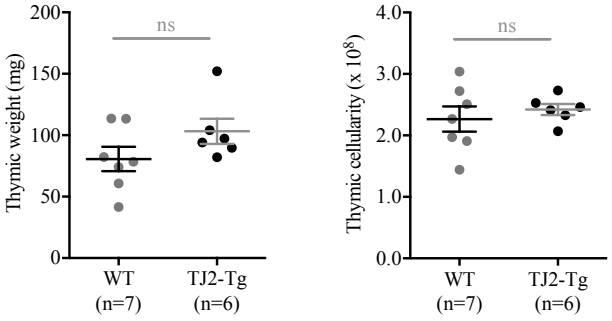

Figure 3.15. Young pre-leukemic TJ2-Tg mice have normal thymic weight and cellularity. Thymic weight and cellularity difference between wild-type (WT) and TJ2-Tg mice at 8 weeks of age. Data presented with mean ± SEM; number of mice is given between parentheses. *P* values determined by two-tailed, unpaired *t*-test (ns, non-significant).

Analysis of 8 to 10 weeks aged-mice, showed enlargement of the thymus as the $CD8^{+}CD25^{+}$ malignant thymocyte population increases (Figure 3.17A). Leukemic cells accumulate in the thymus (due to increased proliferation and/or survival) before spreading to other organs (Fernandes et al., 2015).

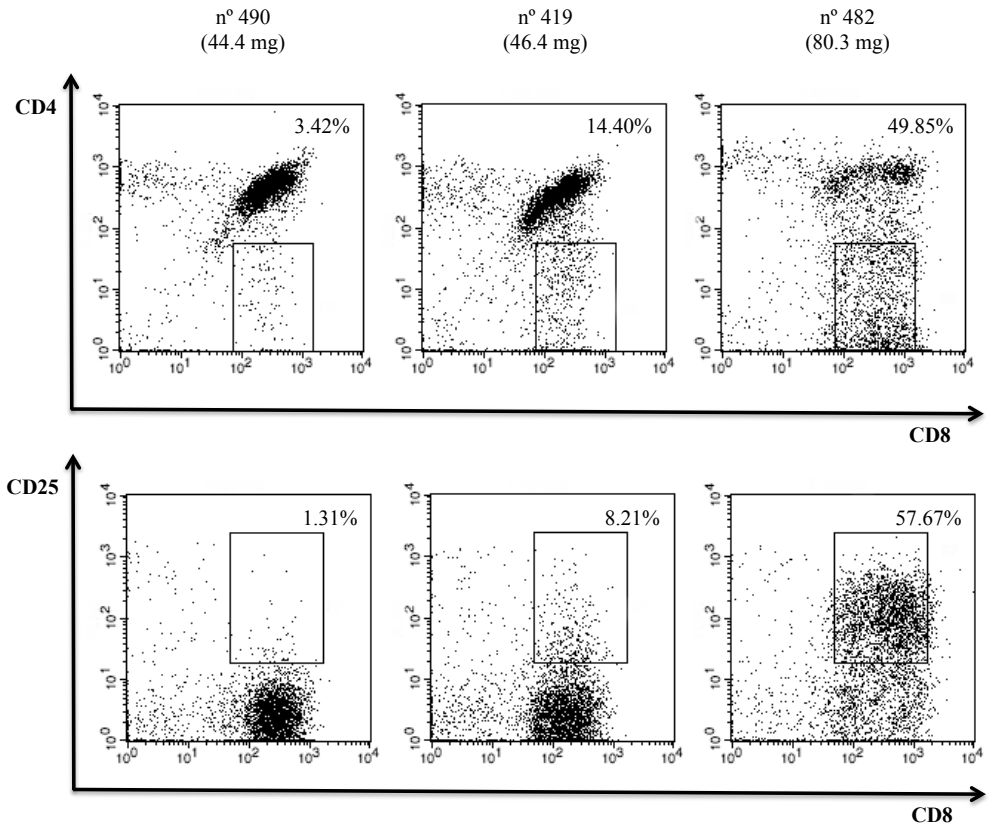

Figure 3.16. Level of progression of the TJ2-induced leukemia can be quantified by presence of $CD8^+CD25^+$ malignant thymocytes. Thymocyte flow cytometry analysis of three representative 8-week-old TJ2-Tg mice (identification and thymic weight of each mouse is indicated). From left to right, representing a healthy TJ2-Tg mouse progressing to a mouse with manifestation of full-blown disease. Plots show an altered pattern of CD4/CD8 expression with an increase in CD8SP cells, co-expressing CD25, correlating with T-cell leukemia progression. Percentage of cells in the respective regions is shown.

To determine the impact of disease initiation on the proportion of TECs, we analyzed by RT-qPCR TEC marker gene expression (*Krt5* and *Krt8*) in whole thymic samples from 8- and 10-week-old TJ2-Tg mice with variable percentages of $CD8^+CD25^+$ cells (Figure 3.17). For these analyses, thymi were collected and weighed. Approximately half of the thymus was used for RNA extraction while the other half was used for thymocyte preparation and flow cytometry analysis. Samples from 8-week-old mice had few $CD8^+CD25^+$ cells, so they were not informative (Figure 3.17B). Analysis of 10-week-old TJ2-Tg mice (Figure 3.17C) indicated that a decrease in the expression of the *Krt5* and *Krt8* TEC genes correlated with an increase in $CD8^+CD25^+$ cell percentages in the thymus. Expression of the *Ccl21a* stromal gene did not show a significant correlation with $CD8^+CD25^+$ cell percentages, but the obtained values indicated that it might nevertheless take place. These findings can be interpreted in two ways: *Krt5*, *Krt8* and *Ccl21a* gene expression is downregulated in thymic

stromal cells from pre-leukemic mice or these cells are themselves proportionally decreased in relation to $CD8^+CD25^+$ and other cells. Considering the aforementioned results indicating TEC underrepresentation in thymic lymphomas, the second hypothesis seems more plausible, i.e. as leukemic cells emerge and expand in the thymus, TECs become underrepresented.

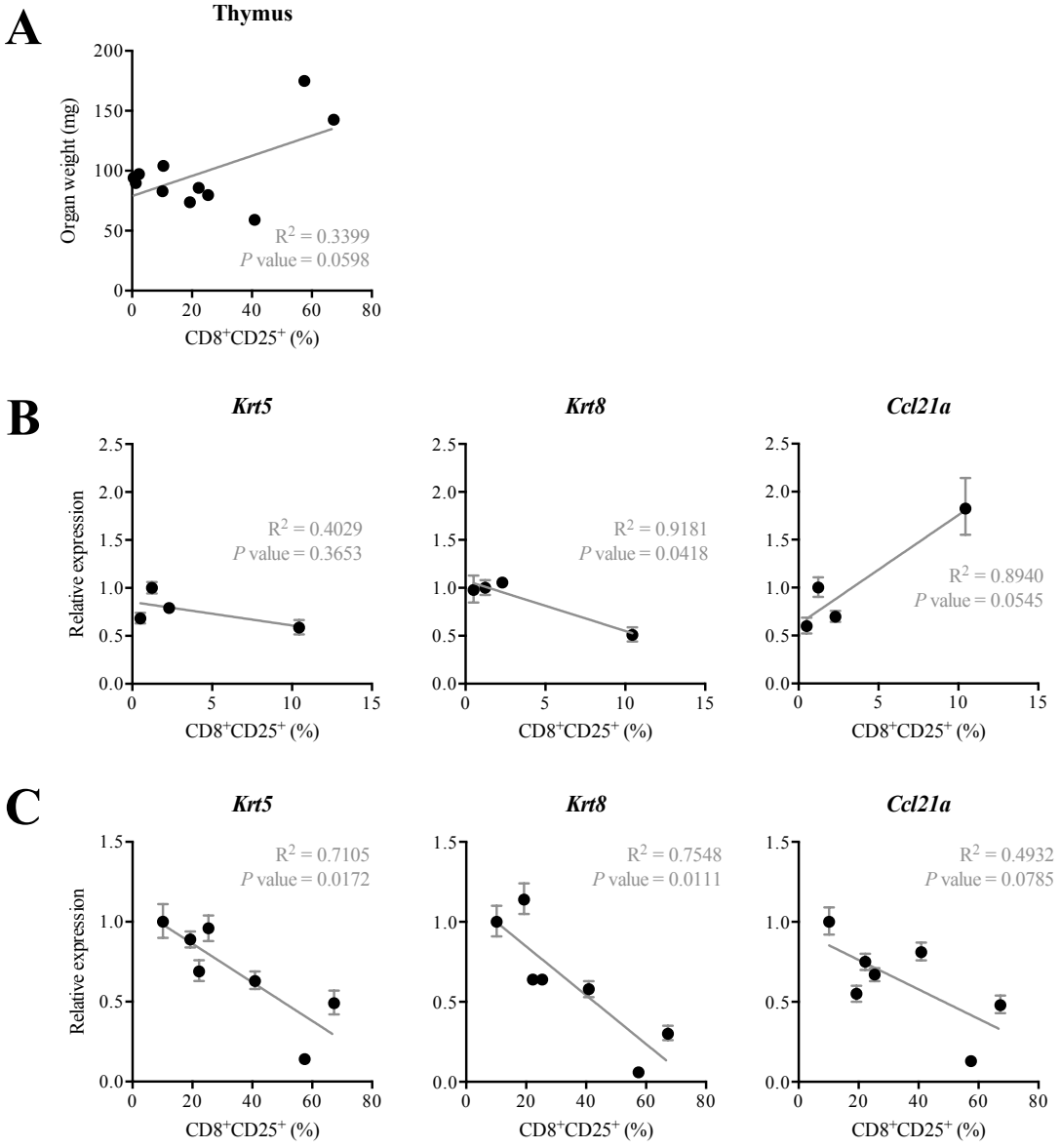

Figure 3.17. Level of disease progression vs. stromal gene expression in TJ2-Tg mice. Thymic weight (A) and gene expression values of *Krt5*, *Krt8* and *Ccl21a* of asymptomatic TJ2-Tg mice of 8 and 10 weeks of age (B and C, respectively) were plotted against the percentage of $CD8^+CD25^+$ malignant thymocytes of each TJ2-Tg mouse. Percentage of $CD8^+CD25^+$ thymocytes was obtained by flow cytometric analysis. Gene expression values were obtained by RT-qPCR, using *Hprt* as an internal reference gene; data presented with error bars for the experimental triplicate, linear regression with R square (R^2) and *P* values.

To gain insights into the nature of the earliest stromal cell alterations in thymic leukemogenesis, we aimed to detect leukemia-associated variations in expression of stromal cell marker genes using a genome-wide transcriptomic approach. Because we aimed to detect gene expression by RNA sequencing in non-purified thymic stromal cells, we set out to analyze small thymic samples at early stages of disease before the massive expansion of leukemic cells, which would mask stromal cell gene expression. To obtain thymic samples with early stage leukemia (less than 25% of $CD8^+CD25^+$ cells), mice were killed at approximately 10 weeks of age or monitored for the presence of blood-borne $CD8^+CD25^+$ cells (Table 3.3 and Figure 3.18). To perform whole-genome RNA sequencing, we obtained through a rudimentary approach stromal cell-enriched fractions from 8-week-old WT mice and from 8- to 10-week-old TJ2-Tg mice with incipient disease. Pilot experiments showed that our fractionation protocol led to enrichment of thymic stromal genes and depletion of thymocyte genes in stromal enriched fractions (Figure 3.19). The initial stage of the disease was confirmed by the nearly normal sized thymi (< 100 mg) and presence of low proportions (10-22%) of $CD8^+CD25^+$ leukemic cells (Table 3.3).

Table 3.3. TJ2-Tg mice monitored for the presence of $CD8^+CD25^+$ leukemic cells.
In bold, samples further processed for RNA-seq analysis.

Mouse identification	Sex	Age (weeks)	Thymic weight (mg)	Thymic sample $CD8^+CD25^+$ (%)	Blood sample $CD8^+CD25^+$ (%)
500	M	10.0	632.0	64.0	n/a
504	M	10.0	58.9	3.1	n/a
505	M	10.6	68.0	6.1	n/a
510	M	10.6	65.3	4.6	n/a
511	**M**	**10.6**	**69.3**	**10.7**	**n/a**
521	M	10.0	56.6	1.1	n/a
528	**M**	**10.0**	**42.1**	**11.0**	**n/a**
355	M	10.0	292.1	72.5	2.86
365	**F**	**8.0**	**96.7**	**22.0**	**2.04**
121	F	15.3	71.0	0.49	0.83
353	F	14.9	95.9	0.63	0.19
363	F	9.9	131.4	5.73	0.19

n/a: non-available.

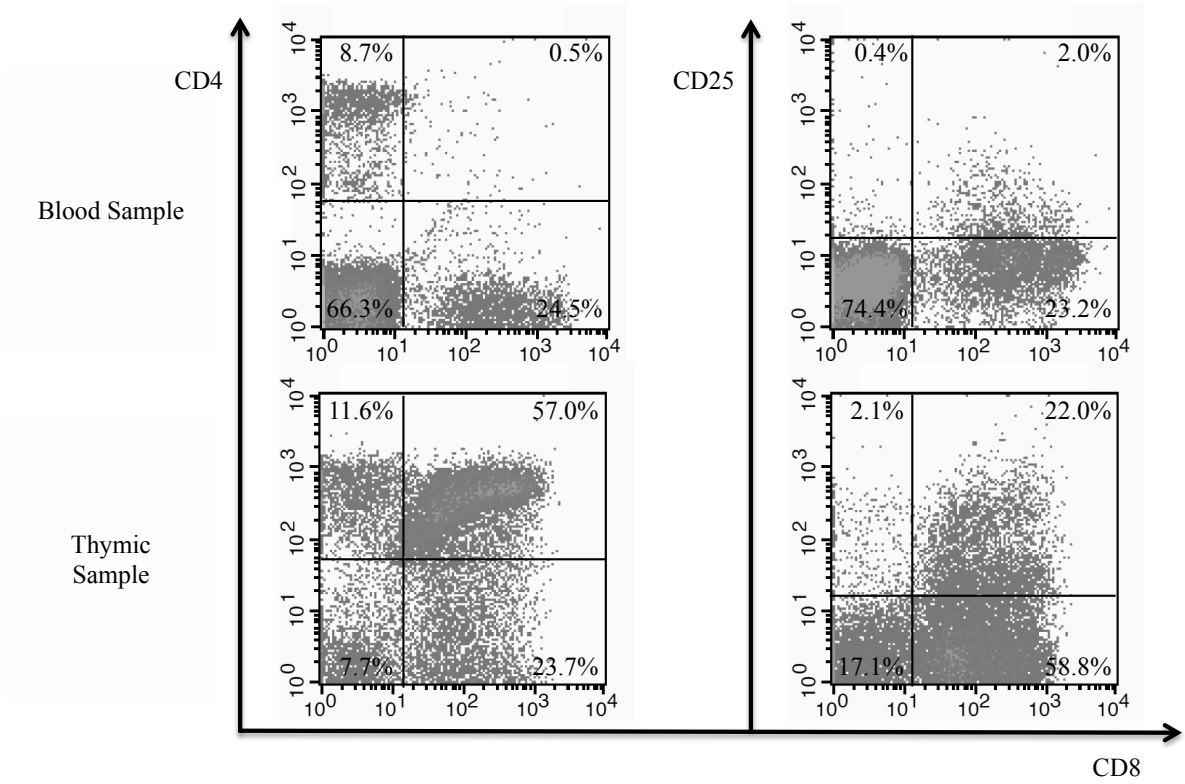

Figure 3.18. Presence of leukemic cells in the blood reveals the onset of TJ2-induced leukemia. Flow cytometry CD4/CD8/CD25 analysis of blood samples collected from the submandibular vein allows monitoring the disease development in TJ2-Tg mice (top panel). Mice with more than 0.5% $CD8^{+}CD25^{+}$ malignant thymocytes in blood were killed. The collected thymic samples were processed for flow cytometry analysis and RNA-seq (bottom panel). Percentage of cells in the respective quadrants is shown.

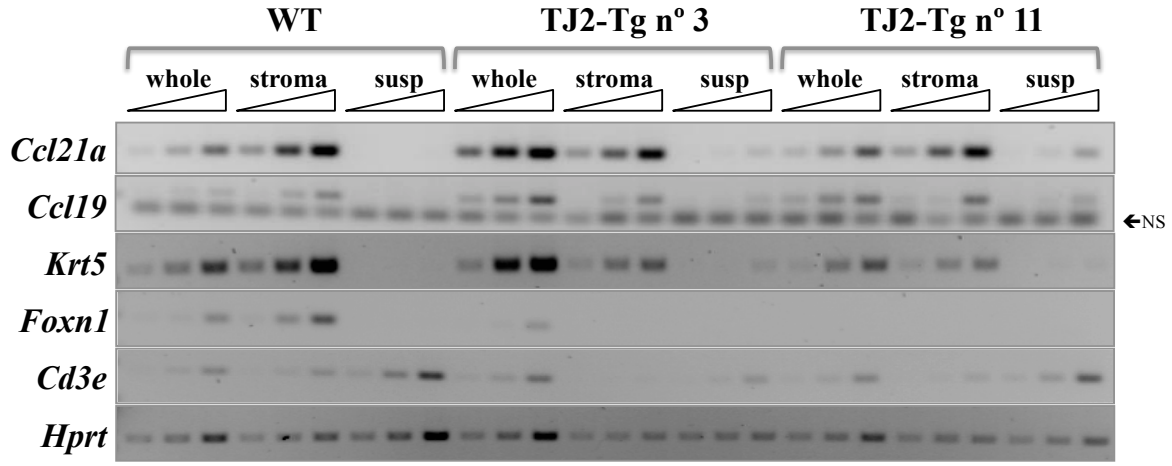

Figure 3.19. Thymic cellular fractions show enriched expression of specific marker genes. Semi-quantitative RT-PCR analysis of the indicated genes for whole thymi (whole), stromal cell-enriched fractions (stroma) and thymic cell suspensions (susp) collected from wild-type (WT) and TJ2-Tg thymic lymphomas (mouse IDs nº 3 and nº 11). Enriched fractions were obtained by simple mechanical separation. (Adapted from Ghezzo, 2009.)

After RNA extraction and mRNA purification with magnetic beads, we pooled mRNA from WT and TJ2-Tg samples for high-throughput sequencing. The pooling of the samples was done to identify gene expression changes common to all leukemic samples. Bioinformatic analysis was performed by Rui Machado (from SysBioLab, led by Dr. Matthias Futschik). Setting the cutoff thresholds for differentially expressed genes (DEGs) at FDR of 0.1 and Log2 fold change > 1, we disclosed 640 DEGs, of which 199 were upregulated in wild-type thymi (Supp. Table 3) and 441 upregulated in TJ2-Tg thymi (Supp. Table 4). As expected from the crude stromal fractionation, several genes differentially expressed between WT and TJ2-Tg samples likely derive from contaminating T lineage cells (e.g., *Ptcra*, *Rag1*, *Rag2*, *Dntt*, *Themis*, etc.) but many could be clearly identified as stromal-derived (e.g. *Ccl25*, *Vim*, *Lepr*, *S100a4*, *Zbtb46*, *Xcl1*, etc.) and were not previously found in TJ2-Tg leukemic cell transcriptomic profiles (GEO GSE51243). To know if these DEGs reflect imbalances in thymic stromal cell proportions, we investigated whether they matched genes highly expressed in thymic stromal cell subsets previously identified by Ki et al. (2014). In this work, the researchers identified DEGs in each stromal cell subset (cTEC, $mTEC^{lo}$, $mTEC^{hi}$, $Sirp\alpha^{-}$ DC, $Sirp\alpha^{+}$ DC and fibroblasts) as genes uniquely up- or down-regulated by > 2-fold relative to all other stromal subsets (Ki et al., 2014). Interestingly, of 116 cTEC-upregulated genes identified in the Ki et al. study, 17 were detected as upregulated in WT thymi compared to TJ2-Tg thymi whereas none was upregulated in TJ2-Tg thymi compared to WT (Figure 3.20 and Supp. Table 5). Conversely, a higher proportion of genes specifically enriched in $mTEC^{lo}$, fibroblast, $Sirp\alpha^{-}$ and $Sirp\alpha^{+}$ DCs subsets were found to be upregulated in TJ2-Tg thymi compared to WT thymi (Figure 3.20 and Supp. Table 5). Of note, nearly 10% of genes upregulated in stroma-enriched TJ2-Tg leukemic samples were specific of $Sirp\alpha^{+}$ DCs.

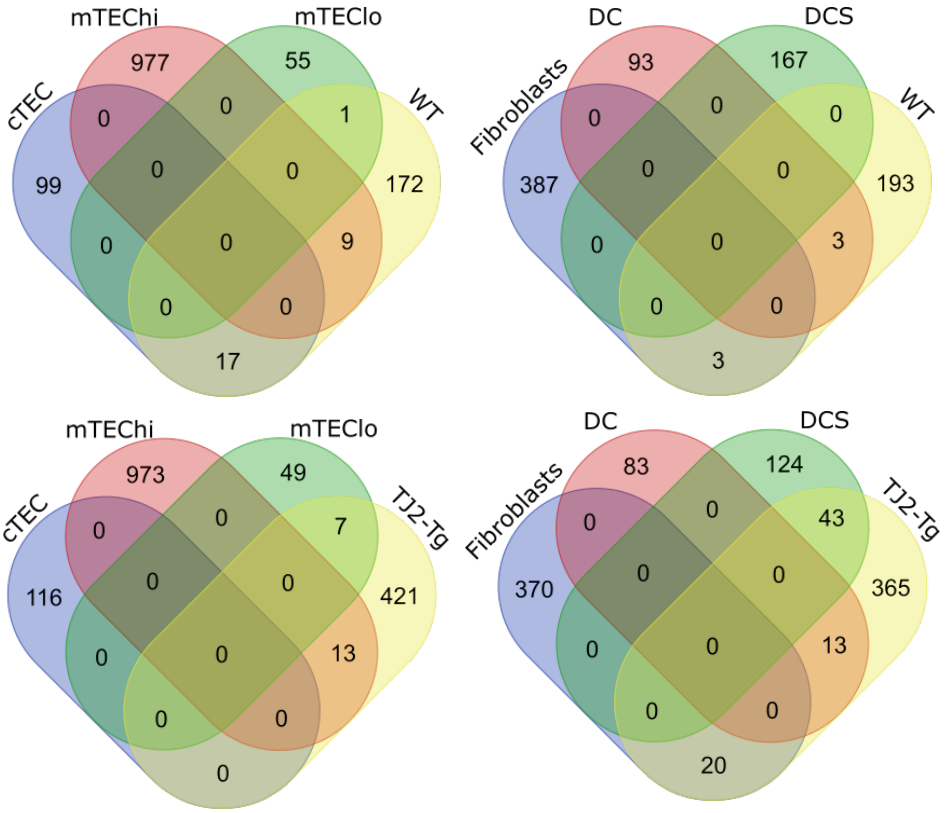

Figure 3.20. Expression of cortical markers becomes reduced from an early stage in TJ2-induced leukemia. Next-generation RNA sequencing of stromal-enriched fractions of wild-type (WT) and TJ2-Tg (with 10-22% $CD8^{+}CD25^{+}$ leukemic thymocytes) samples provided differential gene expression data. Venn diagram to compare cortical thymic epithelial cells (cTEC), medullary thymic epithelial cells ($mTEC^{hi}$ and $mTEC^{lo}$), dendritic cells (DC and DCS, negative and positive for Sirpα, respectively) and fibroblasts subsets from the Ki et al. study (2014) to WT and TJ2-Tg (T-ALL) profiles.

3.2. Role of *Foxn1*-dependent thymic stroma in TEL-JAK2-induced leukemogenesis

3.2.1. *Foxn1* haploinsufficiency delays the onset of TEL-JAK2-induced leukemia

Since TEC marker genes and proteins were found to be altered during thymic lymphomagenesis in TJ2-Tg mice, we set out to test whether these cells were involved in disease development. To this end, we tested the impact of FoxN1 dose reduction in T-ALL

development. The FoxN1 transcription factor is crucial for thymic function, regulating TEC development and maintenance in a dose-dependent manner (Chen et al., 2009). Full inactivation of the *Foxn1* gene leads to a complete loss of the thymus and T cell lineage differentiation (Nehls et al., 1996), so we decided to test the impact of *Foxn1* dose reduction on leukemia development. Cohorts of TJ2-Tg;*Foxn1*$^{+/+}$ and TJ2-Tg;*Foxn1*$^{+/nu}$ were generated and monitored to determine whether *Foxn1* haploinsufficiency influenced leukemogenesis. Indeed, TJ2-Tg mice with only one *Foxn1* allele developed leukemia with delayed onset (with a 7-week median survival difference) (Figure 3.21), revealing that this TEC-specific gene plays a role in the development of TJ2-induced leukemia.

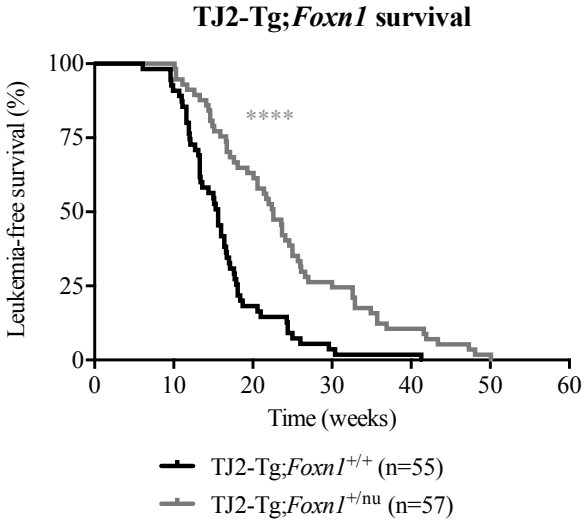

Figure 3.21. *Foxn1* haploinsufficiency delays TEL-JAK2-induced leukemia onset. Kaplan-Meier leukemia-free survival curves for cohorts of TJ2-Tg;*Foxn1*$^{+/+}$ and TJ2-Tg;*Foxn1*$^{+/nu}$ mice (median survival of 16 and 23 weeks, respectively). Log-rank test (****, *P* value < 0.0001). The number of mice in each group is given between parentheses.

Despite the different survival rates of the two cohorts, no significant differences were observed regarding endpoint tumor load of the most affected organs (Figure 3.22). Furthermore, TJ2-Tg mice with *Foxn1* haploinsufficiency presented leukemic cells with *Notch1*-activating mutations (Table 3.1) and thymic lymphomas with Krt5- and Krt8-negative regions (Figure 3.23), further supporting the notion that an identical but delayed disease developed in these mice, as compared to fully *Foxn1*-competent littermates.

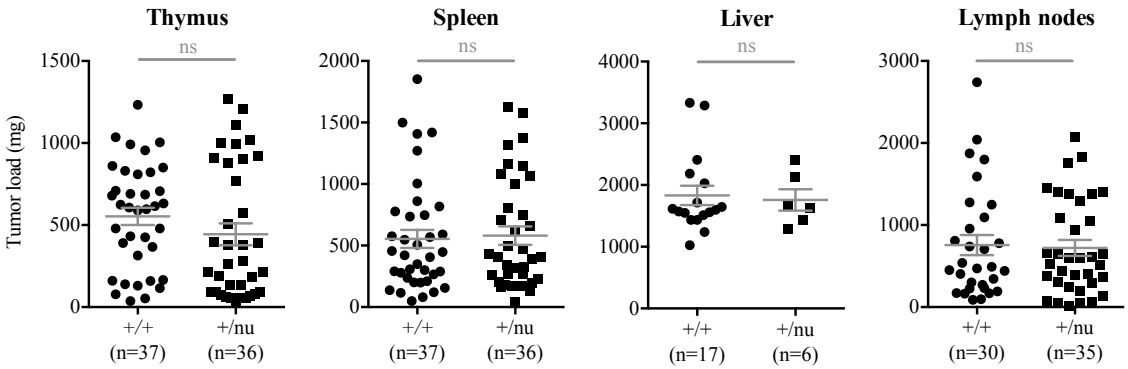

Figure 3.22. *Foxn1* haploinsufficiency does not affect tumor load. Weights of thymus, spleen, lymph nodes and liver collected from euthanized TJ2-Tg;*Foxn1*$^{+/+}$ (+/+) and TJ2-Tg;*Foxn1*$^{+/nu}$ (+/nu) mice, at an advanced stage of the disease. Data presented with mean ± SEM; number of mice is given between parentheses. *P* values determined by two-tailed, unpaired *t*-test (ns, non-significant).

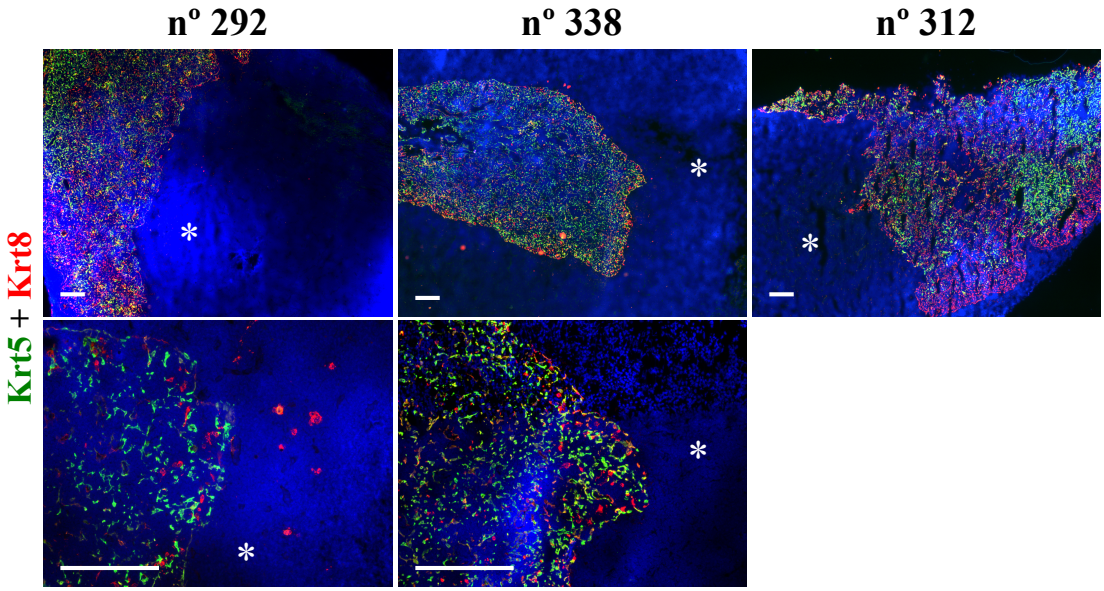

Figure 3.23. *Foxn1* haploinsufficient TJ2-Tg thymic lymphomas also display large KNAs. Endpoint TJ2-Tg;*Foxn1*$^{+/nu}$ thymic lymphomas present the same type of (dis)organization and KNAs as in TJ2-Tg;*Foxn1*$^{+/+}$ samples. Asterisks indicate keratin-negative areas; DAPI staining in blue; sample ID nº at the top; scale bars = 200 µm.

The two mouse cohorts included both males and females. The overall ratio of TJ2-Tg females to males of the total analyzed cases of TJ2-induced leukemia was 1:1.6 (Figure 3.21). Since the average thymic weight and cellularity is lower in males (*Foxn1* mice; data not shown), we wondered whether sex differences could explain differences in leukemia latency. Survival analysis of cohorts of mice within the same genotype (Figure 3.24) disclosed no significant sex differences in survival. By performing the reverse analysis, i.e., by comparing the

survival of TJ2-Tg;*Foxn1*$^{+/nu}$ and TJ2-Tg;*Foxn1*$^{+/+}$ mice within each sex (Figure 3.24), revealed that mice lacking one *Foxn1* allele had prolonged survival, more markedly in males. These differences in mouse survival were not accompanied by differences in endpoint thymic tumor burden (Figure 3.25).

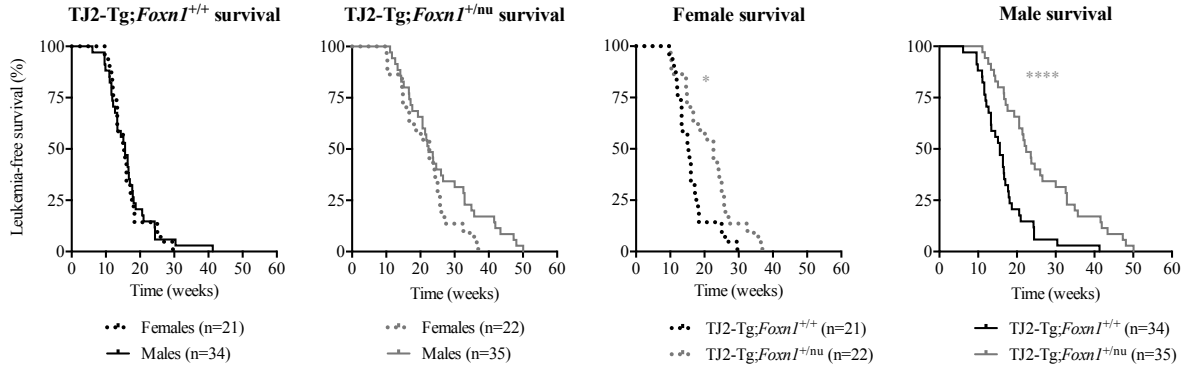

Figure 3.24. Mouse sex does not affect leukemia-free survival. Kaplan-Meier leukemia-free survival curves for cohorts of TJ2-Tg;*Foxn1*$^{+/+}$ and TJ2-Tg;*Foxn1*$^{+/nu}$ mice, separating the mice of each genotype by sex and vice-versa, as indicated in each of the graphic's title and legend. The median survival of females is 15 and 23 weeks (for TJ2-Tg;*Foxn1*$^{+/+}$ and TJ2-Tg;*Foxn1*$^{+/nu}$, respectively) and of males is 16 and 22 weeks (also TJ2-Tg;*Foxn1*$^{+/+}$ and TJ2-Tg;*Foxn1*$^{+/nu}$, respectively). The number of mice in each group is given between parentheses (log-rank test; ****, $P < 0.0001$; *, $P < 0.05$).

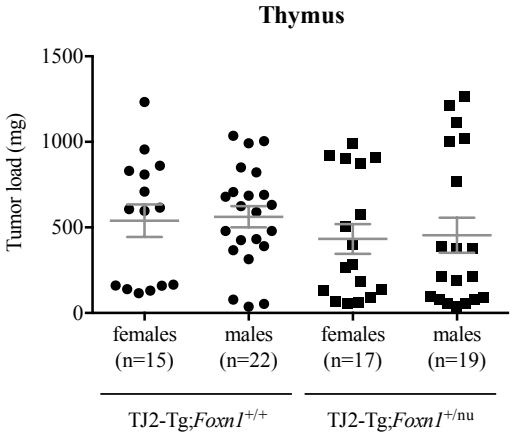

Figure 3.25. Mouse sex does not affect tumor load. Weight of the collected thymic lymphomas of advanced-stage disease of TJ2-Tg;*Foxn1* mice, for each genotype, separated by sex. Data are expressed with mean ± SEM error bars, with number of mice in each group is given between parentheses.

Gene expression analysis on a subset of whole thymic lymphomas by RT-qPCR revealed that at disease endpoint, *Foxn1* haploinsufficiency had no major influence on stromal gene expression (Figure 3.26), including those genes found to be differentially expressed in TJ2-Tg relative to wild-type samples (Figure 3.11). The thymic lymphomas analyzed were

randomly selected and, as expected from our previous data, were collected from significantly older TJ2-Tg;*Foxn1*$^{+/nu}$ mice than TJ2-Tg;*Foxn1*$^{+/+}$ mice (Figure 3.27). Confirming that the analyzed samples were representative of the whole groups, the average thymic tumor load was not significantly different between genotypes. These data support the notion that once it arises, the disease development is similar between both cohorts of TJ2-Tg;*Foxn1* mice.

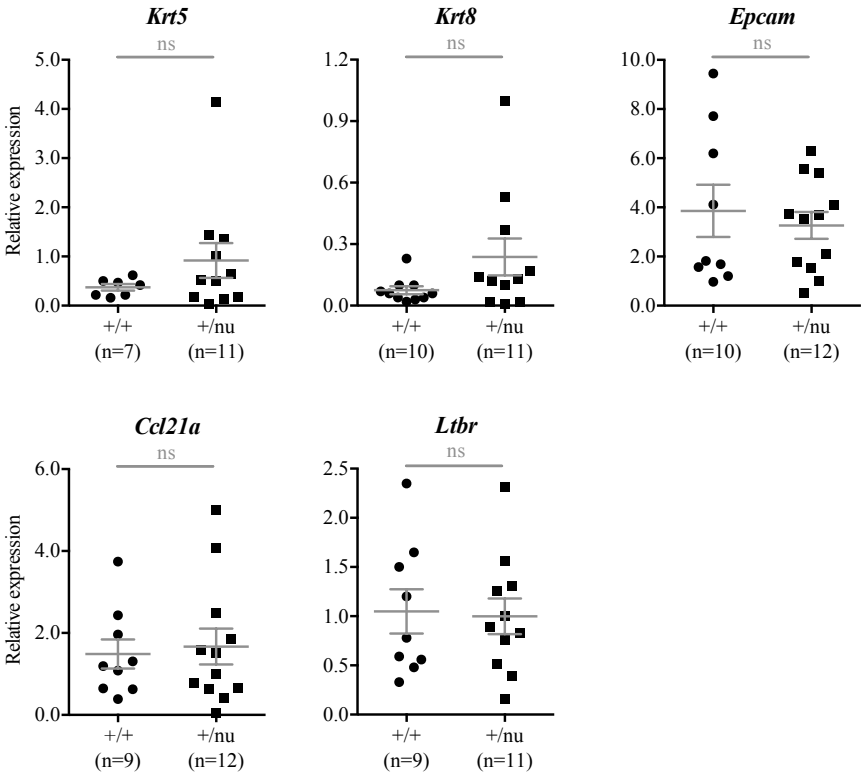

Figure 3.26. *Foxn1* haploinsufficiency has no major influence on gene expression in whole TJ2-Tg thymic lymphomas. RT-qPCR quantification of *Krt5*, *Krt8*, *Epcam*, *Ccl21a* and *Ltbr* thymic stromal gene expression in whole thymic lymphomas of TJ2-Tg;*Foxn1*$^{+/+}$ (+/+) and TJ2-Tg;*Foxn1*$^{+/nu}$ (+/nu) mice, at an advanced stage of the disease. Expression of *Hprt* was used as internal reference. All data are expressed with mean ± SEM error bars, with the number of samples given between parentheses. *P* values determined by two-tailed, unpaired *t*-test with Welch's correction (ns, non-significant).

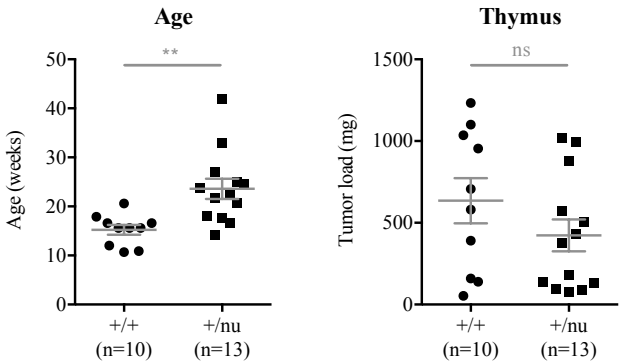

Figure 3.27. Thymic lymphomas used for gene expression analysis from *Foxn1* haploinsufficient mice were older. Age and thymic weight of samples used for RT-qPCR of TJ2-Tg;*Foxn1*$^{+/+}$ (+/+) and TJ2-Tg;*Foxn1*$^{+/nu}$ (+/nu) mice, at an advanced stage of the disease. All data are expressed with mean ± SEM error bars, with the number of samples given between parentheses. *P* values determined by two-tailed, unpaired *t*-test with Welch's correction (**, $P < 0.01$; ns, non-significant).

3.2.2. TJ2-Tg-induced early stage thymic leukemogenesis is delayed by *Foxn1* haploinsufficiency

As previously reported (Fernandes et al., 2015), leukemic cells in TJ2-Tg mice originate in the thymus. To investigate whether *Foxn1* haploinsufficiency delayed the early stages of thymic leukemogenesis, we monitored the stage of disease progression through $CD8^+CD25^+$ leukemic thymocyte detection in 8-week-old TJ2-Tg mice as previously described (Figure 3.16).

Thymic and splenic weights and cellularity of 8-week-old TJ2-Tg;*Foxn1*$^{+/+}$ and TJ2-Tg;*Foxn1*$^{+/nu}$ mice were not significantly different (Figure 3.28) and did not correlate with the percentage of $CD8^+CD25^+$ leukemic cells in the thymus (Figure 3.29B). Yet, in comparison to TJ2-Tg;*Foxn1*$^{+/+}$ thymi, those from TJ2-Tg;*Foxn1*$^{+/nu}$ littermates displayed a significantly lower percentage of $CD8^+CD25^+$ leukemic cells (Figure 3.29A). This delay in the emergence of leukemic cells in TJ2-Tg;*Foxn1*$^{+/nu}$ thymi translated into a mild delay in peripheral blood leukemia, but not in splenic or bone marrow infiltration.

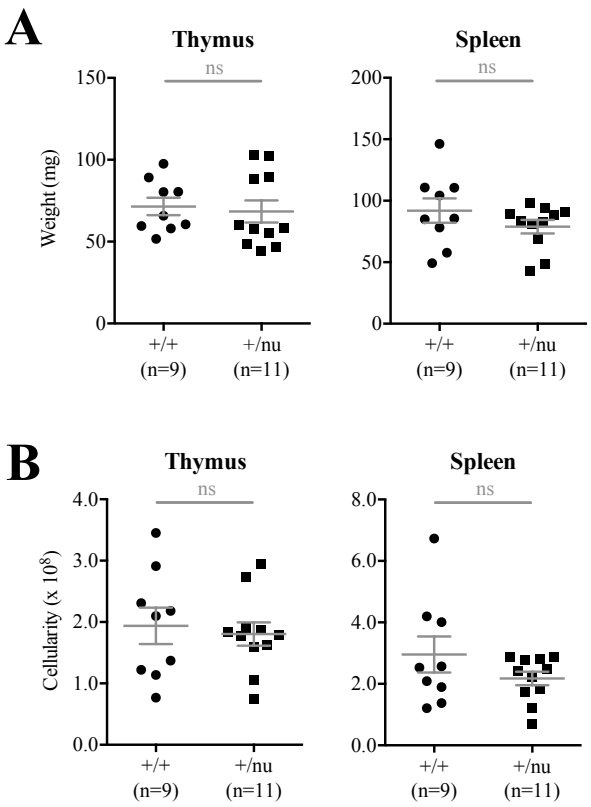

Figure 3.28. *Foxn1* haploinsufficiency does not affect weight or cellularity of young asymptomatic TJ2-Tg mice. Weight (A) and cellularity (B) of thymus and spleen of 8 weeks of age asymptomatic TJ2-Tg;*Foxn1* mice plotted by genotype. Data presented with mean ± SEM; number of mice of TJ2-Tg;*Foxn1*$^{+/+}$ (+/+) and TJ2-Tg;*Foxn1*$^{+/nu}$ (+/nu) mice is given between parentheses. *P* values determined by two-tailed, unpaired *t*-test (ns, non-significant).

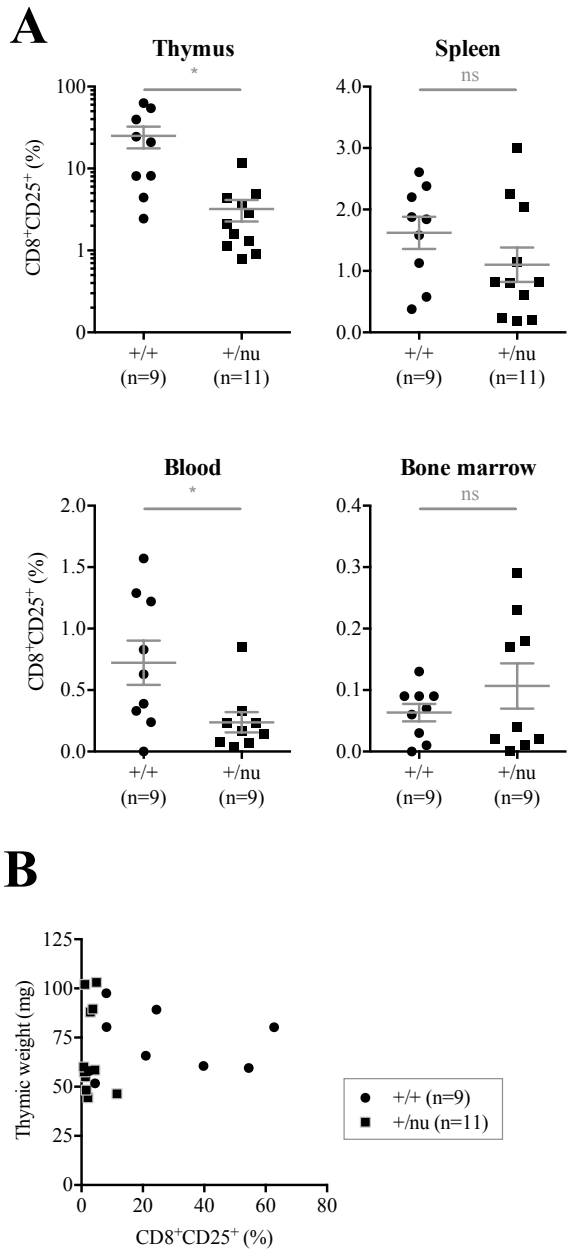

Figure 3.29. TJ2-induced leukemia initiation takes place in the thymus. (A) Percentage of $CD8^+CD25^+$ leukemic cells in thymic, splenic, bone marrow and blood cell suspensions from 8 weeks of age asymptomatic TJ2-Tg;*Foxn1* mice. (B) Thymic weight plotted with percentage of malignant $CD8^+CD25^+$ thymocytes. (A, B) Values of $CD8^+CD25^+$ were obtained by flow cytometry analysis. Data presented with mean ± SEM; number of mice of TJ2-Tg;$Foxn1^{+/+}$ (+/+) and TJ2-Tg;$Foxn1^{+/nu}$ (+/nu) mice is given between parentheses. *P* values determined by two-tailed, unpaired *t*-test with Welch's correction (*, $P < 0.05$; ns, non-significant).

It was previously described that thymic size and cellularity correlated with *Foxn1* dosage (Chen et al., 2009), and that *Foxn1* haploinsufficient pre-adult mice of particular outbred and inbred strains mice presented lower thymic weight than wild-type controls (Kojima et al., 1984; Scheiff et al., 1978). Although no thymic weight differences were found in older (7 to 9 months-old) mice, we observed that the thymic weight of *Foxn1*$^{+/nu}$ mice of 8 or 20 weeks of age was lower than control littermates (Figure 3.30A). However, although *Foxn1*$^{+/+}$ mice presented 1.1-1.3-fold higher thymic weight than *Foxn1*$^{+/nu}$ littermates (Figure 3.30A), TJ2-Tg;*Foxn1*$^{+/+}$ mice at 8 weeks of age presented 7.8-fold more CD8^{+}CD25^{+} leukemic thymocytes (Figure 3.29B) and at 20 weeks of age died from leukemia 2.2-fold more frequently (hazard ratio of 2.93, with 95% CI of 1.90 to 4.51; Figure 3.21) than TJ2-Tg;*Foxn1*$^{+/nu}$ littermates. Thymic weight discrimination by sex showed that at 8-9 weeks and 7-9 months the differences between females of different genotype were not significant (Figure 3.30C), although TJ2-Tg;*Foxn1*$^{+/nu}$ females showed a statistically significant delay in leukemia onset (Figure 3.24). In sum, although we cannot formally exclude that possibility, we consider that reduced thymocyte cellularity in TJ2-Tg;*Foxn1*$^{+/nu}$ mice is not the – or at least not the main – cause of delayed leukemogenesis.

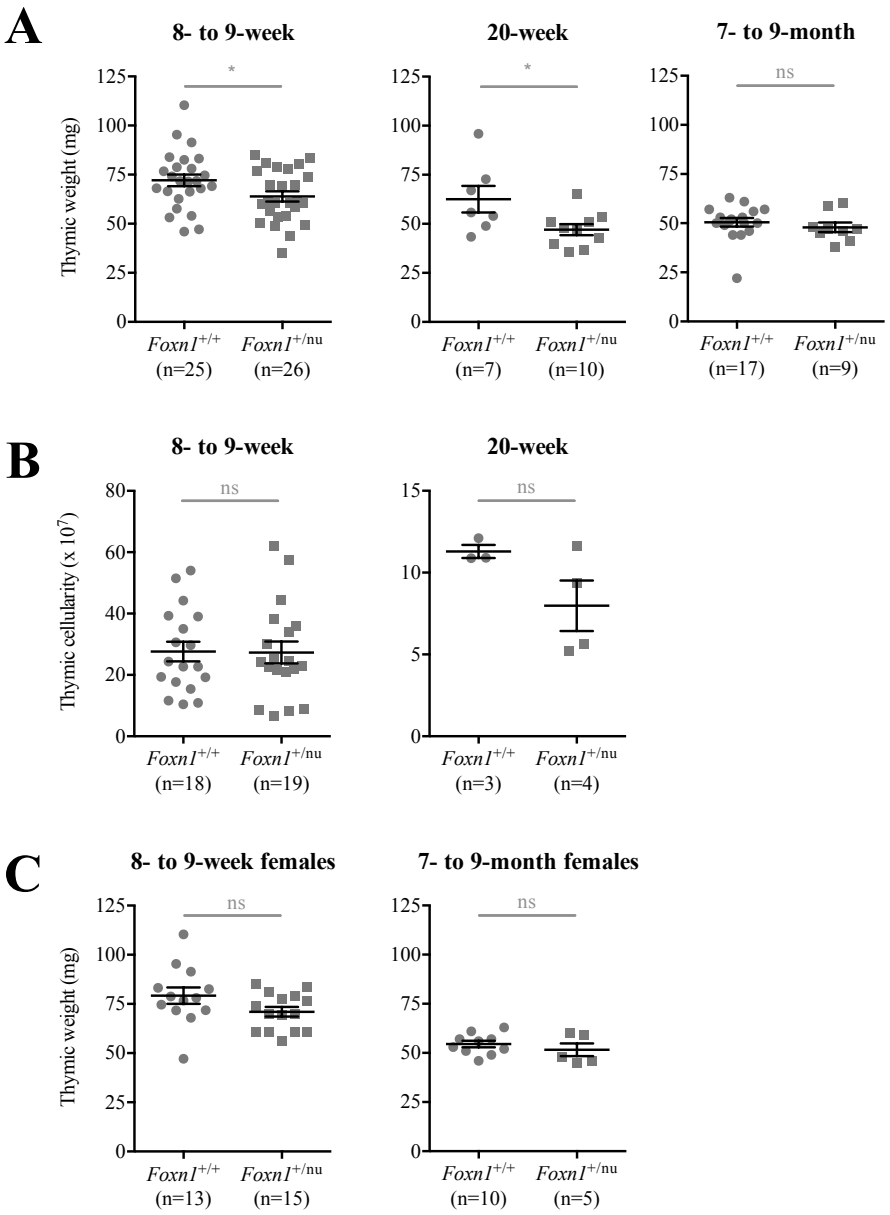

Figure 3.30. *Foxn1* haploinsufficiency leads to mild reduction in thymic weight without causing major perturbations in thymic development. (A) Thymi from healthy 8-9 weeks, 20 weeks and 7-9 months of age mice carrying one (*Foxn1*$^{+/nu}$) or both (*Foxn1*$^{+/+}$) normal *Foxn1* alleles were weighed. (B) Cellularity from 8-9 and 20 weeks of age mice was calculated. (C) Thymic weight from 20 weeks and 7-9 months of age female mice. (A-C) Data sets presented with mean ± SEM error bars; the number of mice is given between parentheses; statistical analysis by two-tailed, unpaired *t*-test (*, $P < 0.05$; ns, non-significant).

3.2.3. The *Foxn1*-dependent thymic microenvironment facilitates leukemic cell expansion

In order to determine the role of *Foxn1*-dependent microenvironment in the maintenance of leukemic cells, these were collected from diseased TJ2-Tg mice and intravenously transplanted into nonconditioned syngeneic *Foxn1*$^{+/nu}$ and *Foxn1*$^{+/+}$ littermate controls (Figure 3.31A). When manifesting signs of disease, recipient mice were killed for analysis. Despite the spleen and liver being the most affected organs, thymi from all recipient mice became infiltrated by leukemic cells, as revealed by flow cytometry detection of CD8^{+}CD25^{+} cells (Figure 3.31B). Results from two independent experiments, one with male and another with female recipients, revealed no statistically significant differences in the thymus, spleen or liver tumor load (Figure 3.31C). However, the thymi tended to be lighter in *Foxn1*$^{+/nu}$ recipients. Since the sample number was low in each experiment, we normalized and pooled the thymic weight values. By doing so, we found that *Foxn1*$^{+/nu}$ mice displayed statistically significant lower thymic weight than *Foxn1*$^{+/+}$ littermates (Figure 3.31D). In contrast, the relative splenic and hepatic tumor load remained similar between *Foxn1*$^{+/+}$ and *Foxn1*$^{+/nu}$ mice (Figure 3.31D). These results indicate therefore that *Foxn1* expression plays a role in facilitating leukemic cell expansion in the thymus.

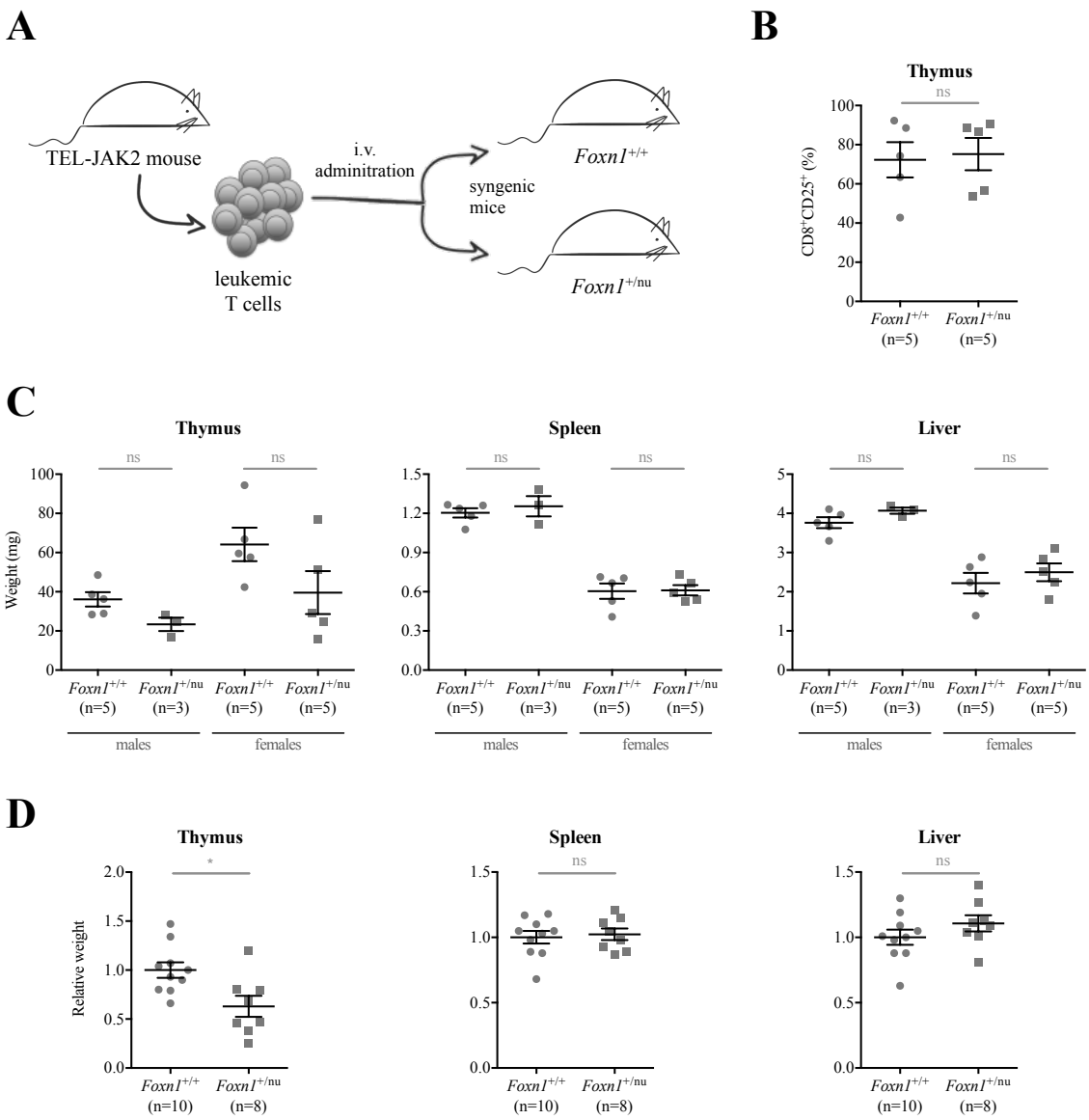

Figure 3.31. *Foxn1* haploinsufficiency impairs leukemic cell expansion in recipient mouse thymi. *Foxn1*$^{+/+}$ and *Foxn1*$^{+/nu}$ mice infused with leukemic cells were killed when manifesting symptoms of disease. (A) Transplantation design schematics. (B) Flow cytometry analysis of thymic cell suspensions showed similar infiltration by $CD8^{+}CD25^{+}$ leukemic cells independently of genotype. Data representative of one of two independent experiments performed with two different leukemic samples. (C) Thymic weight of recipient mice from two independent experiments, one with male and another with female recipients. (C) Relative organ weights from recipient mice of these two transplantation experiments were pooled after normalization based on the average weight of the wild-type (*Foxn1*$^{+/+}$) animals in each experiment. (B-D) Data representing the transplanted *Foxn1*$^{+/+}$ and *Foxn1*$^{+/nu}$ mice, with the number of animals indicated between parentheses. Data presented with mean ± SEM; *P* value determined by two-tailed, unpaired *t*-test (*, $P < 0.05$; ns, non-significant).

3.3. Identification of dose-dependent thymic epithelial cell-specific FoxN1 target genes

3.3.1. *Foxn1* haploinsufficiency is associated with reduced target gene expression

Since FoxN1 is a transcription factor expressed in thymic epithelial cells, its leukemia-promoting role is likely mediated by induction of target genes. By analyzing *Foxn1*$^{+/nu}$ and *Foxn1*$^{+/+}$ whole thymi, we found that *Ccl25*, a well-recognized FoxN1 target gene in TECs (Nowell et al., 2011; Zuklys et al., 2016), was less expressed in the former samples (Figure 3.32). *Foxn1*$^{+/nu}$ thymi also expressed reduced levels of the mTEC marker *Krt5* but *Psmb11*, a FoxN1 target gene in cTECs (Uddin et al., 2017; Zuklys et al., 2016) (Figure 3.32). These gene expression experiments were performed on whole thymic samples, so it is not possible to determine whether variations in gene expression reflect variations in expression in individual cells or variation in number of cells expressing those genes. For example, the lower expression of *Krt5* in *Foxn1* haploinsufficient thymi may be due to a previously observed reduction in mTEC numbers caused by reduced FoxN1 expression (Chen et al., 2009; Cheng et al., 2010), but gene expression experiments in isolated TECs should be performed.

To test the hypothesis that changes in FoxN1 levels influence target gene expression in individual cells, we stably overexpressed *Foxn1* in the murine 1C6 mTEC cell line, which expresses low levels of *Foxn1* (Figure 3.33). After antibiotic selection and clone isolation, RT-qPCR analysis showed that cells with higher *Foxn1* expression also expressed higher levels of *Krt5* and *Ccl25* mRNA (Figure 3.33). The upregulation of these genes was low and the sample number was small, but the data suggest that FoxN1 induces the expression of *Ccl25* and *Krt5*.

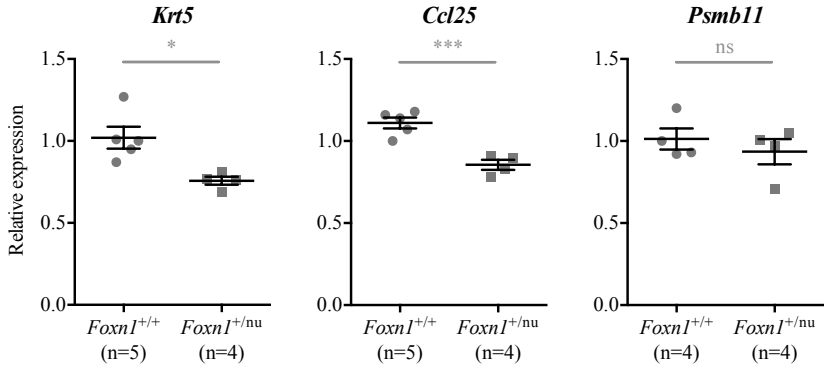

Figure 3.32. *Foxn1* haploinsufficiency leads to reduced target gene expression. Thymic weight and gene expression analysis by RT-qPCR of the *Krt5* mTEC marker, the *Psmb11* cTEC marker, and the *Ccl25* FoxN1 target gene, in whole thymi from the indicated number (n) of wild-type ($Foxn1^{+/+}$) and $Foxn1^{+/nu}$ mice. *Hprt* expression was used as an internal reference. Data presented with mean ± SEM error bars; *P* values determined by two-tailed, unpaired *t*-test (***, $P < 0.001$; *, $P < 0.05$; ns, non-significant).

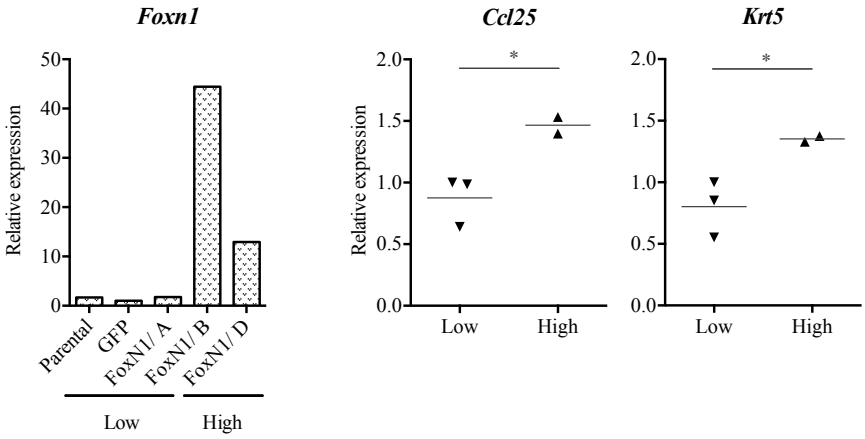

Figure 3.33. Overexpression of *Foxn1* correlates with increased *Ccl25* and *Krt5* expression. A single RT-qPCR expression analysis (in triplicate) of the *Foxn1*, *Ccl25* and *Krt5* genes, relative to the *Gapdh* reference gene was performed for the parental 1C6 cell line and 1C6 clones stably expressing GFP (control plasmid) or FoxN1 (clones FoxN1/A, FoxN1/B and FoxN1/D). For *Krt5* and *Ccl25* gene expression analysis 1C6 cell lines were grouped according to the level of *Foxn1* expression. "Low" includes Parental, GFP and FoxN1/A while "High" includes FoxN1/B and FoxN1/D. Data presented with mean; *P* values determined by two-tailed, unpaired *t*-test (*, $P < 0.05$).

Chapter 4.

Discussion & future perspectives

Although the malignant transformation of thymocytes is triggered by the occurrence of genetic alterations activating or inactivating key regulatory pathways, this process is conditioned and potentially accelerated by the tissue microenvironment. Using a mouse model of JAK/STAT-driven, *Notch1*-mutated T-ALL, our team identified here microenvironmental changes associated with thymic lymphoma development and progression. These included alterations in TECs, with a loss of cortical and an increase of medullary epithelial markers, together with increased proportions of fibroblasts and endothelial cells. Indicating that microenvironmental changes can be involved in the process of disease development, we found that impaired expression of the TEC master regulator FoxN1 transcription factor delayed thymic leukemogenesis.

4.1. Thymic epithelial architectural alterations associated with thymic leukemogenesis

It is well known that the development of normal thymocytes involves interplay between these cells and thymic stromal cells. It is likely that as they emerge, malignant thymocytes also maintain functional interactions with thymic stromal cells. As observed for other malignancies, we hypothesize that, for T-ALL, thymic stromal factors are pro-leukemogenic and that leukemic cells influence stromal cell biology. Supporting the first hypothesis, we found by performing *in vitro* co-cultures that leukemic T cells require the interaction with stromal cells for increased survival. To gain insights on the role of the microenvironment in T-cell leukemia development, we first set out to characterize the thymic lymphoma microenvironment by immunohistology. The data presented here showed severe alterations in the thymic epithelial compartment of TJ2-Tg mice as leukemia progresses.

Diseased TJ2-Tg mice present large thymic lymphomas with loss of cortical-medullary demarcation and frequent disruption of the thymic capsule, as previously reported (Carron et al., 2000; dos Santos et al., 2008) and as observed in other mouse models of T-ALL (Bain et al., 1997; Goodman and Block, 1963; Siegler et al., 1964; Yan et al., 1997). In this work, one striking immunohistological feature observed in advanced TJ2-Tg mouse thymic lymphomas was the presence of conspicuous keratin-negative areas. These were previously found in thymic lymphomas from other mouse models and to increase in size with disease progression

(Davey et al., 1996; Triplett et al., 2016). In TJ2-Tg mice, KNAs contained many fibroblasts and laminin-containing extracellular matrix. Together, these observations lead to the hypothesis that with progression, leukemic cells invade the capsular connective tissue and ultimately expand outwardly from epithelial regions, thus creating KNAs. By studying earlier stage spontaneous thymic lymphomas, we found that the normal corticomedullary demarcation was rapidly lost. This phenomenon was accompanied by a reduction in cortical (Krt8, Ly51) and increase in medullary (Krt5, ICAM-1, Ccl21) marker expression. These findings agree with earlier histological studies reporting cortical atrophy and medullary area increase observed at pre-leukemic stages of several models of viral-induced murine thymic lymphoma (Arnesen, 1958; Dunn et al., 1961; Goodman and Block, 1963; Metcalf, 1966; Siegler and Rich, 1963). Our data thus support the concept that upon emergence of leukemic cells in the thymus, these disseminate throughout all thymic compartments and alter TEC differentiation and/or distribution before invading the thymic capsule and other tissues/organs in more advanced stages.

Although immunohistology of thymi from pre-leukemic TJ2-Tg mice to know whether TEC alterations precede malignancy has not been performed, we think that they are a consequence of thymocyte malignant transformation. In this line, experiments performed in our laboratory led to the observation that leukemic cell colonization of thymi from healthy mice previously intravenously injected with TJ2-Tg leukemic cells resulted in disruption of cortico-medullary organization and loss of cortical areas.

One feature of our animal model is the biomolecular and histological heterogeneity of the TJ2-thymic lymphomas. As an example, that can be observed in the wide range of expression of *Epcam* and *Ccl21a* in endpoint TJ2-Tg thymic lymphomas. Also, occasionally we have found that one of the thymic lobes was more expanded than the other (data not shown). Such events could be caused by different mechanisms, but more likely result from the unilateral initiation and expansion of leukemic cells from one thymic lobe, as reported in another mouse model (Siegler and Rich, 1963). Having the heterogeneity in consideration, we wanted to determine the proportion of thymic epithelial cell subtypes (cortical and medullary TECs) in lymphomas by flow cytometry and their localization in the thymic microenvironment (through immunofluorescence). To perform the TEC characterization, in collaboration from Dr. Nuno L. Alves's group, we separated and analyzed thymic stromal cells through enzymatic matrix digestion and flow cytometry. Since for each thymic lymphoma sample we wanted to obtain information from both flow cytometry and immunofluorescence, we could

not determine the total number of TECs in wild-type and lymphoma thymi, but only qualitative information. Quantitative analyses would be important to assess whether mTEC or cTEC absolute numbers are changed upon disease.

To better understand what are the first histological alterations during thymic leukemogenesis, thymic stromal cell populations should be analyzed at the most early stages of TJ2-induced leukemia, using whole thymic samples from 8- to 10-week mice. Studying not only TEC numbers/percentages, but also expression of TEC genes (i.e. *Krt8*, *Psmb*, *Krt5*, *Icam1*, *Ccl21a*) from sorted TEC samples should determine whether the reduction of thymic epithelial markers we observed in whole samples was due to a diminution of the respective TEC population, an effective reduction in gene expression or a combination of both.

The results here presented reiterate the interconnected fates of thymocytes and stromal cells. Yet, through these experiments alone we were not able to identify the individual factor(s) that is (are) relevant for the development and maintenance of the TJ2-Tg-induced leukemia.

4.2. The FoxN1-dependent thymic microenvironment facilitates thymic leukemogenesis

FoxN1 is a pivotal transcription factor for thymus and skin epithelial cell differentiation in rodents and humans (Romano et al., 2013), but its role in cancer is less clear. Relatively recent evidence indicated that FoxN1 suppresses the transition from benign to malignant keratinocyte lesions (Mandinova et al., 2009). Another report also supporting an anti-oncogenic role showed that *Foxn1* haploinsufficiency accelerated thymic leukemogenesis in the endogenous retroviruses-expressing AKR murine strain (Shisa et al., 1986). In contrast, we report here that loss of one *Foxn1* allele actually hindered both the onset of spontaneous TEL-JAK2-induced leukemia/lymphoma and the thymus colonization by donor leukemic cells. Since leukemogenesis in TJ2-Tg mice is initiated in the thymus (dos Santos et al., 2007; Fernandes et al., 2015) and TECs are the only cells expressing *Foxn1*, we conclude that the delayed leukemogenesis in heterozygotes is caused by FoxN1-mediated defects in these cells and not thymocyte intrinsic defects. FoxN1 was shown to control TEC differentiation in a dose-sensitive manner (Chen et al., 2009). Although *Foxn1* haploinsufficiency does not

appear affect keratinocyte differentiation and hair development, it was shown to cause a moderate reduction in thymic weight of young mice (up to 5 weeks of age) from different outbred and inbred strains (Chen et al., 2009; Kojima et al., 1984; Scheiff et al., 1978). We have observed such reduction in thymic weight in older *Foxn1*$^{+/nu}$ mice (8 and 20 weeks of age) as compared to littermates, but also found that this difference is attenuated with age-associated thymic involution. The reduced thymic weight from birth and concomitant decreased thymocyte production reported in mice with *Foxn1* haploinsufficiency (Chen et al., 2009) could explain the observed delay in TJ2-Tg leukemogenesis, even if that interpretation was apparently unfounded in the context of AKR-induced leukemogenesis, which is accelerated by *Foxn1* haploinsufficiency (Shisa et al., 1986). Supporting the notion that a delay in leukemogenesis caused by *Foxn1* haploinsufficiency cannot be attributed to a mere decrease in thymocyte cellularity, we noticed that the decrease in adult thymic weight caused by loss of one *Foxn1* allele was much less pronounced (1.3-fold) than the delay in both emergence of thymic leukemic cells (9-fold) and leukemia-related death of TJ2-Tg mice (2.2-fold at 20 weeks of age). Since a role for reduced thymocyte cellularity cannot be excluded, we nonetheless acknowledge that the impairment on thymic leukemogenesis caused by *Foxn1* haploinsufficiency might result from both a reduction in thymocyte cellularity and an as yet unidentified mechanism, acting specifically on leukemic cell growth but not on thymocyte development.

4.3. How does TEC-expressed FoxN1 facilitate thymic leukemogenesis?

It is well established that lymphoblastic leukemic T cells need microenvironmental support for survival (Hiai et al., 1981; Ioachim and Furth, 1964; Scupoli et al., 2007; Winter et al., 2001), a concept supported by the observed increased survival of TJ2-Tg mouse leukemic cells in co-culture as compared to monoculture. Our current and previously published data (Fernandes et al., 2015), in agreement with others (Gerby et al., 2014; Hagenbeek and Spits, 2008) indicate the thymus as the site of origin for T-ALL. As previously mentioned, several thymic survival/proliferation factors are involved in disease development. The delayed onset of leukemia displayed by TJ2-Tg;*Foxn1*$^{+/nu}$ mice, but otherwise similar to their littermates in

a more advanced stage, suggests that the thymic microenvironment – specifically the TECs – may play a relevant role not only in progression but also in initiation of TJ2-induced leukemia.

Although the mechanism is not yet clear, we consider that the FoxN1 transcription factor may regulate the expression of target genes/proteins that support leukemogenesis. Being uniquely expressed in the thymus by TECs, the mechanism is likely to be (directly or not) dependent on epithelial cells. Supporting this concept, we observed that *Foxn1* haploinsufficiency was associated with a mild but significantly reduced expression of *Ccl25*, a well-established FoxN1 target gene (Nowell et al., 2011; Zuklys et al., 2016) and a potential growth factor for T-ALL (Mirandola et al., 2012). Future studies should address whether this or other FoxN1 target genes (e.g. *Dll4* and *Cxcl12*) play direct roles in thymic leukemogenesis. Alternatively, *Foxn1* could impinge on leukemogenesis indirectly through changes in TEC biological properties related to communication with other thymic microenvironmental cells, as discussed below.

Since thymic leukemogenesis was found to be accompanied by a relative increase in medullary epithelial markers, we hypothesize that *Foxn1*$^{+/nu}$-associated mTEC differentiation defects underlie the delayed onset of leukemia verified in TJ2-Tg;*Foxn1*$^{+/nu}$ mice. In this line of thought, some investigators (Chen et al., 2009; Cheng et al., 2010) reported that postnatal mTECs were more sensitive to reductions in *Foxn1* expression than cTECs. Others (Nowell et al., 2011), using a different mouse model, concluded that *Foxn1* regulated overall TEC differentiation. Since *Foxn1* null or reduced expression was reported to affect thymic vascularization (Bryson et al., 2013; Mori et al., 2010), it is possible that deficient vascularization underlies delayed leukemogenesis in TJ2-Tg;*Foxn1*$^{+/nu}$ mice. Moreover, TECs were shown to control thymic DC development, differentiation and recruitment (Ito et al., 2006; Lei et al., 2011; Mouri et al., 2014). Thus, it would be interesting to investigate whether *Foxn1* haploinsufficiency is linked to vascular or DC defects.

Previous studies have shown that RelB and LTβR, both mTEC-expressed proteins, are relevant stromal factors in TEL-JAK2-induced leukemogenesis (dos Santos et al., 2008; Fernandes et al., 2015). Additionally, these proteins are essential for thymic medullary development and maintenance, as was shown by the impaired medullary compartment of the respective knock-out mice (Boehm et al., 2003; Burkly et al., 1995). The similarities among RelB, LTβR and FoxN1 regarding their role on leukemogenesis and co-expression in mTECs could be a hint for the job of the mTEC or other medullary cell type in leukemogenesis. To

test this hypothesis, one could test the effect of specifically impairing mTEC differentiation (e.g. Aire knock-out) on leukemogenesis.

4.4. Role for other stromal cells in thymic leukemogenesis

Using a panel of different cellular markers, we detected major numerical and spatial distribution alterations in thymic stromal cell types at early and advanced stages of TJ2-induced leukemia. Most notably, we observed increased staining by CD31 and ER-TR7 antibodies, markers for endothelial cells and thymic fibroblasts, respectively. These findings suggest that angiogenesis, fibroblast proliferation and accrued ECM deposition, which are often associated with cancer (Kalluri, 2016) may favor thymic lymphomagenesis, especially at the most advanced stages. We have also found expression of markers for macrophages (F4/80) and DCs (DEC205) in advanced stage lymphomas. While macrophages have often been noticed in mouse thymic lymphomas (Dunn et al., 1961; Messika et al., 1991; Metcalf, 1966), recent studies indicate that lymphoma-associated macrophages stimulate T-ALL proliferation (Chen et al., 2015). Our findings reinforce the notion that tumor-associated macrophages may be involved in T-cell leukemogenesis, and merit further investigation. DCs are usually associated with an anti-tumoral role via their function in adaptive immunity as tumor antigen-presenting cells (Palucka and Banchereau, 2012). However, it was recently shown that DCs favored survival or proliferation of B and T leukemic cells (Heinig et al., 2014; Triplett et al., 2016). More specifically, Triplett et al. (2016) reported that thymic lymphoma-derived DCs promoted leukemic T cell survival through IGF-1 and PDGF (platelet-derived growth factor) secretion. To test the role of these cell types in leukemogenesis, one could assess the impact of blocking differentiation of these cells on leukemogenesis. That could be achieved by using KO mice for essential proteins, such as NR4A1 for thymic macrophages (Tacke et al., 2015) or Batf3 for thymic DCs (Leventhal et al., 2016).

4.5. Outlook

The thymic microenvironment is composed of an intricate collection of different cell types and factors; being therefore reasonable that more than one cell type/factor could be involved in TJ2-Tg leukemogenesis. In fact, all the previously mentioned studies report the involvement of different cell types, such as TECs and DCs, and different molecular factors, such as chemokines, Notch1, LTβR, RelB and IGF-1 (Figure 4.1). It would be interesting to find if there is one key factor that controls all downstream targets, directly or not, or if different events/signaling pathways act in parallel.

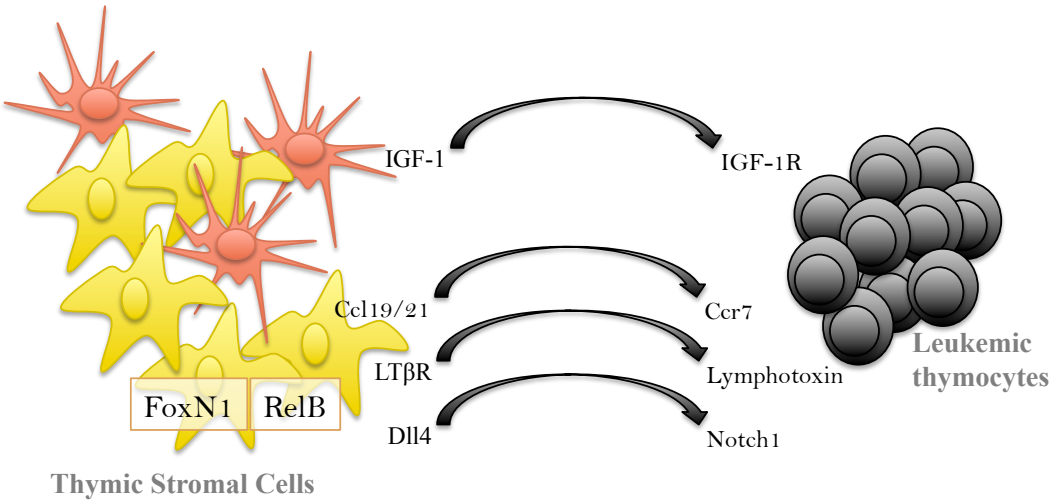

Figure 4.1. Influence of thymic stromal cell signaling in T-ALL. Communication between thymic stromal cells and TJ2-Tg leukemic thymocytes is achieved by different factors, such as IGF-1R, Ccr7, Lymphotoxin and Notch1, expressed by leukemic thymocytes, while FoxN1- and RelB- expressing thymic epithelial cells (represented in yellow) produce Ccl19 and Ccl21, LTβR and Dll4, and dendritic cells (represented in orange) produce IGF-1.

And yet, the influence of FoxN1 in thymic epithelial cells and the fact that *Foxn1* haploinsufficiency is enough to impact the average survival of TJ2-Tg mice indicates that TECs are indeed a key player in leukemogenesis. Although it remains to be determined whether this role is mediated directly by its downstream targets, or indirectly through changes in *Foxn1*-expressing, or other microenvironmental cells remains to be determined (Figure 4.2).

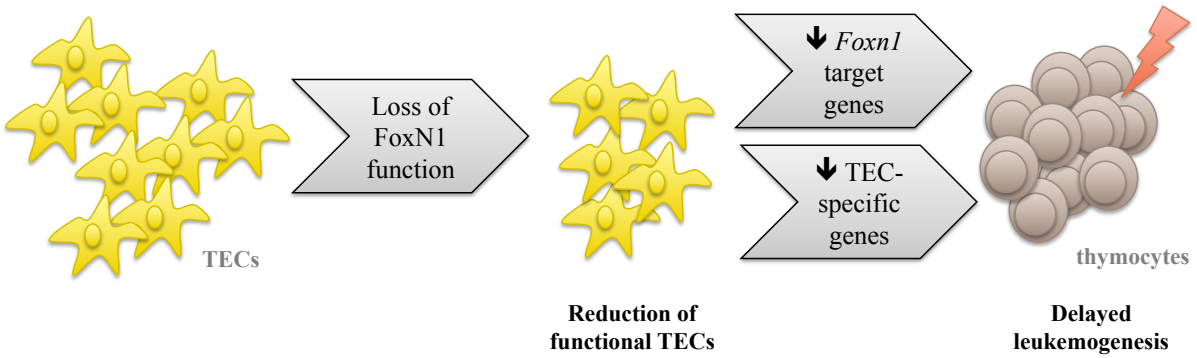

Figure 4.2. Working hypothesis on the role of FoxN1 in TJ2-Tg leukemogenesis. Loss of FoxN1 function by haploinsufficiency in thymic epithelial cells (TECs) causes a decrease in the number of these cells in the thymus, leading to a reduced expression of *Foxn1* target genes and TEC.specific genes. It is still to be determined if the delayed onset of TJ2-Tg leukemia is a consequence of one of these target/specific gene reductions, both or by another unraveled mechanism, yet to be determined.

Following the results here presented, it would be important to further investigate the early stages of TJ2-Tg leukemia, in hope to understand which factors are indeed favoring leukemogenesis. Next-generation sequencing results have already yelded a set of upregulated and downregulated genes in different cell type subsets. Yet to be carried out is the validation of these results, by RT-qPCR, in a more extensive set of wild-type and TJ2-Tg thymic samples (T-cell- and stromal-enriched, and whole thymus) using as candidate genes those most differentially expressed genes. This would allow broadening the number of samples and therefore obtain data, statistically more significant, that would provide meaningful information on the factors that influence the development of TJ2-Tg-induced leukemia. Since our transcriptomic analysis on unsorted cells revealed consistent gene expression differences between wild-type and diseased thymic stromal samples, it would be interesting to perform transcriptomic analyses on purified stromal cells to detect gene expression changes associated with leukemia development. Such experiments could shed light on the functional relationship between stromal cells and malignant T cells.

In addition to the previously mentioned follow-up studies, future studies should also aim to identify and inactivate *in vivo* stromal cells and factors that directly or indirectly promote T-ALL development, for example through *in vivo* expression of toxic molecules (e.g. thymidine kinase or diphtheria toxin) in particular thymic stromal cell types. Understanding how T-ALL develops and what factors are critical in that process may uncover new targets for more efficient treatments, to reduce chemoresistance and relapse, which is the major cause of death in T-ALL cases.

References

Aifantis, I., Raetz, E., and Buonamici, S. (2008). Molecular pathogenesis of T-cell leukaemia and lymphoma. Nat Rev Immunol *8*, 380-390.

Akiyama, T., Shimo, Y., Yanai, H., Qin, J., Ohshima, D., Maruyama, Y., Asaumi, Y., Kitazawa, J., Takayanagi, H., Penninger, J.M.*, et al.* (2008). The tumor necrosis factor family receptors RANK and CD40 cooperatively establish the thymic medullary microenvironment and self-tolerance. Immunity *29*, 423-437.

Akiyama, T., Shinzawa, M., and Akiyama, N. (2012). TNF receptor family signaling in the development and functions of medullary thymic epithelial cells. Front Immunol *3*, 278.

Alexandropoulos, K., and Danzl, N.M. (2012). Thymic epithelial cells: antigen presenting cells that regulate T cell repertoire and tolerance development. Immunol Res *54*, 177-190.

Allman, D., Karnell, F.G., Punt, J.A., Bakkour, S., Xu, L., Myung, P., Koretzky, G.A., Pui, J.C., Aster, J.C., and Pear, W.S. (2001). Separation of Notch1 promoted lineage commitment and expansion/transformation in developing T cells. J Exp Med *194*, 99-106.

Alves, N.L., Huntington, N.D., Rodewald, H.R., and Di Santo, J.P. (2009a). Thymic epithelial cells: the multi-tasking framework of the T cell "cradle". Trends in immunology *30*, 468-474.

Alves, N.L., Richard-Le Goff, O., Huntington, N.D., Sousa, A.P., Ribeiro, V.S., Bordack, A., Vives, F.L., Peduto, L., Chidgey, A., Cumano, A.*, et al.* (2009b). Characterization of the thymic IL-7 niche in vivo. Proc Natl Acad Sci U S A *106*, 1512-1517.

Alves, N.L., Takahama, Y., Ohigashi, I., Ribeiro, A.R., Baik, S., Anderson, G., and Jenkinson, W.E. (2014). Serial progression of cortical and medullary thymic epithelial microenvironments. European journal of immunology *44*, 16-22.

Anderson, G., and Takahama, Y. (2012). Thymic epithelial cells: working class heroes for T cell development and repertoire selection. Trends in immunology *33*, 256-263.

Armstrong, F., Brunet de la Grange, P., Gerby, B., Rouyez, M.C., Calvo, J., Fontenay, M., Boissel, N., Dombret, H., Baruchel, A., Landman-Parker, J.*, et al.* (2009). NOTCH is a key regulator of human T-cell acute leukemia initiating cell activity. Blood *113*, 1730-1740.

Arnesen, K. (1958). Preleukemic and early leukemic changes in the thymus of mice; a study of the AKR/O strain. Acta Pathol Microbiol Scand *43*, 350-364.

Aster, J.C., Xu, L., Karnell, F.G., Patriub, V., Pui, J.C., and Pear, W.S. (2000). Essential roles for ankyrin repeat and transactivation domains in induction of T-cell leukemia by notch1. Mol Cell Biol *20*, 7505-7515.

Bain, G., Engel, I., Robanus Maandag, E.C., te Riele, H.P., Voland, J.R., Sharp, L.L., Chun, J., Huey, B., Pinkel, D., and Murre, C. (1997). E2A deficiency leads to abnormalities in alphabeta T-cell development and to rapid development of T-cell lymphomas. Mol Cell Biol *17*, 4782-4791.

Balkwill, F. (2004). Cancer and the chemokine network. Nat Rev Cancer *4*, 540-550.

Basso, K., Mussolin, L., Lettieri, A., Brahmachary, M., Lim, W.K., Califano, A., Basso, G., Biondi, A., Cazzaniga, G., and Rosolen, A. (2011). T-cell lymphoblastic lymphoma shows differences and similarities with T-cell acute lymphoblastic leukemia by genomic and gene expression analyses. Genes Chromosomes Cancer *50*, 1063-1075.

Belver, L., and Ferrando, A. (2016). The genetics and mechanisms of T cell acute lymphoblastic leukaemia. Nat Rev Cancer *16*, 494-507.

Bene, M.C., Castoldi, G., Knapp, W., Ludwig, W.D., Matutes, E., Orfao, A., and van't Veer, M.B. (1995). Proposals for the immunological classification of acute leukemias. European Group for the Immunological Characterization of Leukemias (EGIL). Leukemia *9*, 1783-1786.

Blackburn, C.C., and Manley, N.R. (2004). Developing a new paradigm for thymus organogenesis. Nat Rev Immunol *4*, 278-289.

Bleul, C.C., Corbeaux, T., Reuter, A., Fisch, P., Monting, J.S., and Boehm, T. (2006). Formation of a functional thymus initiated by a postnatal epithelial progenitor cell. Nature *441*, 992-996.

Boehm, T., Scheu, S., Pfeffer, K., and Bleul, C.C. (2003). Thymic medullary epithelial cell differentiation, thymocyte emigration, and the control of autoimmunity require lympho-epithelial cross talk via LTbetaR. J Exp Med *198*, 757-769.

Boyd, R.L., Tucek, C.L., Godfrey, D.I., Izon, D.J., Wilson, T.J., Davidson, N.J., Bean, A.G., Ladyman, H.M., Ritter, M.A., and Hugo, P. (1993). The thymic microenvironment. Immunol Today *14*, 445-459.

Bredenkamp, N., Nowell, C.S., and Blackburn, C.C. (2014). Regeneration of the aged thymus by a single transcription factor. Development *141*, 1627-1637.

Bromley, S.K., Mempel, T.R., and Luster, A.D. (2008). Orchestrating the orchestrators: chemokines in control of T cell traffic. Nat Immunol *9*, 970-980.

Bryson, J.L., Griffith, A.V., Hughes, B., 3rd, Saito, F., Takahama, Y., Richie, E.R., and Manley, N.R. (2013). Cell-autonomous defects in thymic epithelial cells disrupt endothelial-perivascular cell interactions in the mouse thymus. PLoS One *8*, e65196.

Bunting, M.D., Comerford, I., and McColl, S.R. (2011). Finding their niche: chemokines directing cell migration in the thymus. Immunol Cell Biol *89*, 185-196.

Buonamici, S., Trimarchi, T., Ruocco, M.G., Reavie, L., Cathelin, S., Mar, B.G., Klinakis, A., Lukyanov, Y., Tseng, J.C., Sen, F.*, et al.* (2009). CCR7 signalling as an essential regulator of CNS infiltration in T-cell leukaemia. Nature *459*, 1000-1004.

Burkhardt, B. (2010). Paediatric lymphoblastic T-cell leukaemia and lymphoma: one or two diseases? Br J Haematol *149*, 653-668.

Burkly, L., Hession, C., Ogata, L., Reilly, C., Marconi, L.A., Olson, D., Tizard, R., Cate, R., and Lo, D. (1995). Expression of relB is required for the development of thymic medulla and dendritic cells. Nature *373*, 531-536.

Calderon, L., and Boehm, T. (2011). Three chemokine receptors cooperatively regulate homing of hematopoietic progenitors to the embryonic mouse thymus. Proc Natl Acad Sci U S A *108*, 7517-7522.

Caramalho, I., Nunes-Cabaco, H., Foxall, R.B., and Sousa, A.E. (2015). Regulatory T-Cell Development in the Human Thymus. Front Immunol *6*, 395.

Carron, C., Cormier, F., Janin, A., Lacronique, V., Giovannini, M., Daniel, M.T., Bernard, O., and Ghysdael, J. (2000). TEL-JAK2 transgenic mice develop T-cell leukemia. Blood *95*, 3891-3899.

Chen, E., Staudt, L.M., and Green, A.R. (2012). Janus kinase deregulation in leukemia and lymphoma. Immunity *36*, 529-541.

Chen, J., Jette, C., Kanki, J.P., Aster, J.C., Look, A.T., and Griffin, J.D. (2007). NOTCH1-induced T-cell leukemia in transgenic zebrafish. Leukemia *21*, 462-471.

Chen, L., Xiao, S., and Manley, N.R. (2009). Foxn1 is required to maintain the postnatal thymic microenvironment in a dosage-sensitive manner. Blood *113*, 567-574.

Chen, S.Y., Yang, X., Feng, W.L., Liao, J.F., Wang, L.N., Feng, L., Lin, Y.M., Ren, Q., and Zheng, G.G. (2015). Organ-specific microenvironment modifies diverse functional and phenotypic characteristics of leukemia-associated macrophages in mouse T cell acute lymphoblastic leukemia. Journal of immunology *194*, 2919-2929.

Cheng, L., Guo, J., Sun, L., Fu, J., Barnes, P.F., Metzger, D., Chambon, P., Oshima, R.G., Amagai, T., and Su, D.M. (2010). Postnatal tissue-specific disruption of transcription factor FoxN1 triggers acute thymic atrophy. J Biol Chem *285*, 5836-5847.

Chiaretti, S., Zini, G., and Bassan, R. (2014). Diagnosis and subclassification of acute lymphoblastic leukemia. Mediterr J Hematol Infect Dis *6*, e2014073.

Coffer, P.J., and Burgering, B.M. (2004). Forkhead-box transcription factors and their role in the immune system. Nat Rev Immunol *4*, 889-899.

Condorelli, G.L., Facchiano, F., Valtieri, M., Proietti, E., Vitelli, L., Lulli, V., Huebner, K., Peschle, C., and Croce, C.M. (1996). T-cell-directed TAL-1 expression induces T-cell malignancies in transgenic mice. Cancer Res *56*, 5113-5119.

Cook, G.J., and Pardee, T.S. (2013). Animal models of leukemia: any closer to the real thing? Cancer Metastasis Rev *32*, 63-76.

Cooper, S.L., and Brown, P.A. (2015). Treatment of pediatric acute lymphoblastic leukemia. Pediatr Clin North Am *62*, 61-73.

Corpet, F. (1988). Multiple sequence alignment with hierarchical clustering. Nucleic Acids Res *16*, 10881-10890.

Coustan-Smith, E., Mullighan, C.G., Onciu, M., Behm, F.G., Raimondi, S.C., Pei, D., Cheng, C., Su, X., Rubnitz, J.E., Basso, G.*, et al.* (2009). Early T-cell precursor leukaemia: a subtype of very high-risk acute lymphoblastic leukaemia. Lancet Oncol *10*, 147-156.

Cyster, J.G., and Schwab, S.R. (2012). Sphingosine-1-phosphate and lymphocyte egress from lymphoid organs. Annu Rev Immunol *30*, 69-94.

Davey, G.M., Tucek-Szabo, C.L., and Boyd, R.L. (1996). Characterization of the AKR thymic microenvironment and its influence on thymocyte differentiation and lymphoma development. Leuk Res *20*, 853-866.

De Keersmaecker, K., Real, P.J., Gatta, G.D., Palomero, T., Sulis, M.L., Tosello, V., Van Vlierberghe, P., Barnes, K., Castillo, M., Sole, X.*, et al.* (2010). The TLX1 oncogene drives aneuploidy in T cell transformation. Nat Med *16*, 1321-1327.

Desanti, G.E., Cowan, J.E., Baik, S., Parnell, S.M., White, A.J., Penninger, J.M., Lane, P.J., Jenkinson, E.J., Jenkinson, W.E., and Anderson, G. (2012). Developmentally regulated availability of RANKL and CD40 ligand reveals distinct mechanisms of fetal and adult cross-talk in the thymus medulla. Journal of immunology *189*, 5519-5526.

dos Santos, N.R., Rickman, D.S., de Reynies, A., Cormier, F., Williame, M., Blanchard, C., Stern, M.H., and Ghysdael, J. (2007). Pre-TCR expression cooperates with TEL-JAK2 to transform immature thymocytes and induce T-cell leukemia. Blood *109*, 3972-3981.

dos Santos, N.R., Williame, M., Gachet, S., Cormier, F., Janin, A., Weih, D., Weih, F., and Ghysdael, J. (2008). RelB-Dependent Stromal Cells Promote T-Cell Leukemogenesis. PLoS ONE *3*, e2555.

Doulatov, S., Notta, F., Laurenti, E., and Dick, J.E. (2012). Hematopoiesis: a human perspective. Cell Stem Cell *10*, 120-136.

Dumortier, A., Jeannet, R., Kirstetter, P., Kleinmann, E., Sellars, M., dos Santos, N.R., Thibault, C., Barths, J., Ghysdael, J., Punt, J.A.*, et al.* (2006). Notch activation is an early and critical event during T-Cell leukemogenesis in Ikaros-deficient mice. Mol Cell Biol *26*, 209-220.

Dunn, T.B., Moloney, J.B., Green, A.W., and Arnold, B. (1961). Pathogenesis of a virus-induced leukemia in mice. J Natl Cancer Inst *26*, 189-221.

Eissner, G., Kolch, W., and Scheurich, P. (2004). Ligands working as receptors: reverse signaling by members of the TNF superfamily enhance the plasticity of the immune system. Cytokine Growth Factor Rev *15*, 353-366.

Fernandes, M.T., Dejardin, E., and dos Santos, N.R. (2016). Context-dependent roles for lymphotoxin-beta receptor signaling in cancer development. Biochim Biophys Acta *1865*, 204-219.

Fernandes, M.T., Ghezzo, M.N., Silveira, A.B., Kalathur, R.K., Povoa, V., Ribeiro, A.R., Brandalise, S.R., Dejardin, E., Alves, N.L., Ghysdael, J.*, et al.* (2015). Lymphotoxin-beta receptor in microenvironmental cells promotes the development of T-cell acute lymphoblastic leukaemia with cortical/mature immunophenotype. Br J Haematol *171*, 736-751.

Forster, R., Davalos-Misslitz, A.C., and Rot, A. (2008). CCR7 and its ligands: balancing immunity and tolerance. Nat Rev Immunol *8*, 362-371.

Gerby, B., Tremblay, C.S., Tremblay, M., Rojas-Sutterlin, S., Herblot, S., Hebert, J., Sauvageau, G., Lemieux, S., Lecuyer, E., Veiga, D.F.*, et al.* (2014). SCL, LMO1 and Notch1 reprogram thymocytes into self-renewing cells. PLoS Genet *10*, e1004768.

Ghezzo, M.N. (2009). Identification of the molecular alterations of the thymic microenvironment that favor the onset of T-cell acute lymphoblastic leukemia. MSc Thesis in Biomedical Sciences. Department of Biomedical Sciences and Medicine (Unpublished, University of Algarve).

Ghosh, S., and Hayden, M.S. (2008). New regulators of NF-kappaB in inflammation. Nat Rev Immunol *8*, 837-848.

Golubovskaya, V., and Wu, L. (2016). Different Subsets of T Cells, Memory, Effector Functions, and CAR-T Immunotherapy. Cancers (Basel) *8*.

Goodman, S.B., and Block, M.H. (1963). The Histogenesis of Gross's Viral Induced Mouse Leukemia. Cancer Res *23*, 1634-1640.

Gordon, J., and Manley, N.R. (2011). Mechanisms of thymus organogenesis and morphogenesis. Development *138*, 3865-3878.

Graux, C., Cools, J., Michaux, L., Vandenberghe, P., and Hagemeijer, A. (2006). Cytogenetics and molecular genetics of T-cell acute lymphoblastic leukemia: from thymocyte to lymphoblast. Leukemia *20*, 1496-1510.

Gray, D.H., Chidgey, A.P., and Boyd, R.L. (2002). Analysis of thymic stromal cell populations using flow cytometry. J Immunol Methods *260*, 15-28.

Gray, D.H., Tull, D., Ueno, T., Seach, N., Classon, B.J., Chidgey, A., McConville, M.J., and Boyd, R.L. (2007). A unique thymic fibroblast population revealed by the monoclonal antibody MTS-15. Journal of immunology *178*, 4956-4965.

Hagenbeek, T.J., and Spits, H. (2008). T-cell lymphomas in T-cell-specific Pten-deficient mice originate in the thymus. Leukemia *22*, 608-619.

Hamazaki, Y. (2015). Adult thymic epithelial cell (TEC) progenitors and TEC stem cells: Models and mechanisms for TEC development and maintenance. European journal of immunology *45*, 2985-2993.

Heinig, K., Gatjen, M., Grau, M., Stache, V., Anagnostopoulos, I., Gerlach, K., Niesner, R.A., Cseresnyes, Z., Hauser, A.E., Lenz, P.*, et al.* (2014). Access to follicular dendritic cells is a pivotal step in murine chronic lymphocytic leukemia B-cell activation and proliferation. Cancer Discov *4*, 1448-1465.

Hiai, H., Nishi, Y., Miyazawa, T., Matsudaira, Y., and Nishizuka, Y. (1981). Mouse lymphoid leukemias: symbiotic complexes of neoplastic lymphocytes and their microenvironments. J Natl Cancer Inst *66*, 713-722.

Hikosaka, Y., Nitta, T., Ohigashi, I., Yano, K., Ishimaru, N., Hayashi, Y., Matsumoto, M., Matsuo, K., Penninger, J.M., Takayanagi, H.*, et al.* (2008). The cytokine RANKL produced by positively selected thymocytes fosters medullary thymic epithelial cells that express autoimmune regulator. Immunity *29*, 438-450.

Hirasawa, T., Yamashita, H., and Makino, S. (1998). Genetic typing of the mouse and rat nude mutations by PCR and restriction enzyme analysis. Exp Anim *47*, 63-67.

Hu, D., and Shilatifard, A. (2016). Epigenetics of hematopoiesis and hematological malignancies. Genes Dev *30*, 2021-2041.

Hunger, S.P., and Mullighan, C.G. (2015). Acute Lymphoblastic Leukemia in Children. N Engl J Med *373*, 1541-1552.

Indraccolo, S., Minuzzo, S., Masiero, M., Pusceddu, I., Persano, L., Moserle, L., Reboldi, A., Favaro, E., Mecarozzi, M., Di Mario, G.*, et al.* (2009). Cross-talk between tumor and endothelial cells involving the Notch3-Dll4 interaction marks escape from tumor dormancy. Cancer Res *69*, 1314-1323.

Ioachim, H., and Furth, J. (1964). Intrareticular Cell Multiplication of Leukemic Lymphoblasts in Thymic Tissue Cultures. J Natl Cancer Inst *32*, 339-359.

Irla, M., Hugues, S., Gill, J., Nitta, T., Hikosaka, Y., Williams, I.R., Hubert, F.X., Scott, H.S., Takahama, Y., Hollander, G.A.*, et al.* (2008). Autoantigen-specific interactions with CD4+ thymocytes control mature medullary thymic epithelial cell cellularity. Immunity *29*, 451-463.

Ito, H., Esashi, E., Akiyama, T., Inoue, J., and Miyajima, A. (2006). IL-18 produced by thymic epithelial cells induces development of dendritic cells with CD11b in the fetal thymus. Int Immunol *18*, 1253-1263.

Itoi, M., Tsukamoto, N., Yoshida, H., and Amagai, T. (2007). Mesenchymal cells are required for functional development of thymic epithelial cells. Int Immunol *19*, 953-964.

Jacoby, E., Chien, C.D., and Fry, T.J. (2014). Murine models of acute leukemia: important tools in current pediatric leukemia research. Front Oncol *4*, 95.

Jagannathan-Bogdan, M., and Zon, L.I. (2013). Hematopoiesis. Development *140*, 2463-2467.

Jenkinson, W.E., Jenkinson, E.J., and Anderson, G. (2003). Differential requirement for mesenchyme in the proliferation and maturation of thymic epithelial progenitors. J Exp Med *198*, 325-332.

Jost, T.R., Borga, C., Radaelli, E., Romagnani, A., Perruzza, L., Omodho, L., Cazzaniga, G., Biondi, A., Indraccolo, S., Thelen, M.*, et al.* (2016). Role of CXCR4-mediated bone marrow colonization in CNS infiltration by T cell acute lymphoblastic leukemia. J Leukoc Biol *99*, 1077-1087.

Julien, E., El Omar, R., and Tavian, M. (2016). Origin of the hematopoietic system in the human embryo. FEBS Lett *590*, 3987-4001.

Kalluri, R. (2016). The biology and function of fibroblasts in cancer. Nat Rev Cancer *16*, 582-598.

Kaplan, H.S. (1950). Influence of thymectomy, splenectomy, and gonadectomy on incidence of radiation-induced lymphoid tumors in strain C57 black mice. J Natl Cancer Inst *11*, 83-90.

Karin, M., Cao, Y., Greten, F.R., and Li, Z.W. (2002). NF-kappaB in cancer: from innocent bystander to major culprit. Nat Rev Cancer *2*, 301-310.

Karlsson, A., Ungerback, J., Rasmussen, A., French, J.E., and Soderkvist, P. (2008). Notch1 is a frequent mutational target in chemically induced lymphoma in mouse. Int J Cancer *123*, 2720-2724.

Karrman, K., and Johansson, B. (2017). Pediatric T-cell acute lymphoblastic leukemia. Genes Chromosomes Cancer *56*, 89-116.

Kersey, J., Nesbit, M., Hallgren, H., Sabad, A., Yunis, E., and Gajl-Peczalska, K. (1975). Evidence for origin of certain childhood acute lymphoblastic leukemias and lymphomas in thymus-derived lymphocytes. Cancer *36*, 1348-1352.

Ki, S., Park, D., Selden, H.J., Seita, J., Chung, H., Kim, J., Iyer, V.R., and Ehrlich, L.I. (2014). Global transcriptional profiling reveals distinct functions of thymic stromal subsets and age-related changes during thymic involution. Cell Rep *9*, 402-415.

Klein, L., Kyewski, B., Allen, P.M., and Hogquist, K.A. (2014). Positive and negative selection of the T cell repertoire: what thymocytes see (and don't see). Nat Rev Immunol *14*, 377-391.

Koch, U., and Radtke, F. (2011). Mechanisms of T cell development and transformation. Annu Rev Cell Dev Biol *27*, 539-562.

Kojima, A., Saito, M., Hioki, K., Shimanura, K., and Habu, S. (1984). NFS/N-nu/ + mice can macroscopically be distinguished from NFS/N- +/+ littermates by their thymic size and shape. Exp Cell Biol *52*, 107-110.

Kraal, G., Breel, M., Janse, M., and Bruin, G. (1986). Langerhans' cells, veiled cells, and interdigitating cells in the mouse recognized by a monoclonal antibody. J Exp Med *163*, 981-997.

Kurobe, H., Liu, C., Ueno, T., Saito, F., Ohigashi, I., Seach, N., Arakaki, R., Hayashi, Y., Kitagawa, T., Lipp, M.*, et al.* (2006). CCR7-dependent cortex-to-medulla migration of positively selected thymocytes is essential for establishing central tolerance. Immunity *24*, 165-177.

Lacronique, V., Boureux, A., Valle, V.D., Poirel, H., Quang, C.T., Mauchauffe, M., Berthou, C., Lessard, M., Berger, R., Ghysdael, J.*, et al.* (1997). A TEL-JAK2 fusion protein with constitutive kinase activity in human leukemia. Science *278*, 1309-1312.

Ladi, E., Schwickert, T.A., Chtanova, T., Chen, Y., Herzmark, P., Yin, X., Aaron, H., Chan, S.W., Lipp, M., Roysam, B.*, et al.* (2008). Thymocyte-dendritic cell interactions near sources of CCR7 ligands in the thymic cortex. Journal of immunology *181*, 7014-7023.

Langenau, D.M., Traver, D., Ferrando, A.A., Kutok, J.L., Aster, J.C., Kanki, J.P., Lin, S., Prochownik, E., Trede, N.S., Zon, L.I.*, et al.* (2003). Myc-induced T cell leukemia in transgenic zebrafish. Science *299*, 887-890.

Larson, R.C., Lavenir, I., Larson, T.A., Baer, R., Warren, A.J., Wadman, I., Nottage, K., and Rabbitts, T.H. (1996). Protein dimerization between Lmo2 (Rbtn2) and Tal1 alters thymocyte development and potentiates T cell tumorigenesis in transgenic mice. EMBO J *15*, 1021-1027.

Le Noir, S., Ben Abdelali, R., Lelorch, M., Bergeron, J., Sungalee, S., Payet-Bornet, D., Villarese, P., Petit, A., Callens, C., Lhermitte, L.*, et al.* (2012). Extensive molecular mapping of TCRalpha/delta- and TCRbeta-involved chromosomal translocations reveals distinct mechanisms of oncogene activation in T-ALL. Blood *120*, 3298-3309.

Lei, Y., Ripen, A.M., Ishimaru, N., Ohigashi, I., Nagasawa, T., Jeker, L.T., Bosl, M.R., Hollander, G.A., Hayashi, Y., Malefyt Rde, W.*, et al.* (2011). Aire-dependent production of XCL1 mediates medullary accumulation of thymic dendritic cells and contributes to regulatory T cell development. J Exp Med *208*, 383-394.

Lepique, A.P., Palencia, S., Irjala, H., and Petrie, H.T. (2003). Characterization of vascular adhesion molecules that may facilitate progenitor homing in the post-natal mouse thymus. Clin Dev Immunol *10*, 27-33.

Leventhal, D.S., Gilmore, D.C., Berger, J.M., Nishi, S., Lee, V., Malchow, S., Kline, D.E., Kline, J., Vander Griend, D.J., Huang, H.*, et al.* (2016). Dendritic Cells Coordinate the Development and Homeostasis of Organ-Specific Regulatory T Cells. Immunity *44*, 847-859.

Lin, Y.W., Nichols, R.A., Letterio, J.J., and Aplan, P.D. (2006). Notch1 mutations are important for leukemic transformation in murine models of precursor-T leukemia/lymphoma. Blood *107*, 2540-2543.

Lopes, N., Serge, A., Ferrier, P., and Irla, M. (2015). Thymic Crosstalk Coordinates Medulla Organization and T-Cell Tolerance Induction. Front Immunol *6*, 365.

Luis, T.C., Luc, S., Mizukami, T., Boukarabila, H., Thongjuea, S., Woll, P.S., Azzoni, E., Giustacchini, A., Lutteropp, M., Bouriez-Jones, T.*, et al.* (2016). Initial seeding of the embryonic thymus by immune-restricted lympho-myeloid progenitors. Nat Immunol *17*, 1424-1435.

Ma, F., Manabe, A., Wang, D., Ito, M., Kikuchi, A., Wada, M., Ito, M., Ohara, A., Hosoya, R., Asano, S.*, et al.* (2002). Growth of human T cell acute lymphoblastic leukemia lymphoblasts in NOD/SCID mouse fetal thymus organ culture. Leukemia *16*, 1541-1548.

Malchow, S., Leventhal, D.S., Nishi, S., Fischer, B.I., Shen, L., Paner, G.P., Amit, A.S., Kang, C., Geddes, J.E., Allison, J.P.*, et al.* (2013). Aire-dependent thymic development of tumor-associated regulatory T cells. Science *339*, 1219-1224.

Mandinova, A., Kolev, V., Neel, V., Hu, B., Stonely, W., Lieb, J., Wu, X., Colli, C., Han, R., Pazin, M.J.*, et al.* (2009). A positive FGFR3/FOXN1 feedback loop underlies benign skin keratosis versus squamous cell carcinoma formation in humans. J Clin Invest *119*, 3127-3137.

Marchevsky, A.M., and Wick, M.R. (2014). Pathology of the mediastinum: Cambridge University Press).

Martin, M. (2011). Cutadapt removes adapter sequences from high-throughput sequencing reads. EMBnetjournal *17*, 10-12.

Martins, V.C., Busch, K., Juraeva, D., Blum, C., Ludwig, C., Rasche, V., Lasitschka, F., Mastitsky, S.E., Brors, B., Hielscher, T.*, et al.* (2014). Cell competition is a tumour suppressor mechanism in the thymus. Nature *509*, 465-470.

Matloubian, M., Lo, C.G., Cinamon, G., Lesneski, M.J., Xu, Y., Brinkmann, V., Allende, M.L., Proia, R.L., and Cyster, J.G. (2004). Lymphocyte egress from thymus and peripheral lymphoid organs is dependent on S1P receptor 1. Nature *427*, 355-360.

McCarthy, D.J., Chen, Y., and Smyth, G.K. (2012). Differential expression analysis of multifactor RNA-Seq experiments with respect to biological variation. Nucleic Acids Res *40*, 4288-4297.

McEndy, D.P.B., M. C.; Furth, J. (1944). On the Role of Thymus, Spleen, and Gonads in the Development of Leukemia in a High-Leukemia Stock of Mice. Cancer Res *4*, 377-383.

Medyouf, H., Gusscott, S., Wang, H., Tseng, J.C., Wai, C., Nemirovsky, O., Trumpp, A., Pflumio, F., Carboni, J., Gottardis, M.*, et al.* (2011). High-level IGF1R expression is required for leukemia-initiating cell activity in T-ALL and is supported by Notch signaling. J Exp Med *208*, 1809-1822.

Messika, E., Gallily, R., and Yefenof, E. (1991). Radiation leukemia virus (RadLV)-induced leukemogenesis is associated with an increased number and activity of thymic macrophages. Int J Cancer *48*, 924-930.

Metcalf, D. (1966). Histologic and transplantation studies on preleukemic thymus of the AKR mouse. J Natl Cancer Inst *37*, 425-442.

Metzger, T.C., Khan, I.S., Gardner, J.M., Mouchess, M.L., Johannes, K.P., Krawisz, A.K., Skrzypczynska, K.M., and Anderson, M.S. (2013). Lineage tracing and cell ablation identify a post-Aire-expressing thymic epithelial cell population. Cell Rep *5*, 166-179.

Miller, J.F. (1961). Immunological function of the thymus. Lancet *2*, 748-749.

Minuzzo, S., Agnusdei, V., Pusceddu, I., Pinazza, M., Moserle, L., Masiero, M., Rossi, E., Crescenzi, M., Hoey, T., Ponzoni, M.*, et al.* (2015). DLL4 regulates NOTCH signaling and growth of T acute lymphoblastic leukemia cells in NOD/SCID mice. Carcinogenesis *36*, 115-121.

Mirandola, L., Chiriva-Internati, M., Montagna, D., Locatelli, F., Zecca, M., Ranzani, M., Basile, A., Locati, M., Cobos, E., Kast, W.M.*, et al.* (2012). Notch1 regulates chemotaxis and proliferation by controlling the CC-chemokine receptors 5 and 9 in T cell acute lymphoblastic leukaemia. J Pathol *226*, 713-722.

Misslitz, A., Pabst, O., Hintzen, G., Ohl, L., Kremmer, E., Petrie, H.T., and Forster, R. (2004). Thymic T cell development and progenitor localization depend on CCR7. J Exp Med *200*, 481-491.

Moore, A.J., and Anderson, M.K. (2013). Dendritic cell development: a choose-your-own-adventure story. Adv Hematol *2013*, 949513.

Mori, K., Itoi, M., Tsukamoto, N., and Amagai, T. (2010). Foxn1 is essential for vascularization of the murine thymus anlage. Cell Immunol *260*, 66-69.

Mouri, Y., Nishijima, H., Kawano, H., Hirota, F., Sakaguchi, N., Morimoto, J., and Matsumoto, M. (2014). NF-kappaB-inducing kinase in thymic stroma establishes central tolerance by orchestrating cross-talk with not only thymocytes but also dendritic cells. Journal of immunology *193*, 4356-4367.

Mouri, Y., Yano, M., Shinzawa, M., Shimo, Y., Hirota, F., Nishikawa, Y., Nii, T., Kiyonari, H., Abe, T., Uehara, H.*, et al.* (2011). Lymphotoxin signal promotes thymic organogenesis by eliciting RANK expression in the embryonic thymic stroma. Journal of immunology *186*, 5047-5057.

Mukherjee, S., Richardson, A.M., Rodriguez-Canales, J., Ylaya, K., Erickson, H.S., Player, A., Kawasaki, E.S., Pinto, P.A., Choyke, P.L., Merino, M.J.*, et al.* (2009). Identification of EpCAM as a molecular target of prostate cancer stroma. Am J Pathol *175*, 2277-2287.

Mullighan, C.G. (2010). T-lineage lymphoblastic lymphoma and leukemia-a MASSive problem. Cancer Cell *18*, 297-299.

Murata, S., Sasaki, K., Kishimoto, T., Niwa, S., Hayashi, H., Takahama, Y., and Tanaka, K. (2007). Regulation of CD8+ T cell development by thymus-specific proteasomes. Science *316*, 1349-1353.

Nehls, M., Kyewski, B., Messerle, M., Waldschutz, R., Schuddekopf, K., Smith, A.J., and Boehm, T. (1996). Two genetically separable steps in the differentiation of thymic epithelium. Science *272*, 886-889.

Nitta, T., Murata, S., Sasaki, K., Fujii, H., Ripen, A.M., Ishimaru, N., Koyasu, S., Tanaka, K., and Takahama, Y. (2010). Thymoproteasome shapes immunocompetent repertoire of CD8+ T cells. Immunity *32*, 29-40.

Nitta, T., and Suzuki, H. (2016). Thymic stromal cell subsets for T cell development. Cell Mol Life Sci *73*, 1021-1037.

Nowell, C.S., Bredenkamp, N., Tetelin, S., Jin, X., Tischner, C., Vaidya, H., Sheridan, J.M., Stenhouse, F.H., Heussen, R., Smith, A.J.*, et al.* (2011). Foxn1 regulates lineage progression in cortical and medullary thymic epithelial cells but is dispensable for medullary sublineage divergence. PLoS Genet *7*, e1002348.

O'Neil, J., Calvo, J., McKenna, K., Krishnamoorthy, V., Aster, J.C., Bassing, C.H., Alt, F.W., Kelliher, M., and Look, A.T. (2006). Activating Notch1 mutations in mouse models of T-ALL. Blood *107*, 781-785.

O'Neill, K.E., Bredenkamp, N., Tischner, C., Vaidya, H.J., Stenhouse, F.H., Peddie, C.D., Nowell, C.S., Gaskell, T., and Blackburn, C.C. (2016). Foxn1 Is Dynamically Regulated in Thymic Epithelial Cells during Embryogenesis and at the Onset of Thymic Involution. PLoS One *11*, e0151666.

Orkin, S.H., and Zon, L.I. (2008). Hematopoiesis: an evolving paradigm for stem cell biology. Cell *132*, 631-644.

Owen, J.A., Punt, J., Stranford, S.A., Jones, P.P., and Kuby, J. (2013). Kuby immunology, 7th Ed. (W. H. Freeman and Company).

Palucka, K., and Banchereau, J. (2012). Cancer immunotherapy via dendritic cells. Nat Rev Cancer *12*, 265-277.

Passaro, D., Irigoyen, M., Catherinet, C., Gachet, S., Da Costa De Jesus, C., Lasgi, C., Tran Quang, C., and Ghysdael, J. (2015). CXCR4 Is Required for Leukemia-Initiating Cell Activity in T Cell Acute Lymphoblastic Leukemia. Cancer Cell *27*, 769-779.

Passaro, D., Quang, C.T., and Ghysdael, J. (2016). Microenvironmental cues for T-cell acute lymphoblastic leukemia development. Immunol Rev *271*, 156-172.

Patriarca, C., Macchi, R.M., Marschner, A.K., and Mellstedt, H. (2012). Epithelial cell adhesion molecule expression (CD326) in cancer: a short review. Cancer Treat Rev *38*, 68-75.

Pear, W.S., Aster, J.C., Scott, M.L., Hasserjian, R.P., Soffer, B., Sklar, J., and Baltimore, D. (1996). Exclusive development of T cell neoplasms in mice transplanted with bone marrow expressing activated Notch alleles. J Exp Med *183*, 2283-2291.

Pearse, G. (2006). Normal structure, function and histology of the thymus. Toxicol Pathol *34*, 504-514.

Peeters, P., Raynaud, S.D., Cools, J., Wlodarska, I., Grosgeorge, J., Philip, P., Monpoux, F., Van Rompaey, L., Baens, M., Van den Berghe, H.*, et al.* (1997). Fusion of TEL, the ETS-variant gene 6 (ETV6), to the receptor-associated kinase JAK2 as a result of t(9;12) in a lymphoid and t(9;15;12) in a myeloid leukemia. Blood *90*, 2535-2540.

Perkins, N.D. (2012). The diverse and complex roles of NF-kappaB subunits in cancer. Nat Rev Cancer *12*, 121-132.

Perry, J.S., Lio, C.W., Kau, A.L., Nutsch, K., Yang, Z., Gordon, J.I., Murphy, K.M., and Hsieh, C.S. (2014). Distinct contributions of Aire and antigen-presenting-cell subsets to the generation of self-tolerance in the thymus. Immunity *41*, 414-426.

Petrie, H.T., and Zuniga-Pflucker, J.C. (2007). Zoned out: functional mapping of stromal signaling microenvironments in the thymus. Annu Rev Immunol *25*, 649-679.

Pitt, L.A., Tikhonova, A.N., Hu, H., Trimarchi, T., King, B., Gong, Y., Sanchez-Martin, M., Tsirigos, A., Littman, D.R., Ferrando, A.A.*, et al.* (2015). CXCL12-Producing Vascular Endothelial Niches Control Acute T Cell Leukemia Maintenance. Cancer Cell *27*, 755-768.

Preibisch, S., Saalfeld, S., and Tomancak, P. (2009). Globally optimal stitching of tiled 3D microscopic image acquisitions. Bioinformatics *25*, 1463-1465.

Pui, C.-H. (2006). Childhood leukemias, 2nd Ed. (Cambridge University Press).

Pui, C.H., Carroll, W.L., Meshinchi, S., and Arceci, R.J. (2011). Biology, risk stratification, and therapy of pediatric acute leukemias: an update. J Clin Oncol *29*, 551-565.

Radtke, F., Wilson, A., Mancini, S.J., and MacDonald, H.R. (2004). Notch regulation of lymphocyte development and function. Nat Immunol *5*, 247-253.

Raphael, I., Nalawade, S., Eagar, T.N., and Forsthuber, T.G. (2015). T cell subsets and their signature cytokines in autoimmune and inflammatory diseases. Cytokine *74*, 5-17.

Richmond, A. (2002). Nf-kappa B, chemokine gene transcription and tumour growth. Nat Rev Immunol *2*, 664-674.

Robinson, M.D., McCarthy, D.J., and Smyth, G.K. (2010). edgeR: a Bioconductor package for differential expression analysis of digital gene expression data. Bioinformatics *26*, 139-140.

Romano, R., Palamaro, L., Fusco, A., Giardino, G., Gallo, V., Del Vecchio, L., and Pignata, C. (2013). FOXN1: A Master Regulator Gene of Thymic Epithelial Development Program. Front Immunol *4*, 187.

Rossi, S.W., Chidgey, A.P., Parnell, S.M., Jenkinson, W.E., Scott, H.S., Boyd, R.L., Jenkinson, E.J., and Anderson, G. (2007a). Redefining epithelial progenitor potential in the developing thymus. European journal of immunology *37*, 2411-2418.

Rossi, S.W., Jenkinson, W.E., Anderson, G., and Jenkinson, E.J. (2006). Clonal analysis reveals a common progenitor for thymic cortical and medullary epithelium. Nature *441*, 988-991.

Rossi, S.W., Kim, M.Y., Leibbrandt, A., Parnell, S.M., Jenkinson, W.E., Glanville, S.H., McConnell, F.M., Scott, H.S., Penninger, J.M., Jenkinson, E.J.*, et al.* (2007b). RANK signals from CD4(+)3(-) inducer cells regulate development of Aire-expressing epithelial cells in the thymic medulla. J Exp Med *204*, 1267-1272.

Rothenberg, E.V., Moore, J.E., and Yui, M.A. (2008). Launching the T-cell-lineage developmental programme. Nat Rev Immunol *8*, 9-21.

Scheiff, J.M., Cordier, A.C., and Haumont, S. (1978). The thymus of Nu/+ mice. Anat Embryol (Berl) *153*, 115-122.

Schindelin, J., Arganda-Carreras, I., Frise, E., Kaynig, V., Longair, M., Pietzsch, T., Preibisch, S., Rueden, C., Saalfeld, S., Schmid, B.*, et al.* (2012). Fiji: an open-source platform for biological-image analysis. Nat Methods *9*, 676-682.

Schindelin, J., Rueden, C.T., Hiner, M.C., and Eliceiri, K.W. (2015). The ImageJ ecosystem: An open platform for biomedical image analysis. Molecular Reproduction and Development *82*, 518-529.

Schmieder, R., and Edwards, R. (2011). Quality control and preprocessing of metagenomic datasets. Bioinformatics *27*, 863-864.

Schneider, C.A., Rasband, W.S., and Eliceiri, K.W. (2012). NIH Image to ImageJ: 25 years of image analysis. Nat Meth *9*, 671-675.

Scimone, M.L., Aifantis, I., Apostolou, I., von Boehmer, H., and von Andrian, U.H. (2006). A multistep adhesion cascade for lymphoid progenitor cell homing to the thymus. Proc Natl Acad Sci U S A *103*, 7006-7011.

Scupoli, M.T., Perbellini, O., Krampera, M., Vinante, F., Cioffi, F., and Pizzolo, G. (2007). Interleukin 7 requirement for survival of T-cell acute lymphoblastic leukemia and human thymocytes on bone marrow stroma. Haematologica *92*, 264-266.

Seach, N., Ueno, T., Fletcher, A.L., Lowen, T., Mattesich, M., Engwerda, C.R., Scott, H.S., Ware, C.F., Chidgey, A.P., Gray, D.H.*, et al.* (2008). The lymphotoxin pathway regulates Aire-independent expression of ectopic genes and chemokines in thymic stromal cells. Journal of immunology *180*, 5384-5392.

Sen, L., and Borella, L. (1975). Clinical importance of lymphoblasts with T markers in childhood acute leukemia. N Engl J Med *292*, 828-832.

Shakib, S., Desanti, G.E., Jenkinson, W.E., Parnell, S.M., Jenkinson, E.J., and Anderson, G. (2009). Checkpoints in the development of thymic cortical epithelial cells. Journal of immunology *182*, 130-137.

Shi, Y., Wu, W., Chai, Q., Li, Q., Hou, Y., Xia, H., Ren, B., Xu, H., Guo, X., Jin, C.*, et al.* (2016). LTbetaR controls thymic portal endothelial cells for haematopoietic progenitor cell homing and T-cell regeneration. Nat Commun *7*, 12369.

Shisa, H., Kojima, A., and Hiai, H. (1986). Accelerating effect of nude gene heterozygosity on spontaneous AKR thymic lymphomagenesis. Jpn J Cancer Res *77*, 568-571.

Siegler, R., Geldner, J., and Rich, M.A. (1964). Histogenesis of Thymic Lymphoma Induced by a Murine Leukemia Virus (Rich). Cancer Res *24*, 444-459.

Siegler, R., and Rich, M.A. (1963). Unilateral Histogenesis of Akr Thymic Lymphoma. Cancer Res *23*, 1669-1678.

Silva, A., Laranjeira, A.B., Martins, L.R., Cardoso, B.A., Demengeot, J., Yunes, J.A., Seddon, B., and Barata, J.T. (2011). IL-7 contributes to the progression of human T-cell acute lymphoblastic leukemias. Cancer Res *71*, 4780-4789.

Steelman, L.S., Abrams, S.L., Whelan, J., Bertrand, F.E., Ludwig, D.E., Basecke, J., Libra, M., Stivala, F., Milella, M., Tafuri, A.*, et al.* (2008). Contributions of the Raf/MEK/ERK, PI3K/PTEN/Akt/mTOR and Jak/STAT pathways to leukemia. Leukemia *22*, 686-707.

Su, D.M., Navarre, S., Oh, W.J., Condie, B.G., and Manley, N.R. (2003). A domain of Foxn1 required for crosstalk-dependent thymic epithelial cell differentiation. Nat Immunol *4*, 1128-1135.

Sun, L., Li, H., Luo, H., and Zhao, Y. (2014). Thymic epithelial cell development and its dysfunction in human diseases. Biomed Res Int *2014*, 206929.

Sun, L., Sun, C., Liang, Z., Li, H., Chen, L., Luo, H., Zhang, H., Ding, P., Sun, X., Qin, Z.*, et al.* (2015). FSP1(+) fibroblast subpopulation is essential for the maintenance and regeneration of medullary thymic epithelial cells. Sci Rep *5*, 14871.

Suniara, R.K., Jenkinson, E.J., and Owen, J.J. (2000). An essential role for thymic mesenchyme in early T cell development. J Exp Med *191*, 1051-1056.

Tacke, R., Hilgendorf, I., Garner, H., Waterborg, C., Park, K., Nowyhed, H., Hanna, R.N., Wu, R., Swirski, F.K., Geissmann, F.*, et al.* (2015). The transcription factor NR4A1 is essential for the development of a novel macrophage subset in the thymus. Sci Rep *5*, 10055.

Takaba, H., Morishita, Y., Tomofuji, Y., Danks, L., Nitta, T., Komatsu, N., Kodama, T., and Takayanagi, H. (2015). Fezf2 Orchestrates a Thymic Program of Self-Antigen Expression for Immune Tolerance. Cell *163*, 975-987.

Takahama, Y. (2006). Journey through the thymus: stromal guides for T-cell development and selection. Nat Rev Immunol *6*, 127-135.

Terszowski, G., Muller, S.M., Bleul, C.C., Blum, C., Schirmbeck, R., Reimann, J., Pasquier, L.D., Amagai, T., Boehm, T., and Rodewald, H.R. (2006). Evidence for a functional second thymus in mice. Science *312*, 284-287.

Tlsty, T.D., and Coussens, L.M. (2006). Tumor stroma and regulation of cancer development. Annu Rev Pathol *1*, 119-150.

Tosello, V., and Ferrando, A.A. (2013). The NOTCH signaling pathway: role in the pathogenesis of T-cell acute lymphoblastic leukemia and implication for therapy. Ther Adv Hematol *4*, 199-210.

Touw, I., Pouwels, K., van Agthoven, T., van Gurp, R., Budel, L., Hoogerbrugge, H., Delwel, R., Goodwin, R., Namen, A., and Lowenberg, B. (1990). Interleukin-7 is a growth factor of precursor B and T acute lymphoblastic leukemia. Blood *75*, 2097-2101.

Trampont, P.C., Tosello-Trampont, A.C., Shen, Y., Duley, A.K., Sutherland, A.E., Bender, T.P., Littman, D.R., and Ravichandran, K.S. (2010). CXCR4 acts as a costimulator during thymic beta-selection. Nat Immunol *11*, 162-170.

Tremblay, M., Tremblay, C.S., Herblot, S., Aplan, P.D., Hebert, J., Perreault, C., and Hoang, T. (2010). Modeling T-cell acute lymphoblastic leukemia induced by the SCL and LMO1 oncogenes. Genes Dev *24*, 1093-1105.

Trinquand, A., Dos Santos, N.R., Tran Quang, C., Rocchetti, F., Zaniboni, B., Belhocine, M., Da Costa de Jesus, C., Lhermitte, L., Tesio, M., Dussiot, M.*, et al.* (2016). Triggering the TCR Developmental Checkpoint Activates a Therapeutically Targetable Tumor Suppressive Pathway in T-cell Leukemia. Cancer Discov *6*, 972-985.

Triplett, T.A., Cardenas, K.T., Lancaster, J.N., Hu, Z., Selden, H.J., Jasso, G.J., Balasubramanyam, S., Chan, K., Li, L., Chen, X.*, et al.* (2016). Endogenous dendritic cells from the tumor microenvironment support T-ALL growth via IGF1R activation. Proc Natl Acad Sci U S A *113*, E1016-1025.

Tscharke, D.C., Croft, N.P., Doherty, P.C., and La Gruta, N.L. (2015). Sizing up the key determinants of the CD8(+) T cell response. Nat Rev Immunol *15*, 705-716.

Uddin, M.M., Ohigashi, I., Motosugi, R., Nakayama, T., Sakata, M., Hamazaki, J., Nishito, Y., Rode, I., Tanaka, K., Takemoto, T.*, et al.* (2017). Foxn1-beta5t transcriptional axis controls CD8+ T-cell production in the thymus. Nat Commun *8*, 14419.

Ueda, Y., Katagiri, K., Tomiyama, T., Yasuda, K., Habiro, K., Katakai, T., Ikehara, S., Matsumoto, M., and Kinashi, T. (2012). Mst1 regulates integrin-dependent thymocyte trafficking and antigen recognition in the thymus. Nat Commun *3*, 1098.

Ueno, T., Saito, F., Gray, D.H., Kuse, S., Hieshima, K., Nakano, H., Kakiuchi, T., Lipp, M., Boyd, R.L., and Takahama, Y. (2004). CCR7 signals are essential for cortex-medulla migration of developing thymocytes. J Exp Med *200*, 493-505.

Uzan, B., Poglio, S., Gerby, B., Wu, C.L., Gross, J., Armstrong, F., Calvo, J., Cahu, X., Deswarte, C., Dumont, F.*, et al.* (2014). Interleukin-18 produced by bone marrow-derived stromal cells supports T-cell acute leukaemia progression. EMBO Mol Med *6*, 821-834.

Vainchenker, W., and Constantinescu, S.N. (2013). JAK/STAT signaling in hematological malignancies. Oncogene *32*, 2601-2613.

Van Vlierberghe, P., and Ferrando, A. (2012). The molecular basis of T cell acute lymphoblastic leukemia. J Clin Invest *122*, 3398-3406.

Van Vlierberghe, P., Pieters, R., Beverloo, H.B., and Meijerink, J.P. (2008). Molecular-genetic insights in paediatric T-cell acute lymphoblastic leukaemia. Br J Haematol *143*, 153-168.

Van Vliet, E., Melis, M., Foidart, J.M., and Van Ewijk, W. (1986). Reticular fibroblasts in peripheral lymphoid organs identified by a monoclonal antibody. The journal of histochemistry and cytochemistry : official journal of the Histochemistry Society *34*, 883-890.

Webb, L.V., Ley, S.C., and Seddon, B. (2016). TNF activation of NF-kappaB is essential for development of single-positive thymocytes. J Exp Med *213*, 1399-1407.

Weerkamp, F., van Dongen, J.J., and Staal, F.J. (2006). Notch and Wnt signaling in T-lymphocyte development and acute lymphoblastic leukemia. Leukemia *20*, 1197-1205.

Weng, A.P., Ferrando, A.A., Lee, W., Morris, J.P.t., Silverman, L.B., Sanchez-Irizarry, C., Blacklow, S.C., Look, A.T., and Aster, J.C. (2004). Activating mutations of NOTCH1 in human T cell acute lymphoblastic leukemia. Science *306*, 269-271.

Winter, S.S., Sweatman, J., Shuster, J.J., Link, M.P., Amylon, M.D., Pullen, J., Camitta, B.M., and Larson, R.S. (2002). Bone marrow stroma-supported culture of T-lineage acute lymphoblastic leukemic cells predicts treatment outcome in children: a Pediatric Oncology Group study. Leukemia *16*, 1121-1126.

Winter, S.S., Sweatman, J.J., Lawrence, M.B., Rhoades, T.H., Hart, A.L., and Larson, R.S. (2001). Enhanced T-lineage acute lymphoblastic leukaemia cell survival on bone marrow stroma requires involvement of LFA-1 and ICAM-1. Br J Haematol *115*, 862-871.

Wu, L. (2006). T lineage progenitors: the earliest steps en route to T lymphocytes. Curr Opin Immunol *18*, 121-126.

Yan, W., Young, A.Z., Soares, V.C., Kelley, R., Benezra, R., and Zhuang, Y. (1997). High incidence of T-cell tumors in E2A-null mice and E2A/Id1 double-knockout mice. Mol Cell Biol *17*, 7317-7327.

You, M.J., Medeiros, L.J., and Hsi, E.D. (2015). T-lymphoblastic leukemia/lymphoma. Am J Clin Pathol *144*, 411-422.

Yui, M.A., and Rothenberg, E.V. (2014). Developmental gene networks: a triathlon on the course to T cell identity. Nat Rev Immunol *14*, 529-545.

Zarin, P., Chen, E.L., In, T.S., Anderson, M.K., and Zuniga-Pflucker, J.C. (2015). Gamma delta T-cell differentiation and effector function programming, TCR signal strength, when and how much? Cell Immunol *296*, 70-75.

Zhong, Y., Jiang, L., Hiai, H., Toyokuni, S., and Yamada, Y. (2007). Overexpression of a transcription factor LYL1 induces T- and B-cell lymphoma in mice. Oncogene *26*, 6937-6947.

Zlotoff, D.A., Sambandam, A., Logan, T.D., Bell, J.J., Schwarz, B.A., and Bhandoola, A. (2010). CCR7 and CCR9 together recruit hematopoietic progenitors to the adult thymus. Blood *115*, 1897-1905.

Zook, E.C., Krishack, P.A., Zhang, S., Zeleznik-Le, N.J., Firulli, A.B., Witte, P.L., and Le, P.T. (2011). Overexpression of Foxn1 attenuates age-associated thymic involution and prevents the expansion of peripheral CD4 memory T cells. Blood *118*, 5723-5731.

Zuklys, S., Handel, A., Zhanybekova, S., Govani, F., Keller, M., Maio, S., Mayer, C.E., Teh, H.Y., Hafen, K., Gallone, G.*, et al.* (2016). Foxn1 regulates key target genes essential for T cell development in postnatal thymic epithelial cells. Nat Immunol.

Annex.
Supplementary data

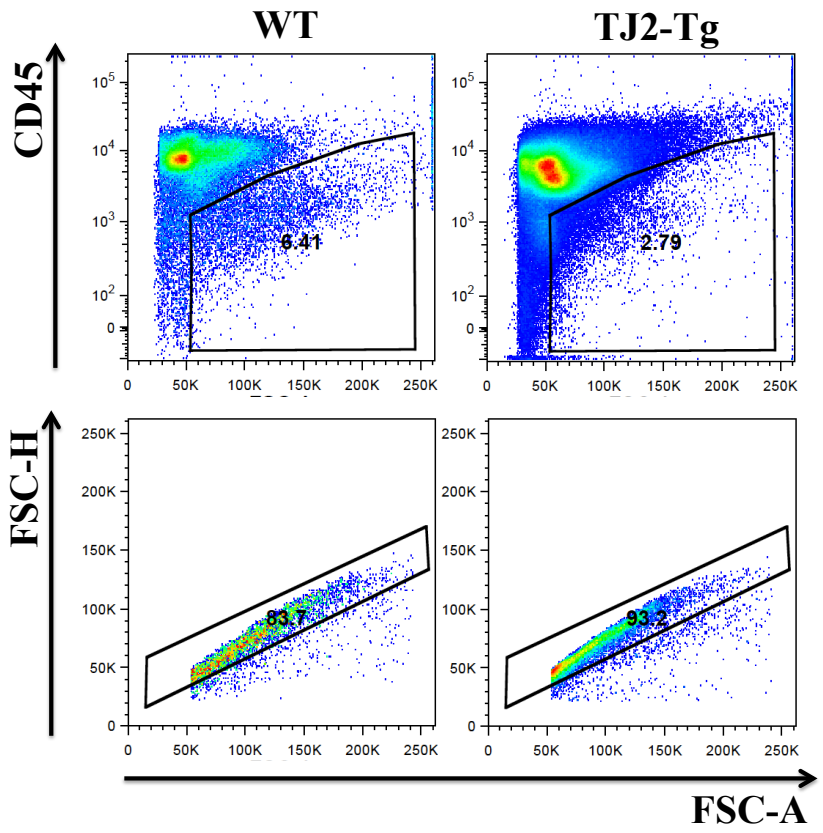

Supp. Figure 1. Exclusion of CD45^{+} cells and doublets prior to flow cytometry analysis of TEC subpopulations. Analysis of TEC subpopulations initiated by eliminating the majority of CD45^{hi} cell population (top panel) and selecting single cells (bottom panel). Here represented are one wild-type (WT) and one TJ2-Tg (mouse ID nº 146) sample.

Supp. Table 1. High frequency of exon 34 *Notch1* mutations in TJ2-Tg-induced leukemia samples with distinct genetic backgrounds.

Samples	*Notch1* ex34.2	Mutated codon	Mutation
TJ2-Tg;*Rag2*$^{+/-}$			
3	**mut**	2351	Ins ATTA
4	**mut**	2399	Ins CGGG
5	**mut**	2362	Ins GG
20	wt	-	-
21	**mut**	2457	Ins T
99	wt	-	-
103	wt	-	-
TJ2-Tg;*Rag2*$^{-/-}$			
15	wt	-	-
18 (Prim.)	**mut**	2380	Ins A
18 (Pass. 2)	**mut**	2380	Ins A
28 (Prim.)	**mut**	2398	Ins AGGGAAT
28 (Pass. 2)	**mut**	2361	Del GGCTGGCAAC, Ins CCCTCGAGCGG
31	wt	-	-
68	**mut**	2361	Del G, Ins CC
132 (Prim.)	**mut**	2399	Ins GG
132 (Pass. 2)	**mut**	2399	Ins GG
140	wt	-	-
268	**mut**	2361	Del G, Ins AGAAAAAAAG
1248 (Prim.)	**mut**	2361	Del G, Ins CC
1248 (Pass. 2)	**mut**	2361	Del G, Ins CC
1267	wt	-	-
TJ2-Tg;*Ltbr*$^{+/-}$			
19	**mut**	2361	Ins CT
194	**mut**	2399	Ins AGGG
203	wt	-	-
212	**mut**	2361	Ins AGGG
214	**mut**	2361	Del C, Ins GG
215	**mut**	ND	Ins 4 nt
217	**mut**	2361	Del C, Ins GGA
TJ2-Tg;*Ltbr*$^{-/-}$			
26	**mut**	2361	Del CG, Ins 24 nt
31	**mut**	2399	Ins GG
76	wt	-	-
88	**mut**	2404	Ins 22 nt
144	wt	-	-
189	**mut**	2384	Ins C
198	wt	-	-
204	**mut**	2361	Del G, Ins AAA
224	**mut**	2398	Ins CCTC

Prim., primary sample; Pass., passaged in transplanted mice; mut, mutated sequence; wt, wild-type sequence; ND, not determined.

Supp. Table 2. Endpoint TJ2-Tg thymic lymphoma samples analyzed by immunofluorescence.

Genotype	ID	Age (weeks)	Thymus (mg)	Double immunofluorescence sets*
TJ2-Tg;*Foxn1*$^{+/+}$	128	17	1393	9
	133	18	1000	2
	269	20	589	9
	341	12	631	9
	335	18	165	2
TJ2-Tg;*Foxn1*$^{+/nu}$	312	23	265	2
	292	15	530	2
	338	20	378	2

*** 9**: ICAM-1/Krt5, Krt8/Krt5, UEA-1/Krt5, DEC205/Krt5, ER-TR7/Krt5, Laminin/Krt8, CD31/Krt5 and F4/80 with Krt5. **2**: ICAM-1/Krt5 and Krt8 with Krt5.

Supp. Table 3. DEGs upregulated in WT sample.

Gene	T-ALL counts	WT counts	logFC	logCPM	*P* value	FDR
Hnrnpa2b1	855	1400	1,264	9,782	0,003	0,099
Tbata	619	1035	1,295	9,337	0,002	0,087
Bcl11b	558	934	1,296	9,189	0,002	0,088
Trpm7	174	297	1,324	7,529	0,003	0,097
Top2b	281	482	1,331	8,225	0,002	0,081
Rorc	289	497	1,335	8,268	0,002	0,080
Tapt1	303	527	1,351	8,348	0,002	0,071
Osbpl8	145	254	1,361	7,293	0,002	0,086
Kif11	126	223	1,376	7,102	0,002	0,084
Sesn1	183	324	1,377	7,639	0,002	0,072
Zfp266	98	174	1,380	6,744	0,002	0,093
Sp3	155	276	1,385	7,406	0,002	0,074
Cxcl12	694	1238	1,388	9,569	0,001	0,051
Atp13a3	192	347	1,406	7,730	0,001	0,062
Pcm1	110	199	1,407	6,929	0,002	0,077
Pkp1	89	162	1,416	6,631	0,002	0,087
Ubxn7	120	219	1,420	7,063	0,002	0,068
Mmp9	126	230	1,420	7,134	0,002	0,067
Hadh	89	163	1,425	6,638	0,002	0,084
Fabp4	497	914	1,432	9,119	0,001	0,042
Pan3	262	482	1,432	8,196	0,001	0,046
Ssbp2	66	122	1,438	6,218	0,003	0,096
Camkk1	73	135	1,438	6,363	0,002	0,093
Ccng2	103	191	1,443	6,860	0,002	0,066
Nfatc3	237	444	1,458	8,071	0,001	0,043
Cdkn2aip	51	96	1,463	5,868	0,003	0,099
Cry1	55	104	1,470	5,981	0,003	0,097
Calcrl	77	146	1,474	6,466	0,002	0,069
Nusap1	61	116	1,478	6,135	0,002	0,088
Diras2	83	158	1,480	6,577	0,001	0,066
Cnot7	75	143	1,482	6,434	0,002	0,067
Orc4	45	86	1,485	5,705	0,003	0,099
G2e3	54	104	1,496	5,974	0,002	0,084
Zfp664	83	160	1,498	6,591	0,001	0,058
Pten	154	298	1,505	7,484	0,001	0,038
Eif3e	53	103	1,509	5,956	0,002	0,077
Lef1	166	323	1,513	7,598	0,001	0,035
Ccrl1	41	80	1,514	5,594	0,003	0,097
Arglu1	285	558	1,522	8,383	0,000	0,027
Gabpa	93	183	1,528	6,776	0,001	0,044
Mbnl3	47	93	1,535	5,803	0,002	0,075
Plekhf2	47	93	1,535	5,803	0,002	0,075
Tmpo	377	748	1,541	8,801	0,000	0,023
Mmgt1	35	70	1,549	5,395	0,003	0,097
Nqo1	47	94	1,550	5,814	0,002	0,070

(cont.)

Supp. Table 3. DEGs upregulated in WT sample. (Continuation.)

Gene	T-ALL counts	WT counts	logFC	logCPM	*P* value	FDR
Tfdp2	60	120	1,551	6,164	0,001	0,059
Cdh4	92	184	1,552	6,777	0,001	0,039
Sh2d1a	76	154	1,570	6,517	0,001	0,043
Clic5	141	286	1,573	7,407	0,000	0,028
Tmem194	62	126	1,574	6,228	0,001	0,047
Epm2aip1	150	305	1,576	7,499	0,000	0,026
Ctcf	172	352	1,586	7,703	0,000	0,023
Lpl	116	238	1,589	7,138	0,000	0,028
Eif2s3y	60	124	1,598	6,198	0,001	0,045
Aqp11	96	199	1,603	6,877	0,000	0,028
Neil3	46	96	1,611	5,828	0,001	0,053
Fasn	819	1707	1,613	9,973	0,000	0,013
C330027C09Rik	53	112	1,630	6,044	0,001	0,042
Senp7	89	189	1,638	6,794	0,000	0,026
Tcf7	1073	2283	1,642	10,385	0,000	0,011
Dck	144	307	1,644	7,491	0,000	0,017
C1galt1	51	109	1,646	6,001	0,001	0,038
Mbtd1	111	238	1,652	7,122	0,000	0,021
Suz12	105	226	1,658	7,046	0,000	0,021
Tef	97	209	1,659	6,933	0,000	0,021
Zfp62	72	156	1,667	6,511	0,000	0,027
Ppp1r9a	23	50	1,667	4,888	0,002	0,091
Dntt	429	929	1,668	9,082	0,000	0,011
Myb	609	1319	1,668	9,588	0,000	0,010
Ets2	288	624	1,668	8,508	0,000	0,012
Pds5b	189	411	1,673	7,904	0,000	0,013
Scai	65	142	1,678	6,373	0,000	0,027
Snhg11	305	666	1,679	8,599	0,000	0,011
Zmym1	37	81	1,680	5,568	0,001	0,052
Tube1	46	101	1,685	5,882	0,001	0,036
Thrsp	72	158	1,685	6,524	0,000	0,024
Fopnl	70	154	1,689	6,487	0,000	0,024
Acsl1	74	163	1,690	6,568	0,000	0,022
Gtf2a2	23	51	1,696	4,909	0,002	0,082
Ptprd	37	82	1,697	5,581	0,001	0,048
Gucy1a2	26	58	1,705	5,088	0,002	0,079
Nnt	66	147	1,706	6,415	0,000	0,023
Dgat2	47	105	1,710	5,932	0,001	0,031
Mxi1	37	83	1,715	5,594	0,001	0,044
Dbi	33	75	1,733	5,445	0,001	0,048
Ddx3y	91	210	1,758	6,916	0,000	0,012
Ndc80	18	42	1,767	4,619	0,002	0,091
Psmb11	170	395	1,769	7,825	0,000	0,007
Itm2a	73	171	1,779	6,616	0,000	0,012
Slc16a1	134	315	1,785	7,494	0,000	0,008
Zfp280c	45	106	1,786	5,927	0,000	0,021
P2rx1	33	78	1,790	5,488	0,000	0,031
Camk4	176	416	1,793	7,894	0,000	0,006

(cont.)

Supp. Table 3. DEGs upregulated in WT sample. (Continuation.)

Gene	T-ALL counts	WT counts	logFC	logCPM	*P* value	FDR
Cep97	136	323	1,800	7,527	0,000	0,007
Casc5	46	110	1,808	5,975	0,000	0,018
2610018G03Rik	51	122	1,809	6,123	0,000	0,015
Glcci1	270	647	1,813	8,526	0,000	0,004
Nwd1	27	65	1,815	5,222	0,001	0,043
Mbd4	19	46	1,821	4,733	0,002	0,068
Lpar6	202	489	1,828	8,119	0,000	0,004
Snap91	20	49	1,838	4,818	0,001	0,065
Aldh6a1	36	88	1,838	5,648	0,000	0,023
Atp1a2	38	93	1,840	5,727	0,000	0,023
Acbd4	48	119	1,860	6,076	0,000	0,014
Arpp21	222	551	1,864	8,283	0,000	0,003
Fgf14	22	55	1,868	4,973	0,001	0,036
Enpep	98	248	1,891	7,126	0,000	0,005
Zfp101	26	66	1,891	5,226	0,000	0,030
Neurl2	81	207	1,905	6,862	0,000	0,005
Trp53inp1	329	840	1,905	8,883	0,000	0,002
F13a1	39	100	1,908	5,816	0,000	0,012
Sgol2	21	54	1,908	4,938	0,001	0,044
Prss16	1551	4000	1,920	11,132	0,000	0,001
2610307P16Rik	15	39	1,921	4,480	0,002	0,079
Unc79	15	39	1,921	4,480	0,002	0,079
AI504432	121	313	1,923	7,455	0,000	0,003
Chek1	18	47	1,929	4,738	0,001	0,043
Satb1	830	2167	1,938	10,244	0,000	0,001
Zfp386	30	79	1,945	5,470	0,000	0,017
Nadkd1	18	48	1,959	4,761	0,001	0,038
Sgol1	22	59	1,969	5,050	0,000	0,023
Jrkl	13	35	1,970	4,319	0,002	0,066
Dgke	128	345	1,982	7,583	0,000	0,002
Alcam	133	364	2,005	7,655	0,000	0,001
Zfp943	25	69	2,011	5,263	0,000	0,017
Atl2	108	298	2,016	7,364	0,000	0,002
Osbpl6	18	50	2,018	4,806	0,000	0,027
Ccl25	864	2389	2,020	10,368	0,000	0,001
Cdh24	41	114	2,025	5,978	0,000	0,006
Chml	16	45	2,035	4,654	0,001	0,044
Cd28	109	306	2,041	7,398	0,000	0,001
Pgm2l1	32	91	2,056	5,649	0,000	0,009
Ccr9	390	1111	2,063	9,254	0,000	0,001
Cdo1	33	95	2,074	5,707	0,000	0,006
Cyp2e1	18	52	2,075	4,849	0,000	0,021
Xkrx	12	35	2,084	4,295	0,001	0,050
Chpt1	23	67	2,089	5,205	0,000	0,012
Dnajb4	27	79	2,096	5,438	0,000	0,008
Dgkg	11	33	2,123	4,206	0,002	0,069
Kif18a	12	36	2,124	4,325	0,001	0,037
Zfp770	19	58	2,155	4,987	0,000	0,013

(cont.)

Supp. Table 3. DEGs upregulated in WT sample. (Continuation.)

Gene	T-ALL counts	WT counts	logFC	logCPM	*P* value	FDR
Nefm	16	49	2,158	4,748	0,000	0,024
Zfp40	16	49	2,158	4,748	0,000	0,024
Pth	15	46	2,159	4,659	0,000	0,024
Serpinb2	14	43	2,160	4,565	0,000	0,027
Akap17b	10	31	2,169	4,111	0,001	0,062
Zfp280d	102	318	2,192	7,424	0,000	0,000
Themis	104	330	2,217	7,473	0,000	0,000
A630033H20Rik	9	29	2,223	4,009	0,001	0,064
Ces1d	19	62	2,251	5,063	0,000	0,008
BB031773	14	46	2,257	4,640	0,000	0,016
Dbp	16	53	2,271	4,837	0,000	0,009
Abat	22	73	2,276	5,291	0,000	0,004
Chchd10	18	61	2,305	5,030	0,000	0,006
Fn3k	7	24	2,307	3,739	0,002	0,069
2010012O05Rik	6	21	2,332	3,558	0,002	0,070
Lcorl	10	35	2,343	4,244	0,001	0,031
Rmnd5a	319	1111	2,353	9,202	0,000	0,000
Spink5	13	46	2,363	4,621	0,000	0,011
Car3	63	225	2,387	6,890	0,000	0,000
Pdk4	15	54	2,390	4,842	0,000	0,008
Rag2	53	192	2,407	6,658	0,000	0,000
Slc2a13	9	34	2,451	4,185	0,000	0,023
Yod1	9	34	2,451	4,185	0,000	0,023
Adipoq	37	142	2,489	6,209	0,000	0,000
Medag	10	39	2,499	4,367	0,000	0,014
Arxes2	6	24	2,524	3,702	0,001	0,036
D330041H03Rik	6	24	2,524	3,702	0,001	0,036
Scd1	523	2131	2,580	10,108	0,000	0,000
Nron	5	21	2,588	3,515	0,002	0,070
Rag1	759	3112	2,589	10,653	0,000	0,000
Ptprn2	5	22	2,655	3,566	0,001	0,056
Zfp9	4	18	2,679	3,302	0,002	0,090
Mettl23	4	19	2,756	3,360	0,002	0,070
Rasd1	6	29	2,796	3,915	0,000	0,011
Nphs2	3	15	2,815	3,054	0,002	0,090
Rtkn2	5	26	2,895	3,754	0,000	0,019
Zfp708	3	16	2,908	3,122	0,002	0,069
Mpc2	16	86	2,968	5,420	0,000	0,000
Ptcra	9	49	2,977	4,617	0,000	0,001
Ror1	3	17	2,995	3,187	0,001	0,052
Scn1a	13	73	3,028	5,178	0,000	0,000
Gpd1	43	249	3,083	6,942	0,000	0,000
Utp14b	4	24	3,092	3,623	0,000	0,017
Olfr920	3	19	3,154	3,311	0,001	0,031
Cdhr5	2	13	3,161	2,838	0,002	0,084
Cidec	6	38	3,185	4,237	0,000	0,001
Atp2a1	2	14	3,268	2,917	0,001	0,062
Odf3b	2	15	3,366	2,991	0,001	0,045

(cont.)

Supp. Table 3. DEGs upregulated in WT sample. (Continuation.)

Gene	T-ALL counts	WT counts	logFC	logCPM	*P* value	FDR
Ppara	3	24	3,490	3,582	0,000	0,007
Pck1	27	230	3,637	6,775	0,000	0,000
Cox8b	6	60	3,842	4,820	0,000	0,000
Elovl3	1	14	4,171	2,848	0,000	0,016
Npm2	3	40	4,224	4,223	0,000	0,000
Sptssb	1	15	4,270	2,926	0,000	0,012
Ucp1	12	181	4,451	6,378	0,000	0,000
Cidea	5	102	4,863	5,530	0,000	0,000
Atp13a5	0	10	6,639	2,394	0,001	0,064
Mir301	0	10	6,639	2,394	0,001	0,064

FC, fold-change; CPM, count-per-million; FDR, false discovery rate.

Supp. Table 4. DEGs upregulated in TJ2-Tg sample.

Gene	T-ALL counts	WT counts	logFC	logCPM	*P* value	FDR
Xist	1130	0	-12.892	8.434	0.000	0.000
Gldc	74	0	-8.962	4.666	0.000	0.000
Gzmb	942	2	-8.255	8.179	0.000	0.000
Prol1	32	0	-7.756	3.600	0.000	0.000
Scgb1b27	32	0	-7.756	3.600	0.000	0.000
Scgb2b27	28	0	-7.565	3.438	0.000	0.001
Klra2	27	0	-7.513	3.394	0.000	0.001
Cd200r4	20	0	-7.082	3.040	0.000	0.012
Gpr55	20	0	-7.082	3.040	0.000	0.012
Cabp4	19	0	-7.009	2.981	0.000	0.016
Siglece	19	0	-7.009	2.981	0.000	0.016
Tgtp2	19	0	-7.009	2.981	0.000	0.016
A730020M07Rik	16	0	-6.763	2.787	0.001	0.031
Moxd1	16	0	-6.763	2.787	0.001	0.031
A2m	15	0	-6.671	2.716	0.001	0.044
Car6	15	0	-6.671	2.716	0.001	0.044
Gzmk	15	0	-6.671	2.716	0.001	0.044
Tgtp1	15	0	-6.671	2.716	0.001	0.044
Krt6a	13	0	-6.467	2.562	0.002	0.092
Serpina3f	111	1	-6.104	5.219	0.000	0.000
Gbp1	101	1	-5.968	5.094	0.000	0.000
Glycam1	180	2	-5.869	5.878	0.000	0.000
Spt1	85	1	-5.719	4.868	0.000	0.000
Ccl8	402	6	-5.489	7.000	0.000	0.000
Cd163l1	1541	25	-5.387	8.910	0.000	0.000
Fcgr4	124	2	-5.331	5.380	0.000	0.000
Cd79a	53	1	-5.040	4.263	0.000	0.000
Hk3	192	4	-4.997	5.984	0.000	0.000
Apol10b	50	1	-4.956	4.190	0.000	0.000
Cxcl9	2156	49	-4.903	9.405	0.000	0.000
Ffar2	48	1	-4.897	4.139	0.000	0.000
Prg4	209	5	-4.804	6.107	0.000	0.000
Pax5	45	1	-4.804	4.059	0.000	0.001
Zbtb32	44	1	-4.772	4.031	0.000	0.001
Chst5	43	1	-4.739	4.003	0.000	0.001
Siglecg	116	3	-4.674	5.307	0.000	0.000
Cd19	289	8	-4.604	6.563	0.000	0.000
Gbp10	39	1	-4.598	3.883	0.000	0.002
Il1b	36	1	-4.483	3.786	0.000	0.004
Ccl2	34	1	-4.401	3.718	0.000	0.005
Megf11	33	1	-4.358	3.682	0.000	0.007

(cont.)

Supp. Table 4. DEGs upregulated in TJ2-Tg sample. (Continuation.)

Gene	T-ALL counts	WT counts	logFC	logCPM	*P* value	FDR
Serpina3n	815	28	-4.305	8.037	0.000	0.000
Ifng	31	1	-4.269	3.608	0.000	0.012
Adamts4	29	1	-4.173	3.529	0.000	0.015
Prf1	81	3	-4.156	4.846	0.000	0.000
Nkg7	392	16	-4.053	7.014	0.000	0.000
Lilrb3	190	8	-4.000	6.008	0.000	0.000
Gbp6	49	2	-3.995	4.196	0.000	0.001
Cxcr3	95	4	-3.983	5.067	0.000	0.000
C6	25	1	-3.960	3.357	0.001	0.041
Crtac1	25	1	-3.960	3.357	0.001	0.041
Lcn2	91	4	-3.921	5.012	0.000	0.000
Syndig1l	24	1	-3.901	3.310	0.001	0.052
Tigit	24	1	-3.901	3.310	0.001	0.052
Ccdc164	152	7	-3.868	5.709	0.000	0.000
Haao	43	2	-3.807	4.038	0.000	0.003
Rab20	22	1	-3.777	3.211	0.002	0.069
Shisa3	22	1	-3.777	3.211	0.002	0.069
C4b	260	13	-3.758	6.457	0.000	0.000
Gbp5	359	18	-3.757	6.908	0.000	0.000
F2rl2	21	1	-3.710	3.159	0.002	0.090
I830077J02Rik	21	1	-3.710	3.159	0.002	0.090
Lrrc25	77	4	-3.680	4.803	0.000	0.000
Naaa	581	32	-3.625	7.596	0.000	0.000
Bst1	70	4	-3.543	4.686	0.000	0.000
Gm13498	121	7	-3.539	5.419	0.000	0.000
Cpxm1	411	24	-3.539	7.114	0.000	0.000
Fam19a3	35	2	-3.511	3.793	0.000	0.011
Scimp	35	2	-3.511	3.793	0.000	0.011
P2rx2	34	2	-3.469	3.759	0.000	0.014
Myl10	98	6	-3.455	5.140	0.000	0.000
Ctla4	161	10	-3.443	5.816	0.000	0.000
Gp49a	33	2	-3.426	3.725	0.000	0.017
Pla2g5	80	5	-3.421	4.871	0.000	0.000
Ifitm1	63	4	-3.391	4.557	0.000	0.001
Cd22	291	19	-3.377	6.641	0.000	0.000
Napsa	230	15	-3.377	6.314	0.000	0.000
Fam46c	31	2	-3.337	3.652	0.000	0.027
Stk32c	31	2	-3.337	3.652	0.000	0.027
Gzma	762	54	-3.263	8.011	0.000	0.000
Fut7	29	2	-3.241	3.576	0.001	0.035
Itih4	29	2	-3.241	3.576	0.001	0.035
Serpina3g	731	53	-3.230	7.955	0.000	0.000

(cont.)

Supp. Table 4. DEGs upregulated in TJ2-Tg sample. (Continuation.)

Gene	T-ALL counts	WT counts	logFC	logCPM	*P* value	FDR
Ccdc12	28	2	-3.190	3.536	0.001	0.044
Tbc1d2	28	2	-3.190	3.536	0.001	0.044
Gbp2	1319	100	-3.167	8.804	0.000	0.000
Adra2a	53	4	-3.143	4.349	0.000	0.005
Msr1	40	3	-3.141	3.987	0.000	0.011
Mtus2	40	3	-3.141	3.987	0.000	0.011
Cd244	52	4	-3.115	4.327	0.000	0.006
Cxcl11	52	4	-3.115	4.327	0.000	0.006
Ppm1j	52	4	-3.115	4.327	0.000	0.006
Tbx21	51	4	-3.087	4.304	0.000	0.008
Fam26f	113	9	-3.083	5.362	0.000	0.000
Cxcl10	991	80	-3.076	8.404	0.000	0.000
Il2rb	701	57	-3.065	7.912	0.000	0.000
Susd3	49	4	-3.030	4.257	0.000	0.011
Slamf8	227	19	-3.019	6.327	0.000	0.000
Pld4	650	56	-2.981	7.813	0.000	0.000
Batf2	47	4	-2.970	4.208	0.000	0.013
Olig3	47	4	-2.970	4.208	0.000	0.013
Hmox1	241	21	-2.961	6.417	0.000	0.000
Fcer1g	240	21	-2.955	6.412	0.000	0.000
Clec4a3	34	3	-2.908	3.800	0.000	0.030
Atf3	45	4	-2.907	4.157	0.000	0.018
Thbs4	110	10	-2.894	5.344	0.000	0.000
Eml1	55	5	-2.881	4.420	0.000	0.008
Tgm2	1238	116	-2.862	8.746	0.000	0.000
Sostdc1	54	5	-2.855	4.399	0.000	0.010
5830411N06Rik	404	38	-2.854	7.154	0.000	0.000
Fhl2	32	3	-2.821	3.732	0.001	0.045
Gm12250	236	23	-2.800	6.405	0.000	0.000
Bcar1	122	12	-2.782	5.497	0.000	0.000
Naip2	41	4	-2.773	4.050	0.001	0.031
Fcrla	51	5	-2.773	4.332	0.000	0.014
Foxp3	51	5	-2.773	4.332	0.000	0.014
Ch25h	71	7	-2.771	4.768	0.000	0.003
Vit	71	7	-2.771	4.768	0.000	0.003
Nptx1	50	5	-2.744	4.310	0.000	0.016
Lepr	40	4	-2.738	4.022	0.001	0.038
Cfb	555	57	-2.728	7.618	0.000	0.000
Cacna1i	30	3	-2.728	3.660	0.002	0.070
Fcgr1	98	10	-2.727	5.205	0.000	0.001
Timp1	203	21	-2.714	6.206	0.000	0.000
Ifitm2	145	15	-2.712	5.741	0.000	0.000

(cont.)

Supp. Table 4. DEGs upregulated in TJ2-Tg sample. (Continuation.)

Gene	T-ALL counts	WT counts	logFC	logCPM	*P* value	FDR
Man1c1	57	6	-2.674	4.488	0.000	0.011
Tbxas1	57	6	-2.674	4.488	0.000	0.011
Srpk3	38	4	-2.664	3.964	0.000	0.031
Kcnk5	75	8	-2.660	4.853	0.000	0.005
Thbs1	343	37	-2.656	6.947	0.000	0.000
Fgl2	268	29	-2.651	6.601	0.000	0.000
Mea1	56	6	-2.649	4.468	0.000	0.012
Gbp11	28	3	-2.629	3.583	0.002	0.088
Ttc16	28	3	-2.629	3.583	0.002	0.088
Tyms-ps	28	3	-2.629	3.583	0.002	0.088
Cd5l	46	5	-2.624	4.214	0.000	0.027
Zbtb46	54	6	-2.597	4.426	0.000	0.016
Xcl1	124	14	-2.585	5.542	0.000	0.001
Ifi205	62	7	-2.576	4.610	0.000	0.010
Aif1	123	14	-2.573	5.532	0.000	0.001
Col8a1	53	6	-2.570	4.404	0.000	0.016
Ctss	1883	217	-2.563	9.386	0.000	0.000
Gbp3	397	46	-2.554	7.167	0.000	0.000
Mcam	405	47	-2.551	7.195	0.000	0.000
Cd7	258	30	-2.547	6.561	0.000	0.000
Tifab	95	11	-2.546	5.184	0.000	0.003
Pgpep1l	35	4	-2.546	3.872	0.001	0.045
Tgfbi	763	89	-2.545	8.096	0.000	0.000
Lsr	129	15	-2.543	5.601	0.000	0.001
Mybpc2	69	8	-2.540	4.756	0.000	0.011
Tlr1	128	15	-2.532	5.592	0.000	0.001
C1qtnf6	94	11	-2.531	5.172	0.000	0.003
Itgb7	908	107	-2.531	8.346	0.000	0.000
Clec10a	60	7	-2.529	4.572	0.000	0.013
Pak6	43	5	-2.527	4.137	0.001	0.044
Cd79b	267	32	-2.504	6.615	0.000	0.000
Pla2g2d	307	37	-2.496	6.812	0.000	0.000
Phf11b	42	5	-2.493	4.111	0.001	0.053
Ly6a	1354	164	-2.492	8.924	0.000	0.000
Rgs16	50	6	-2.486	4.338	0.000	0.027
Dock4	66	8	-2.476	4.705	0.000	0.016
Tyrobp	441	54	-2.474	7.327	0.000	0.000
Pik3ap1	106	13	-2.465	5.344	0.000	0.003
Podnl1	41	5	-2.459	4.084	0.001	0.053
Gprin3	49	6	-2.457	4.315	0.001	0.031
Lyl1	49	6	-2.457	4.315	0.001	0.031
Hck	202	25	-2.456	6.232	0.000	0.000

(cont.)

Supp. Table 4. DEGs upregulated in TJ2-Tg sample. (Continuation.)

Gene	T-ALL counts	WT counts	logFC	logCPM	*P* value	FDR
Igsf23	73	9	-2.453	4.842	0.000	0.011
B430306N03Rik	32	4	-2.417	3.773	0.002	0.084
Gm12185	32	4	-2.417	3.773	0.002	0.084
Ctsw	452	58	-2.407	7.372	0.000	0.000
Aprt	148	19	-2.402	5.809	0.000	0.001
Xcr1	179	23	-2.402	6.072	0.000	0.001
Vash1	70	9	-2.393	4.794	0.000	0.014
Casp4	93	12	-2.391	5.176	0.000	0.005
Slc34a2	100	13	-2.381	5.276	0.000	0.005
Ncam1	77	10	-2.380	4.923	0.000	0.011
Itgax	373	49	-2.373	7.105	0.000	0.000
Ms4a6d	69	9	-2.372	4.777	0.000	0.016
Rnase6	69	9	-2.372	4.777	0.000	0.016
S100a11	76	10	-2.361	4.908	0.000	0.011
Tmem243	38	5	-2.349	4.000	0.002	0.091
Iigp1	1027	138	-2.342	8.551	0.000	0.000
Itgae	365	49	-2.341	7.079	0.000	0.000
Ppp3cc	45	6	-2.334	4.220	0.001	0.052
Clca2	178	24	-2.333	6.075	0.000	0.001
Cmklr1	67	9	-2.330	4.744	0.000	0.021
Dnase1l3	479	65	-2.326	7.466	0.000	0.000
Wdfy4	707	96	-2.326	8.020	0.000	0.000
S100a4	271	37	-2.316	6.664	0.000	0.001
H2-DMb2	139	19	-2.312	5.736	0.000	0.003
Neurl3	247	34	-2.304	6.536	0.000	0.001
Plaur	44	6	-2.302	4.195	0.001	0.062
Ifit3	94	13	-2.292	5.204	0.000	0.009
Lyz2	2503	349	-2.289	9.838	0.000	0.000
Ly86	200	28	-2.279	6.245	0.000	0.001
Psme2	43	6	-2.269	4.169	0.002	0.072
Ccdc102a	50	7	-2.267	4.366	0.001	0.043
Pkig	50	7	-2.267	4.366	0.001	0.043
Trpm2	329	47	-2.252	6.947	0.000	0.001
Anpep	175	25	-2.250	6.064	0.000	0.002
Plat	91	13	-2.245	5.167	0.000	0.012
Coro2a	257	37	-2.240	6.602	0.000	0.001
Plek	236	34	-2.239	6.483	0.000	0.001
Ckb	49	7	-2.238	4.344	0.001	0.050
Hpse	55	8	-2.214	4.499	0.001	0.036
Snai3	55	8	-2.214	4.499	0.001	0.036
Slamf7	157	23	-2.213	5.919	0.000	0.003
Fzd2	136	20	-2.207	5.722	0.000	0.005

(cont.)

Supp. Table 4. DEGs upregulated in TJ2-Tg sample. (Continuation.)

Gene	T-ALL counts	WT counts	logFC	logCPM	*P* value	FDR
Gpx3	1161	172	-2.201	8.750	0.000	0.000
Lrg1	196	29	-2.200	6.230	0.000	0.002
Themis2	148	22	-2.192	5.841	0.000	0.005
Cd160	54	8	-2.187	4.478	0.001	0.043
Gna15	54	8	-2.187	4.478	0.001	0.043
Tlr11	67	10	-2.180	4.766	0.000	0.031
Gpr35	80	12	-2.174	5.004	0.000	0.016
AF251705	60	9	-2.171	4.620	0.001	0.045
Socs3	396	60	-2.167	7.223	0.000	0.001
Fcgr3	157	24	-2.152	5.929	0.000	0.004
Chst3	72	11	-2.147	4.867	0.000	0.027
Angpt2	52	8	-2.133	4.437	0.001	0.048
Pou2f2	84	13	-2.130	5.077	0.000	0.023
H2-DMb1	225	35	-2.128	6.434	0.000	0.003
Tmem173	494	77	-2.127	7.544	0.000	0.001
Serpinb1a	274	43	-2.116	6.713	0.000	0.002
Ms4a1	70	11	-2.106	4.835	0.000	0.030
Ccl6	76	12	-2.100	4.947	0.000	0.024
Chst12	57	9	-2.097	4.563	0.001	0.060
Trip6	82	13	-2.095	5.050	0.000	0.026
Irf1	1090	174	-2.093	8.679	0.000	0.001
Cdc42ep1	44	7	-2.083	4.226	0.003	0.096
Cxcl13	50	8	-2.077	4.394	0.002	0.066
Mefv	50	8	-2.077	4.394	0.002	0.066
C1s	626	102	-2.063	7.893	0.000	0.001
Golm1	123	20	-2.062	5.608	0.000	0.011
Serping1	1021	167	-2.058	8.592	0.000	0.001
Adcy4	147	24	-2.057	5.854	0.000	0.009
Pdgfc	49	8	-2.048	4.372	0.002	0.076
Gpr114	249	41	-2.047	6.591	0.000	0.003
Il2ra	643	106	-2.046	7.934	0.000	0.001
Irgm1	582	96	-2.046	7.792	0.000	0.001
Slc27a3	85	14	-2.041	5.107	0.000	0.028
Sox18	151	25	-2.037	5.895	0.000	0.008
Il10ra	641	107	-2.028	7.933	0.000	0.001
Zbp1	359	60	-2.026	7.110	0.000	0.002
Ecscr	84	14	-2.024	5.094	0.001	0.031
Cst7	60	10	-2.021	4.643	0.001	0.066
Tgm1	54	9	-2.020	4.504	0.002	0.091
Ube2l6	155	26	-2.018	5.935	0.000	0.011
Plvap	573	97	-2.008	7.777	0.000	0.002
Lmo2	77	13	-2.005	4.980	0.001	0.044

(cont.)

Supp. Table 4. DEGs upregulated in TJ2-Tg sample. (Continuation.)

Gene	T-ALL counts	WT counts	logFC	logCPM	*P* value	FDR
Ifi30	793	135	-2.000	8.242	0.000	0.001
Cxcr6	65	11	-2.000	4.754	0.001	0.055
Fcrl1	65	11	-2.000	4.754	0.001	0.055
Fxyd5	552	94	-2.000	7.726	0.000	0.002
4930503E24Rik	106	18	-1.999	5.415	0.000	0.023
5430435G22Rik	94	16	-1.995	5.252	0.000	0.025
Adam19	310	53	-1.993	6.909	0.000	0.003
Sh3bp5	158	27	-1.992	5.966	0.000	0.011
Gm4951	117	20	-1.990	5.552	0.000	0.016
Selp	117	20	-1.990	5.552	0.000	0.016
Sh3tc1	82	14	-1.989	5.068	0.001	0.035
Uap1l1	76	13	-1.986	4.966	0.001	0.044
Asb2	122	21	-1.980	5.611	0.000	0.015
Gpr124	64	11	-1.977	4.737	0.001	0.055
C1qa	739	128	-1.975	8.146	0.000	0.002
Pisd	75	13	-1.967	4.951	0.001	0.049
Ubd	761	133	-1.962	8.191	0.000	0.002
Clca1	69	12	-1.961	4.840	0.001	0.047
Sema4a	651	114	-1.959	7.968	0.000	0.002
Osbpl3	233	41	-1.951	6.515	0.000	0.007
Cish	419	74	-1.947	7.344	0.000	0.003
Ncf4	170	30	-1.946	6.076	0.000	0.011
Gm2a	921	163	-1.944	8.467	0.000	0.002
Med28	68	12	-1.940	4.824	0.001	0.053
Igtp	838	149	-1.938	8.333	0.000	0.002
Cd72	157	28	-1.930	5.969	0.000	0.013
Meox1	73	13	-1.928	4.921	0.001	0.062
Lap3	212	38	-1.924	6.388	0.000	0.009
Blk	67	12	-1.919	4.808	0.001	0.060
Fcer2a	67	12	-1.919	4.808	0.001	0.060
Anxa8	100	18	-1.915	5.350	0.001	0.035
Pdlim4	100	18	-1.915	5.350	0.001	0.035
Rabep2	111	20	-1.914	5.493	0.000	0.024
A4galt	61	11	-1.908	4.684	0.002	0.081
Tlr9	94	17	-1.908	5.267	0.001	0.033
Hip1	176	32	-1.903	6.133	0.000	0.014
Fxyd6	88	16	-1.900	5.179	0.001	0.041
Tnfaip8l2	104	19	-1.894	5.408	0.001	0.031
Sdc3	758	139	-1.893	8.199	0.000	0.003
Ccr5	93	17	-1.892	5.256	0.001	0.033
C1qb	1294	238	-1.889	8.966	0.000	0.002
Clec12a	158	29	-1.889	5.985	0.000	0.016

(cont.)

Supp. Table 4. DEGs upregulated in TJ2-Tg sample. (Continuation.)

Gene	T-ALL counts	WT counts	logFC	logCPM	*P* value	FDR
Samhd1	943	174	-1.884	8.513	0.000	0.003
Nlrc5	1001	185	-1.882	8.599	0.000	0.003
Josd2	65	12	-1.875	4.775	0.002	0.076
Adap1	108	20	-1.874	5.463	0.000	0.031
C1qc	940	176	-1.863	8.513	0.000	0.003
Il18bp	238	45	-1.847	6.566	0.000	0.012
Dpp7	69	13	-1.847	4.860	0.002	0.087
Socs2	95	18	-1.841	5.294	0.001	0.049
Scn3b	100	19	-1.837	5.365	0.001	0.044
Rrad	89	17	-1.829	5.208	0.001	0.048
B3gnt3	68	13	-1.826	4.845	0.003	0.097
C1ra	94	18	-1.826	5.283	0.001	0.054
Rnf19b	333	64	-1.825	7.044	0.000	0.010
Lama5	264	51	-1.817	6.718	0.000	0.012
Aebp1	217	42	-1.814	6.443	0.000	0.015
Irf5	165	32	-1.810	6.061	0.000	0.023
Apobr	62	12	-1.807	4.724	0.003	0.097
Gimap7	67	13	-1.804	4.829	0.002	0.082
Isg15	82	16	-1.798	5.102	0.002	0.067
Csf2rb	569	112	-1.791	7.812	0.000	0.007
Ctsz	551	109	-1.784	7.767	0.000	0.008
Kit	182	36	-1.782	6.204	0.000	0.023
Npdc1	106	21	-1.777	5.456	0.001	0.045
Serpine1	121	24	-1.776	5.639	0.001	0.038
Fes	225	45	-1.766	6.504	0.000	0.019
Alox5ap	159	32	-1.756	6.021	0.000	0.031
Clec9a	144	29	-1.755	5.883	0.001	0.032
Cndp2	297	60	-1.753	6.897	0.000	0.015
Sirpa	803	163	-1.747	8.313	0.000	0.008
Pigs	74	15	-1.743	4.974	0.003	0.097
Lgals1	706	144	-1.740	8.131	0.000	0.009
Plac8	365	75	-1.728	7.194	0.000	0.014
Notch4	112	23	-1.726	5.542	0.001	0.058
Tnfsf10	310	64	-1.721	6.965	0.000	0.017
Lfng	358	74	-1.720	7.169	0.000	0.015
Irgm2	377	78	-1.718	7.242	0.000	0.015
Fgd2	372	77	-1.718	7.224	0.000	0.014
Prr13	193	40	-1.715	6.300	0.000	0.027
Plekho2	255	53	-1.711	6.692	0.000	0.020
Plod3	163	34	-1.705	6.066	0.001	0.035
Cfp	439	92	-1.700	7.463	0.000	0.015
C3	3977	837	-1.695	10.623	0.000	0.008

(cont.)

Supp. Table 4. DEGs upregulated in TJ2-Tg sample. (Continuation.)

Gene	T-ALL counts	WT counts	logFC	logCPM	*P* value	FDR
Efhd2	233	49	-1.694	6.568	0.000	0.024
Olfm1	81	17	-1.693	5.106	0.002	0.087
Tie1	190	40	-1.692	6.283	0.000	0.029
H2-Eb1	6415	1357	-1.688	11.314	0.000	0.008
Hcst	90	19	-1.685	5.251	0.002	0.090
Hsd3b7	160	34	-1.678	6.046	0.001	0.040
Slc25a39	113	24	-1.678	5.565	0.001	0.066
Dhx58	155	33	-1.675	6.003	0.001	0.043
Lgmn	463	99	-1.671	7.545	0.000	0.016
Tap1	1680	362	-1.661	9.391	0.000	0.011
Pion	144	31	-1.659	5.904	0.001	0.045
Hvcn1	347	75	-1.655	7.139	0.000	0.023
H2-Aa	6323	1368	-1.655	11.300	0.000	0.010
Lgals3	217	47	-1.652	6.478	0.001	0.033
Arid5a	244	53	-1.648	6.644	0.000	0.030
Sfpi1	115	25	-1.644	5.596	0.002	0.068
Naga	220	48	-1.641	6.500	0.001	0.033
Sh3bp2	165	36	-1.640	6.097	0.001	0.049
Rpl32	334	73	-1.639	7.089	0.000	0.023
Ninj1	128	28	-1.636	5.746	0.002	0.068
Adam11	210	46	-1.635	6.436	0.001	0.038
Slc25a45	146	32	-1.634	5.929	0.001	0.059
Cybb	255	56	-1.632	6.709	0.001	0.032
Bax	159	35	-1.628	6.049	0.001	0.048
Rusc1	95	21	-1.620	5.339	0.003	0.097
Ushbp1	113	25	-1.619	5.577	0.002	0.079
Bcl3	140	31	-1.619	5.874	0.001	0.059
Ciita	795	177	-1.613	8.330	0.000	0.018
Pla2g7	135	30	-1.613	5.824	0.001	0.065
Ctsh	363	81	-1.610	7.214	0.000	0.026
Gimap3	465	104	-1.606	7.566	0.000	0.023
Vim	2190	491	-1.604	9.786	0.000	0.015
Slc24a6	258	58	-1.598	6.734	0.001	0.035
Gbp7	489	110	-1.598	7.640	0.000	0.023
H2-D1	2619	590	-1.597	10.045	0.000	0.015
Pced1b	129	29	-1.597	5.765	0.002	0.075
H2-Ob	244	55	-1.594	6.656	0.001	0.041
H2-K1	9300	2102	-1.592	11.872	0.000	0.014
Kbtbd11	380	86	-1.589	7.284	0.000	0.028
Vwa1	189	43	-1.581	6.301	0.001	0.052
Rasa4	381	87	-1.576	7.290	0.000	0.029
Rasip1	114	26	-1.576	5.599	0.002	0.088

(cont.)

Supp. Table 4. DEGs upregulated in TJ2-Tg sample. (Continuation.)

Gene	T-ALL counts	WT counts	logFC	logCPM	*P* value	FDR
Ldha	689	158	-1.571	8.136	0.000	0.023
Cyth4	662	152	-1.569	8.079	0.000	0.024
Tnfrsf1b	453	104	-1.569	7.538	0.000	0.029
Lgals3bp	1204	277	-1.566	8.936	0.000	0.021
Wars	504	116	-1.565	7.691	0.000	0.028
Clec7a	152	35	-1.563	6.001	0.002	0.069
Plcg2	204	47	-1.563	6.412	0.001	0.054
Anxa6	869	201	-1.558	8.471	0.000	0.024
Lamc2	695	161	-1.556	8.152	0.000	0.025
H2-DMa	466	108	-1.555	7.582	0.000	0.031
Gimap4	461	107	-1.553	7.567	0.001	0.031
Irf8	724	169	-1.545	8.213	0.000	0.027
Ctsd	3558	831	-1.545	10.499	0.000	0.020
Csf2rb2	294	69	-1.537	6.933	0.001	0.045
Chd7	221	52	-1.532	6.531	0.001	0.058
H2-M3	233	55	-1.528	6.607	0.001	0.058
Unc93b1	937	222	-1.524	8.587	0.000	0.027
Glipr2	177	42	-1.520	6.223	0.002	0.075
Plbd1	530	126	-1.519	7.774	0.001	0.035
Oas3	139	33	-1.518	5.887	0.002	0.093
Cd74	9395	2249	-1.509	11.908	0.000	0.023
Myo6	309	74	-1.508	7.010	0.001	0.051
Tmem176a	519	125	-1.500	7.749	0.001	0.038
C2	220	53	-1.498	6.533	0.002	0.067
Bhlhe40	199	48	-1.496	6.393	0.002	0.072
Grn	812	198	-1.482	8.393	0.001	0.036
Lyn	197	48	-1.482	6.382	0.002	0.079
Stab1	201	49	-1.481	6.411	0.002	0.074
Csf1r	544	133	-1.478	7.822	0.001	0.043
Ifitm3	1029	252	-1.476	8.734	0.001	0.035
Mgp	909	223	-1.474	8.557	0.001	0.037
AW112010	385	95	-1.465	7.333	0.001	0.053
Entpd1	286	71	-1.456	6.914	0.002	0.067
Tspo	402	100	-1.453	7.397	0.001	0.055
Rogdi	185	46	-1.453	6.301	0.003	0.096
Runx3	229	57	-1.451	6.601	0.002	0.079
Clu	930	232	-1.449	8.596	0.001	0.042
H2-T23	866	218	-1.436	8.497	0.001	0.045
Oas2	254	64	-1.434	6.752	0.002	0.075
Cxcl16	388	99	-1.416	7.356	0.002	0.069
App	1120	286	-1.416	8.871	0.001	0.047
Fgr	223	57	-1.413	6.574	0.003	0.097

(cont.)

Supp. Table 4. DEGs upregulated in TJ2-Tg sample. (Continuation.)

Gene	T-ALL counts	WT counts	logFC	logCPM	*P* value	FDR
Nod1	344	88	-1.413	7.187	0.002	0.075
Serpinh1	745	191	-1.410	8.289	0.001	0.054
Jak3	456	117	-1.409	7.588	0.002	0.067
Hspg2	829	213	-1.407	8.442	0.001	0.054
Ifi47	673	173	-1.406	8.144	0.001	0.058
Mpeg1	1269	328	-1.398	9.055	0.001	0.051
Cd48	309	80	-1.395	7.039	0.002	0.086
Cybasc3	432	112	-1.394	7.515	0.002	0.073
Bst2	451	117	-1.393	7.577	0.002	0.073
Synpo	265	69	-1.387	6.824	0.003	0.100
Cyba	372	97	-1.385	7.305	0.002	0.079
Piezo1	390	102	-1.381	7.373	0.002	0.083
Mvp	426	112	-1.373	7.501	0.002	0.082
Psmb9	598	158	-1.366	7.986	0.002	0.072
Lrrc58	2181	579	-1.360	9.844	0.001	0.059
Ctsb	2583	689	-1.353	10.090	0.001	0.061
Tagln2	845	227	-1.343	8.487	0.002	0.075
H2-Ab1	6227	1680	-1.337	11.362	0.001	0.064
Pkm	444	120	-1.334	7.571	0.003	0.096
Itgb4	651	178	-1.317	8.121	0.003	0.094
Lcp1	1310	364	-1.294	9.130	0.002	0.090
Psap	6569	1848	-1.276	11.456	0.002	0.088

FC, fold-change; CPM, count-per-million; FDR, false discovery rate.

Supp. Table 5. Overlapping genes between the high-throughput RNA-sequencing and the study performed by Ki and colleagues (2014).

Stromal subsets	WT (n=199)		TJ2-Tg (n=441)	
cTEC	**17 (8.5%)**		**0 (0.0%)**	
	Alcam	*Nefm*	-	
	Aldh6a1	*Nqo1*		
	Ccl25	*Prss16*		
	Ccrl1	*Psmb11*		
	Cdh4	*Scn1a*		
	Clic5	*Snhg11*		
	Cxcl12	*Tbata*		
	Diras2	*Tef*		
	Fgf14			
mTEC^{lo}	**1 (0.5%)**		**7 (1.6%)**	
	Cidea		*Clca1*	*Sostdc1*
			Clca2	*Tnfsf10*
			Ncam1	*Vit*
			Scn3b	
mTEC^{hi}	**9 (4.5%)**		**13 (2.9%)**	
	Adipoq	*Spink5*	*A2m*	*Gzmb*
	Car3	*Thrsp*	*Car6*	*Ifng*
	Cdhr5		*Ccdc164*	*Itih4*
	Fabp4		*Cd163l1*	*Prg4*
	Pck1		*Crtac1*	*Spt1*
	Rasd1		*Cxcl13*	*Tbx21*
	Serpinb2		*Gbp1*	
Fibroblasts	**3 (1.5%)**		**20 (4.5%)**	
	Itm2a		*Adamts4*	*Mcam*
	Lpl		*Adra2a*	*Meox1*
	Pten		*Aebp1*	*Mgp*
			C1ra	*Pkig*
			C1s	*Plat*
			C3	*Plvap*
			C4b	*Rgs16*
			Cdc42ep1	*Serping1*
			Ifitm1	*Serpinh1*
			Lepr	*Thbs4*

(cont.)

Supp. Table 5. Overlapping genes between the high-throughput RNA-sequencing and the study performed by Ki and colleagues (2014). (Continuation.)

Stromal subsets	WT (n=199)	TJ2-Tg (n=441)	
Sirpα$^-$ DCs (DC)	**3 (1.5%)**	**13 (2.9%)**	
	C330027C09Rik	*5430435G22Rik*	*Itgae*
	Kif11	*Apobr*	*Naaa*
	Tmpo	*Bst1*	*Notch4*
		Cxcr3	*Osbpl3*
		Fcrla	*Slc24a6*
		Fgd2	*Xcr1*
		Irf8	
Sirpα$^+$ DCs (DCS)	**0 (0.0%)**	**43 (9.8%)**	
	-	*AF251705*	*Fcgr4*
		C1qa	*Hvcn1*
		C1qb	*Il18bp*
		C1qc	*Lgals3*
		Ccr5	*Lgals3bp*
		Cd200r4	*Lgmn*
		Cd22	*Ly86*
		Cd72	*Lyz2*
		Cfp	*Mefv*
		Clec4a3	*Ms4a6d*
		Clec7a	*Msr1*
		Csf1r	*Neurl3*
		Cst7	*Ninj1*
		Ctsb	*Pla2g2d*
		Ctsd	*Pla2g7*
		Ctsz	*S100a4*
		Cybb	*Sirpa*
		Dpp7	*Stab1*
		Fam26f	*Tgfbi*
		Fcer1g	*Tlr1*
		Fcgr1	*Tnfrsf1b*
		Fcgr3	